1-1-2014

Augmenting the Protein C Pathway with Endothelial Targeted Biotherapeutics: Strategies to Promote Partnering of TM and EPCR

Colin F. Greineder
University of Pennsylvania, cfg_25@yahoo.com

Augmenting the Protein C Pathway with Endothelial Targeted Biotherapeutics: Strategies to Promote Partnering of TM and EPCR

Abstract
The design of targeted recombinant biotherapeutics is a rapidly growing area of translational biomedical research, with particular relevance to acute and life-threatening conditions, in which the available treatment options have narrow therapeutic indices. Although vascular immunotargeting typically has been thought of as a strategy for controlling and altering pharmacokinetics, in the context of biotherapeutic delivery, precise localization may be the primary goal, allowing optimal interaction of drug with endogenous partners. The protein C pathway has important protective roles in a variety of human illnesses, including sepsis and acute lung injury. We recently reported a strategy for augmenting this pathway by anchoring thrombomodulin (TM, CD141) to the endothelium via an affinity ligand to platelet endothelial cell adhesion molecule-1 (PECAM-1, CD31). Endothelial PECAM-1, however, is believed to localize to a different portion of the cell membrane than the majority of endogenous TM and its key co-factor, the endothelial protein C receptor (EPCR, CD201). The current document includes new data indicating that recombinant TM anchored to endothelial PECAM-1 does not partner effectively with EPCR and describes the design, implementation, and validation of two strategies for more effectively replicating the enzymatic partnering of these two molecules. In both cases, proximity of these co-factors on the surface of the endothelial membrane appears to be the key variable and has significant implications, affecting not only functional activity in vitro but therapeutic efficacy in vivo. These findings underscore the complexity of targeting biotherapeutics to the plasmalemma, and suggest that precision on a nanometer scale is necessary for optimal biotherapeutic effect.

Degree Type
Dissertation

Degree Name
Doctor of Philosophy (PhD)

Graduate Group
Pharmacology

First Advisor
Vladimir R. Muzykantov

Keywords
Endothelial Protein C Receptor, Endothelium, Targeted Drug Delivery, Thrombomodulin

Subject Categories
Biomedical | Pharmacology

AUGMENTING THE PROTEIN C PATHWAY WITH ENDOTHELIAL TARGETED BIOTHERAPEUTICS:

STRATEGIES TO PROMOTE PARTNERING OF TM AND EPCR

Dr. Colin F. Greineder, MD

A DISSERTATION

in

Pharmacology
Presented to the Faculties of the University of Pennsylvania
In
Partial Fulfillment of the Requirements for the Degree of Doctor of Philosophy
2014

Supervisor of Dissertation

_____

Vladimir R Muzykantov, MD, PhD
Professor of Pharmacology

Graduate Group Chairperson

_____

Julie Blendy, PhD
Professor of Pharmacology

Dissertation Committee
Dr. Mortimer Poncz, MD, Professor of Pediatrics (Chair)
Dr. Steven M. Albelda, MD, Professor of Medicine
Dr. Sriram Krishnaswamy, PhD, Professor of Pediatrics
Dr. Emer M. Smyth, PhD, Research Associate Professor of Pharmacology
Dr. Stephen R. Thom, MD, PhD, Professor of Emergency Medicine

AUGMENTING THE PROTEIN C PATHWAY WITH ENDOTHELIAL TARGETED BIOTHERAPEUTICS: STRATEGIES TO PROMOTE PARTNERING OF TM AND EPCR

DEDICATION

To my mother and father, who instilled in me a love of knowledge, dedication to hard work, and commitment to help others. I miss you both and strive to honor your memory every day.

ACKNOWLEDGEMENTS

Like every PhD student on the verge of graduation, I look back at the last several years of my life and can scarcely begin to think of all of the people that deserve acknowledgement for helping me to complete this body of work. Countless conversations come to mind – some which had major impact on the choices I made and some which simply helped me keep going in the face of frustration, disillusionment, and disappointment. As many friends and colleagues have heard me say over the past 5 years, working in the emergency room is about 95% success, and much of the challenge is in learning to deal with the rare, but devastating failures. Working in the laboratory, on the other hand, seems to be about 95% failure, and much of the challenge is in learning to subsist on the rare, but rewarding successes. All who are reading this are likely to have played some part in teaching me to be patient, persistent, honest, and ethical, in spite of the many challenges and temptations that have arisen along the way. Each of you has contributed to the development of what I hope will be a long career spent in pursuit of novel diagnostics and therapeutics for the sickest amongst us.

In particular, I would like to express my deep gratitude to my advisor, Dr. Vladimir Muzykantov, who saw in me the desire not only to develop hypotheses and conduct experiments, but to constantly ask “why are we doing this?” and “how do we plan to apply this to the real world?” Although my initial impulses may have been naïve and my ideas poorly developed, Vladimir did not crush them, but rather stoked my enthusiasm and molded me into a (more) mature scientist. He introduced me to the field of Drug Targeting, as I have introduced him to the practice of Emergency Medicine. I hope to have a long career together, and that one day (not too far off, please!), our work will contribute to patient care.

I also wish to thank the members of the Department of Emergency Medicine who helped to bring me to Penn and convinced me to pursue this rather atypical path.

In particular, I want to acknowledge Bob Neumar, who first suggested that a PhD would be the best preparation for my career as a physician scientist. Bob's institutional grant from SAEM supported my first two years, and although he has moved on from Penn, he remains a mentor, friend, and trusted advisor. Likewise, I am grateful to Steve Thom, now at the University of Maryland, and Lance Becker, who always seem willing to take time out of their incredibly busy schedules to offer their advice, or simply talk about science and medicine. Finally, I want to mention John Younger, who took me into his lab while still a resident in Michigan and encouraged my interest in basic science. All four of you are pioneers and I draw great motivation from the examples that you provide.

Next, I wish to thank Sarah Squire, our graduate group coordinator, and each of the members of my Thesis Committee. With my atypical circumstances and crazy schedule, I certainly have not been the easiest graduate student to deal with! I want to specifically thank Emer Smyth for understanding the challenges of doing science while having little children at home. Emer's door has always seemed open to me and she has taken the time to provide me much needed advice and support during the most trying of times. Likewise, Dr. Albelda, with his vast experience mentoring physician scientists, has been a consistent source of advice and guidance regarding my chosen career path. I want to thank Drs. Poncz and Krishnaswamy, two giants in the field of experimental hematology, for providing me a unique perspective on my work and challenging me to cut to the chase and focus my work. I have already mentioned Dr. Thom, of course, but he deserves double thanks for his work on my committee.

I want to express my deep gratitude to each and every member of the Muzykantov laboratory. I have had the good fortune to work alongside an amazing set of post-docs and research scientists, who have taught me more than I can possibly acknowledge. I must specifically thank Drs. Ann Marie Chacko, Blaine Zern, Elizabeth Hood, Ronald Carnemolla, Sergei Zaytsev, Melissa

Howard, Jingyan Han, Vladimir Shuvaev, and Samira Tliba. You have tolerated my foibles, listened to my stories, laughed at my jokes, and opened your lives to me. I am deeply indebted to each of you and hope we will stay close going forward.

Of course, the biggest thanks must go to my loving wife, Sarah, my two sons, Max and Niels, and my sisters, Kirsten and Britt. The last few years have been a juggling act, to say the least, and without the support of my family, I would no doubt have been swallowed up long ago. To Sarah, in particular, I want to express my gratitude, but I find that I have no words, other than to say that I could never have accomplished any of this without your help, patience, support, and belief in me. This dissertation may pale in significance, in comparison to our two greatest accomplishments together, but nonetheless I treasure the fact that you share my vision of the future and want to get there together.

ABSTRACT

AUGMENTING THE PROTEIN C PATHWAY WITH ENDOTHELIAL TARGETED BIOTHERAPEUTICS: STRATEGIES TO PROMOTE PARTNERING OF TM AND EPCR

Dr. Colin F. Greineder

Dr. Vladimir R. Muzykantov

The design of targeted recombinant biotherapeutics is a rapidly growing area of translational biomedical research, with particular relevance to acute and life-threatening conditions, in which the available treatment options have narrow therapeutic indices. Although vascular immunotargeting typically has been thought of as a strategy for controlling and altering pharmacokinetics, in the context of biotherapeutic delivery, precise localization may be the primary goal, allowing optimal interaction of drug with endogenous partners. The protein C pathway has important protective roles in a variety of human illnesses, including sepsis and acute lung injury. We recently reported a strategy for augmenting this pathway by anchoring thrombomodulin (TM, CD141) to the endothelium via an affinity ligand to platelet endothelial cell adhesion molecule-1 (PECAM-1, CD31). Endothelial PECAM-1, however, is believed to localize to a different portion of the cell membrane than the majority of endogenous TM and its key co-factor, the endothelial protein C receptor (EPCR, CD201). The current document includes new data indicating that recombinant TM anchored to endothelial PECAM-1 does not partner effectively with EPCR and describes the design, implementation, and validation of two strategies for more effectively replicating the enzymatic partnering of these two molecules. In both cases, proximity of these co-factors on the surface of the endothelial membrane appears to be the key variable and has significant implications, affecting not only functional activity *in vitro* but therapeutic efficacy *in vivo*. These findings underscore the complexity of targeting biotherapeutics to the plasmalemma, and suggest that precision on a nanometer scale is necessary for optimal biotherapeutic effect.

TABLE OF CONTENTS

LIST OF FIGURES

CHAPTER ONE: INTRODUCTION

I. A Brief review of Drug Targeting

Over the past four decades, thousands of scientists and clinicians have contributed to the study of drug targeting, resulting in the development and testing of hundreds of strategies for the delivery of therapeutics to various locations in the body. By the late 1990s, annual sales of Advanced Drug Delivery Systems (ADDS) in the United States exceeded $10 billion, and they have continued to rise rapidly[1]. While a comprehensive survey of the field is clearly beyond the scope of this document, it is instructive to briefly review the origins of drug targeting and its progression from the controlled release of small lipophilic drugs to the precise subcellular localization of macromolecular biotherapeutics.

Magischen Kugeln: the origins of targeted drug delivery

With few exceptions, the pharmaceuticals in clinical use distribute throughout the body based on their physical characteristics (size, charge, lipophilicity, etc.) and the physiologic state of the patient to which they are administered. Without any specific control over pharmacokinetics, most drugs do not accumulate at their intended site of therapeutic action. In order to achieve adequate concentration at the required location, large doses, repeated administration, or even continuous infusion may be required, increasing the cost, risk of harmful side-effects, and likelihood that patients will not adhere to the proper regimen. Far from theoretical, these factors lead to the failure of the majority of prospective therapeutics[2,3], as well as millions of dollars of annual health care expenses related to adverse drug events and medication non-compliance[4,5]. With the development of monoclonal antibodies (mAbs) and advances in polymeric chemistry in the 1970s, a new field of scientific investigation emerged, dedicated to the development of delivery systems for the

controlled release, distribution, and permeation of drugs across cellular membranes[6].

The basic concepts of drug targeting were formulated long before any technology existed to apply them to biological systems. The Nobel laureate, Paul Ehrlich, is largely credited with advancing the theory of *Seitenketten* ("side chains"), or cellular receptors, in the early 20th century[7]. He postulated that these receptors were responsible for the binding of bacterial toxins to particular cells – e.g. the attachment of tetanospasmin to the neuromuscular junction[8]. Ehrlich went on coin the famous term *magischen Kugeln* ("magic bullets") to refer to therapeutics that would mimic the action of these toxins, going directly to their intended cellular targets and attacking diseased tissue while inflicting no harm to the remainder of the body[9]. While Ehrlich's vision has yet to be fully realized, substantial progress has been made, with the design and implementation of hundreds of ADDS. Research efforts have followed a natural progression from relatively basic strategies of therapeutic delivery to more sophisticated approaches. Each new technology has been accompanied by practical applications, allowing physicians and scientists to tackle increasingly difficult biological questions and clinical challenges[10].

The polymeric drug depot: the first ADDS

Perhaps the first and most elementary therapeutic delivery system was that of the polymeric drug depot, a device intended for the gradual and controlled release of pharmaceuticals. The earliest drug depots, such as the Norplant® device, consisted of non-biodegradable polymers and aimed at reducing the cost and complexity of treatment regimens[11]. Norplant®, a series of silicone capsules containing the steroid hormone, levonorgestrel, produced highly effective, long-term contraception[12]. Although the device achieved notoriety in the United States as the subject of a number of class action lawsuits, it continues to be utilized in the developing world, where it has the major advantage of long-term efficacy without the need for consumable supplies[13]. Silicone and other non-

degradable polymers were ultimately replaced by materials such as poly(lactic-co-glycolic) acid, or PLGA[14]. Biodegradable polymers allow for repeated administration, and their development enabled new clinical applications, such as monthly dosing of gonadotropins for the treatment of endometriosis, prostate cancer, and children with precocious puberty[15,16]. The most recent depot technologies have achieved actual "drug targeting", in the sense that they release therapeutics at a site of disease, rather than into the systemic circulation. The most widely publicized and medically significant example is that of the drug-eluting stent (DES), a polymer-coated expandable metal tube, which is deployed within an atherosclerotic artery as a means to maintain blood flow following angioplasty. Bare metal stents, used prior to the invention of DES, were complicated by high rates of in-stent restenosis (ISR), a pathological process in which vascular smooth muscle cell proliferation, or "neointimal hyperplasia", leads to vessel re-occlusion[17]. DES, which slowly release immunosuppressive or anti-proliferative agents from their polymer coating, achieve high local concentrations of drug with minimal side effects and have dramatically reduced the incidence of ISR[18–20].

Mobile drug delivery systems and a focus tumor targeting

While polymeric depots remain the most significant achievement of the drug delivery field from both a medical and commercial standpoint, even the most sophisticated examples employ an elementary targeting strategy – i.e. the direct implantation of drug at its intended site of action. Since many diseases are disseminated (e.g. metastatic cancer) or inaccessible to implantable depots, the focus of the drug delivery field has largely turned to mobile targeting systems. These are capable of carrying therapeutics to diseased sites throughout the body, where local factors stimulate release[10]. The vast majority of this work has dealt with the delivery of inherently toxic agents, such as antimicrobials and antineoplastics, which are limited in their dosing and efficacy due to narrow therapeutic indices. In particular, the treatment of cancer has dominated the field

of targeted drug delivery for nearly two decades, perhaps because of the obvious and intuitive appeal of delivering chemotherapeutic drugs to tumor, while sparing normal tissues[21].

As in other cases, the simplest strategies have been explored first, amongst them the passive leakage of drug carriers into tumor. The landmark observation that liposomes and other nanoparticles (NPs) accumulate in neoplastic tissue in excess of proportional blood flow has been termed the "Enhanced Permeability and Retention (EPR)" effect[22]. As the name implies, EPR is believed to be the result of a combination of phenomena. First, NPs that are normally too large to cross the endothelial barrier are able to permeate through defective and discontinuous neovasculature, which is formed by rapidly growing tumors. Second, NPs are poorly cleared from tumor interstitium due to impaired lymphatic drainage[23]. The EPR effect has had a profound and lasting impact on the development of drug targeting systems, despite the fact that it only applies to treatment of cancer, and specifically, the targeting of solid tumors. In general, priority has been placed on the development of long-circulating drug carriers, which maintain the high plasma concentrations needed to drive passive tumor targeting. Since anti-neoplastic drugs are typically toxic, retention of drug carrier in the bloodstream has the added benefit of preventing access to normal tissues (e.g. the bone marrow), thus reducing dose-limiting side effects[24].

Lessons from the clinic: liposomes and early polymer conjugates

The most successful drug carriers – from a clinical standpoint – have been passively targeted liposomal formulations of small molecule chemotherapeutics. The prime example is that of doxorubicin, a highly effective anticancer drug, which unfortunately causes cumulative, dose-dependent, and irreversible cardiomyopathy[25]. Loading doxorubicin into long-circulating polyethylene glycol (PEG)-coated liposomes leads to a drastic reduction in its plasma clearance rate (0.1L/hr vs. 45L/hr for free drug) and volume of distribution (4L as opposed to 254L for free drug), confirming the ability of the drug carrier to limit access to

normal tissues[26]. The first FDA approved nanoparticle, Doxil® (PEGylated doxorubicin liposomes) demonstrated significantly less cardiotoxicity in clinical trials than free doxorubicin[27]. At the same time, the EPR-mediated tumor targeting suggested by early pharmacokinetic studies[26], failed to translate into a marked improvement in clinical efficacy, with overall survival rates similar to those of free doxorubicin, depending on the type of cancer being treated and combination of therapies utilized[27,28].

The development of another liposomal drug, amphotericin B, is a remarkably similar story. Amphotericin is a highly effective anti-fungal agent whose utility is limited by dose-dependent and often irreversible nephrotoxicity. Early studies suggested that incorporation of amphotericin into liposomes could prevent its interaction with mammalian cell membranes[29]. Moreover, a passive targeting mechanism was discovered based on non-specific binding of the drug carrier to the fungal cell wall. Electron microscopy revealed that amphotericin-loaded liposomes were disrupted by this interaction and free drug released into the fungal cytoplasm[30]. This exciting pre-clinical work led to industrial development and clinical testing of AmBisome (liposomal amphotericin B), which demonstrated significant reductions in nephrotoxicity, as compared to free drug. As with Doxil®, however, AmBisome has been somewhat of a disappointment in that the antimicrobial efficacy appears to be similar to free amphotericin[31]. Given these relatively modest clinical results, it is not surprising that both therapeutics have faded from widespread use. AmBisome has been largely eclipsed by the equally effective and less toxic echinocandin class of antifungals[32], and Doxil® has been in nearly continuous nationwide shortage since going off patent in 2009, with no generic form of the drug available[25]. In February, 2013, the FDA approved generic doxorubicin HCl liposomes, but it remains to be seen to what extent the drug will regain use after this hiatus[33].

Liposomal formulations are by no means the only ADDS available for the delivery of toxic, small molecule drugs. In fact, liposomes have relatively short circulation times in comparison to many newer drug carriers, in part because of

their limited capacity for PEGylation[34]. More stable carriers have been developed based on N-(2-hydroxypropyl)-methacrylamide (HPMA), polyglutamic acid (PGA), cyclodextrin, and diblock PEG/PLGA copolymers[35]. The elucidation of endocytic pathways in the 1950s and 60s lead to an important realization by the Nobel laureate Christian De Duve, who suggested that the lysosome might be a useful target for polymeric drug carriers[36]. Peptide linkers susceptible to lysosomal proteases, such as Gly-Phe-Leu-Gly, were used to conjugate drugs to HPMA, such that the resulting complex would be stable in the circulation, but susceptible to cleavage once the conjugate had been internalized by endocytosis[24]. Other polymers, like PGA, are directly degraded by lysosomal proteases[37], whereas some incorporate pH sensitive bonds to encourage degradation in the lysosome and release of free drug within the cell[38]. A few classes of polymer conjugates have advanced sufficiently to reach clinical trials. The first, HPMA copolymer-Gly-Phe-Leu-Gly-doxorubicin, or PK1 (FCE28068), was tested in patients with non-small-cell lung cancer (NSCLC), colon cancer, and anthracycline-resistant breast cancer. No cardiotoxicity was observed, even in patients receiving large cumulative doses of doxorubicin, but the drug produced only partial therapeutic responses, and clinical trials were not continued[39]. The most extensive clinical testing to date has been with a PGA conjugate, paclitaxel poliglumex, or Xyotax. After early trials in NSCLC were positive, multiple phase III trials were conducted, all of which missed their primary endpoint of improved survival. Although Xyotax appears to decrease incidence of paclitaxel-induced side effects, this was not enough to sustain its clinical development[37]. In general, the lesson may be that passive targeting strategies, while capable of reducing off-target side effects from toxic small-molecule drugs, are not enough to produce the “magic bullets” envisioned by Paul Ehrlich and long-expected by the medical community.

Ligand-targeted therapeutics

The limited success of liposomal carriers and early polymer conjugates has turned attention to the development of more sophisticated targeting strategies. In particular drug carriers have been decorated with nutrients, peptide hormones, antibodies, and other molecules designed to promote binding and uptake by target cells. The renewed interest in ligand targeting is not entirely surprising, given the recent commercial success of monoclonal antibody (mAb) therapeutics. One of the most successful examples has been that of folate targeting. While folic acid is essential for proliferation of all mammalian cells, only a few cell types, amongst them cancer cells, express high affinity folate receptors (FRs)[40]. A variety of potent anti-cancer drugs have been generated by conjugation of toxic agents to folate. These conjugates bind FRs and are internalized. In some cases, such as the pseudomonas exotoxin PE38, the cargo has a built-in mechanism of endosomal escape[41]. In other cases, conjugates have been designed with disulfide linkages, resulting in the discharge of free drug in the reducing environment of the endosome[42]. Most importantly, the development of folate-targeted therapeutics has been accompanied by cognate imaging agents, which allow for the identification and selection of patients whose tumors overexpress FRs. The pairing of molecular imaging and targeted drug delivery is a powerful concept, which has led to unprecedented success and multiple ongoing clinical trials[43].

New priorities: the emergence of macromolecular biotherapeutics

Perhaps the most significant shift in the field of drug targeting is the one currently underway, which has been driven by the rapid growth of a new class of drugs, macromolecular biotherapeutics. In the thirty years since the FDA approval of recombinant human insulin, biotherapeutics (also referred to as “biologics”) have become a major force in the pharmaceutical industry[44]. This rapidly growing category now accounts for 5 of the top 10 best-selling drugs and more than 50% of the portfolio of most pharmaceutical companies[45]. The most

successful examples have been recombinant proteins that boost natural protective mechanisms, which are deficient or defunct in human disease. Examples include erythropoietin (EPO) administered to boost red cell production in patients with chronic renal failure and granulocyte colony-stimulating factor (G-CSF) used to combat chemotherapy-induced neutropenia[46]. While both EPO and G-CSF have achieved widespread use and commercial success[47], they represent a relatively small subset of biotherapeutics that require no site-specific delivery. Like small molecule drugs, most macromolecules (one notable exception being mAbs) do not inherently accumulate at their intended site of therapeutic action. If anything, the size, complexity, and biocompatibility of these drugs limits their ability to permeate cell membranes and makes them more susceptible to the body's mechanisms of inactivation and elimination[48]. Moreover, the greatest advantage of biotherapeutics – their extreme specificity for particular endogenous biological pathways – also represents one of their greatest challenges, in that these agents require precise delivery to specific locations in order to exert optimal activity.

A good example is that of small interfering ribonucleic acids (siRNA), which are, in principle, able to reversibly silence the expression of any gene of interest. siRNA could become the most important class of therapeutics in history, with the capacity to modulate the pathogenesis of nearly any disease. However, they must be delivered to a specific multiprotein complex, the RNA-induced silencing complex (RISC), in order to have an effect. Numerous obstacles stand between siRNA and the RISC, including RNAse-mediated destruction, immune recognition and clearance, lack of tissue targeting, inefficient cellular uptake, and inability to escape endosomal compartments and reach the perinuclear region of the cytoplasm[49]. As a result, most of the RNA therapeutics in early clinical trials either require direct application of genetic material to the organ of interest (e.g. intravitreal injection) or target the liver via lipid nanoparticles naturally taken up through the fenestrated endothelium[50].

Another interesting example is that of fibrinolytic enzymes. Nearly two decades after the landmark 1995 NINDS trial[51], which demonstrated a long-term benefit of recombinant tissue plasminogen activator (t-PA) in the setting of acute ischemic stroke, less than 5% of stroke patients receive fibrinolytic therapy[52]. The strict eligibility criteria, which exclude the vast majority of patients, are the result of a narrow therapeutic window and potentially life-threatening toxicity, intracranial hemorrhage[53]. As is often the case, poor pharmacokinetics resulting from extremely rapid clearance (the plasma half-life of free t-PA is approximately 3-1/2 minutes)[54] and the presence of a circulating inhibitor[55], necessitate large bolus doses and continuous infusion in order to achieve effective thrombolysis. This increases the cost and risk of side effects and has severely limited clinical use. A variety of efforts have been made to alter pharmacokinetics and protect the drug en route to its therapeutic site, including PEGylation of the enzyme, genetic modification, and encapsulation in a variety of liposomal and polymeric drug carriers[34]. While these modifications have improved circulation time, many simultaneously impede clot permeation and accessibility to fibrin. Correspondingly, none of these approaches have proven to have a decisive advantage over t-PA in the treatment of acute stroke[56].

The general lesson appears to be that targeting of macromolecular biotherapeutics may be quite different from the delivery of inherently toxic, small molecule drugs, especially in applications unrelated to cancer. Characteristics which may be ideal for an ADDS carrying doxorubicin or paclitaxel, such as prolonged circulation time and impaired entry into normal tissues, may be disadvantageous in the delivery of biotherapeutics. Attachment to targeting ligands, polymers, or stealth agents (e.g. PEG) may impair access to the necessary site of action or block partnering with cofactors. Until technology is developed to precisely localize biotherapeutics and optimize their interaction with endogenous partners, the clinical development of numerous candidate drugs will be stifled, and the translation of many scientific discoveries will remain impossible.

II. Developing Therapeutics for Acute Vascular Disorders

The obstacles encountered in the development and clinical testing of recombinant fibrinolytics demonstrate the enormous challenges which face the scientific and medical community in designing therapeutics for the treatment of acute vascular disorders. Cardiovascular disease is already the most common cause of death in industrialized nations, and its incidence is on the rise[57]. The acute manifestations are typically unforeseeable and life-threatening, meaning that candidate therapeutics must work after the onset of symptoms, achieve rapid efficacy, and demonstrate limited off-target side effects. The most severe vascular disorders, including sepsis, acute lung injury, and post-traumatic multi-organ failure, have been labeled “critical illnesses”, owing to the lack of disease-specific therapies and reliance on sophisticated supportive measures in treating afflicted patients[58]. Despite substantial improvements in emergency and intensive care, the morbidity and mortality of these conditions has remained essentially unchanged[59,60].

Endothelial cells: a critical target

The vascular endothelium, once thought to be a passive barrier between blood and tissue, is now recognized to have an important role in many of these same diseases in which the medical field has struggled to achieve improved outcomes[61–63]. Endothelial cells (ECs) project a variety of protein complexes into the vascular lumen, which interact with circulating blood components and allow ECs to sense and respond to changes in flow, coagulation, nutrient delivery, and inflammation[64,65]. In the last several decades, scientists have elucidated a variety of endothelial mechanisms, which help to maintain blood fluidity, control vascular tone and permeability, and regulate the innate immune response[66]. Advances in tissue culture have allowed the study of these mechanisms not only at rest, but under different patterns of flow[67]. Molecular biology has enabled the identification of many of the proteins involved in these protective pathways, as well as variations in their level of expression in segments of the vasculature

exposed to high or low shear stress. Finally, the creation of endothelial-specific genetic modifications in animals and the identification of disease-linked polymorphisms in patients have provided insight into the relative importance of these endothelial pathways in human disease[68–70].

Despite the enormous accumulation of knowledge regarding endothelial biology, physicians and scientists remain largely unable to influence the endothelial mechanisms known to play a part in acute vascular disorders in humans. Only a small number of drugs have significant effects on ECs and those that do typically have little endothelial specificity (e.g. non-steroidal anti-inflammatory drugs), require complex regimens of administration (e.g. epoprostenol)[71], or are meant for the treatment of chronic conditions like systemic hypertension (e.g. angiotensin converting enzyme-inhibitors). Biotherapeutics, in particular, tend to have no innate affinity for the endothelium, and only a tiny fraction of administered dose is typically retained at the vascular margin. While the field of drug targeting has begun to take an interest in endothelial delivery, efforts have focused on directing therapeutics to tumor-associated neovasculature[72]. Only a small number of investigators have prioritized the delivery of biotherapeutics to normal ECs, and limited capacity exists to target specific vascular beds or areas of endothelial activation[73–76].

The Protein C pathway and its role in acute vascular disease

Amongst the endogenous endothelial systems considered for pharmacologic intervention, the protein C pathway has attracted perhaps the most intense interest, in part because of its involvement in the coagulation cascade, the innate immune response, and the control of vascular permeability[77]. The existence of protein C (PC) was first predicted in 1970 by Ewa Marciniak, who described a “coagulation inhibitor elicited by thrombin”[78]. In 1976, this factor was identified as vitamin K dependent and named “protein C” by Johan Stenflo, because it was present in the third major peak eluted off of an anion exchange column following the barium citrate adsorption of bovine plasma[79]. Like other

vitamin K-activated, gamma-carboxyglutamate (Gla) containing factors, PC was found to be a zymogen, cleavable by thrombin and Russell's viper venom[80]. Unlike other coagulation zymogens, however, the majority of PC could be recovered in serum[81]. Indeed, its slow rate of activation in clotting assays led Charles Esmon to search for an endothelial cofactor capable of accelerating the generation of activated protein C (APC). By perfusing discarded pig's ears (collected from a local slaughterhouse) with thrombin and PC, Esmon discovered that such a cofactor was present, and subsequent efforts led to the isolation of thrombomodulin (TM)[82].

TM was ultimately characterized as an endothelial transmembrane glycoprotein capable of altering the enzymatic specificity of thrombin. When bound to TM, thrombin no longer activates fibrinogen, Factor V, or platelets, but instead generates APC[83]. Although it is often thought of as an anticoagulant, TM differs substantially from molecules like antithrombin, heparin, hirudin, and the new direct thrombin inhibitors (e.g. dabigatran). Rather than simply inhibiting thrombin activity, TM couples it to the generation of APC, which has anti-inflammatory, anti-apoptotic, and endothelial barrier stabilizing activity, in addition to anticoagulant functions. The importance of the protein C pathway is demonstrated by the uniform lethality of homozygous protein C deficiency, which manifests as neonatal purpura fulminans[84]. No genetic form of human TM deficiency exists, presumably due to embryonic lethality. In fact, even mice homozygous for a single point mutation in TM, which disrupts thrombin binding, have a severe prothrombotic and hyperinflammatory phenotype[85].

The role of the protein C pathway in maintaining homeostasis is also demonstrated, albeit in less absolute terms, by the nearly universal finding of endothelial TM deficiency in the presence of human vascular disease. Loss of TM has been demonstrated in nearly every condition involving acute or chronic vascular inflammation, from sepsis and ischemia/reperfusion injury to atherosclerosis and diabetic neuropathy[86–89]. In addition to transcriptional downregulation, there is evidence to suggest that TM is internalized, inactivated,

and cleaved from the endothelial membrane in these conditions. A wide variety of mediators have been implicated, including cytokines, reactive oxygen species, and neutrophil-derived proteases[90–93]. Given its pervasive nature, it seems likely that this process must have conferred a selective advantage in some evolutionary situations, such as localized infection or trauma. In the context of contemporary human medicine, however, loss of endothelial TM is no longer advantageous and has become an important component of the pathogenesis of numerous vascular diseases.

In addition to TM and PC, a third molecule, the endothelial protein C receptor (EPCR), has a critical role in the protective functions of this system. APC generation by the TM/thrombin complex is accelerated between 5 and 20 fold when PC is bound to EPCR, depending on whether measurements are made *in vitro* or *in vivo*[94,95]. Moreover, EPCR appears to play a central role in mediating the anti-inflammatory, anti-apoptotic, and barrier stabilizing effects of APC[84]. Although EPCR has a short cytoplasmic tail and no direct intracellular signaling activity, it co-localizes with the protease-activated receptor 1 (PAR1) in caveolin-1 rich microdomains and participates in its activation by APC[96]. Specifically, APC must be bound to EPCR to cleave PAR1[97]. Some *in vitro* experiments indicate a second mechanism of protective signaling through PAR1, in which the specificity of thrombin is altered when EPCR is occupied by PC, switching it from a pro-inflammatory to anti-inflammatory signal[98]. The APC/EPCR complex also appears to signal through additional receptors, including the sphingosine-1-phosphate receptor (S1PR) and PAR3[99–101]. Like TM, EPCR is cleaved from the endothelial membrane in the presence of systemic inflammation. Plasma levels of a soluble form of EPCR (sEPCR) are elevated in human sepsis and a variety of autoimmune disorders and correlate with the severity of underlying disease[102–104]. *In vitro* studies indicate that a matrix metalloprotease is responsible for EPCR cleavage and that release of sEPCR is stimulated by inflammatory mediators, reactive oxygen species, and coagulation factors[105].

Studies with genetically modified mice have confirmed the role of EPCR in mediating protective effects of the protein C pathway *in vivo*. These results are particularly significant because of the distinct tissue distribution of TM and EPCR, the former predominantly found on capillaries and smaller vessels and the latter with higher expression on large vessels[106]. These differing patterns of expression have led to questions about the importance of EPCR and its partnering with TM *in vivo*. Nonetheless, EPCR is clearly involved in mediating protective effects, based on observations that mice with genetically-induced EPCR deficiency (~10% of normal expression levels) are more susceptible to endotoxemia than wild type controls, whereas animals with endothelial-specific overexpression of EPCR (150 times normal expression levels) are markedly more resistant[69,107]. One theory is that the level of colocalization of TM, EPCR, and PAR1 might vary depending on the vascular bed examined, and that this might explain the overall importance of this signaling pathway, despite distinct patterns of expression noted in some organs[84]. Consistent with this idea, one recent study investigated the importance of EPCR in maintaining endothelial barrier function in various organs and found significant variation depending on the vascular bed involved[108]. Figure 1.1 shows the major components of the Protein C Pathway, in schematic form, and their primary functions at the luminal endothelial cell membrane.

III. Biotherapeutic Interventions into the Protein C Pathway

Multiple approaches have been proposed to reverse the pathogenic suppression of the protein C pathway, including endothelial gene therapy and the infusion of recombinant proteins. The former approach has intuitive appeal and has provided proof-of-principle for replenishing endothelial TM[109–111], and potentially EPCR as well. Nonetheless, it requires the site-specific delivery of siRNA or other genetic material – not only to endothelial cells, but a specific compartment of the EC cytoplasm. As alluded to above, significant technological limitations exist which make gene therapy unrealistic, except in rare clinical

contexts (e.g. *ex vivo* viral transduction of ECs in harvested vein segments prior to bypass grafting)[112]. Even if the technical limitations are overlooked, temporal considerations are unlikely to permit this approach in the treatment of emergent conditions like sepsis, stroke, and acute lung injury.

Xigris® and other recombinant proteins

In 1987, Taylor and Esmon reported that recombinant human APC (rhAPC) protected baboons from an otherwise lethal infusion of bacteria[113]. The timing of this discovery was fortuitous, coinciding not only with the emergence of biotherapeutics as a viable class of pharmaceuticals, but also the recognition of systemic inflammation and derangements in coagulation as important components of human sepsis[114]. rhAPC was developed by the pharmaceutical industry and became one of a number of recombinant proteins tested in septic patients in the late 1990s. Ultimately, the phase III PROWESS trial demonstrated a survival benefit in patients randomized to rhAPC (28-day mortality of 24.7% vs. 30.8% with placebo), and led to the FDA approval of drotrecogin alfa (rhAPC), or Xigris®[115]. Unfortunately, as in the case of recombinant t-PA, poor pharmacokinetics severely limited its clinical utility. In fact, the similarities to t-PA are striking: rhAPC is rapidly cleared (the plasma half-life of free APC is approximately 13 minutes)[116] and inactivated by a circulating inhibitor, and these factors led to the decision to administer the drug via continuous infusion. This in turn increased the cost and risk of life-threatening hemorrhage, and ultimately, the drug was withdrawn from the market when its risks were shown to outweigh any potential benefit[117].

A variety of efforts have been made to replicate the beneficial effects seen with rhAPC, while avoiding its negative characteristics. Genetically modified forms have been created which demonstrate reduced inactivation of Factors Va and VIIIa[118]. These mutants lack the anti-coagulant and pro-fibrinolytic effects of wild type APC, while preserving other beneficial activities. In fact, the lack of anti-coagulant effect actually results in indirect anti-inflammatory

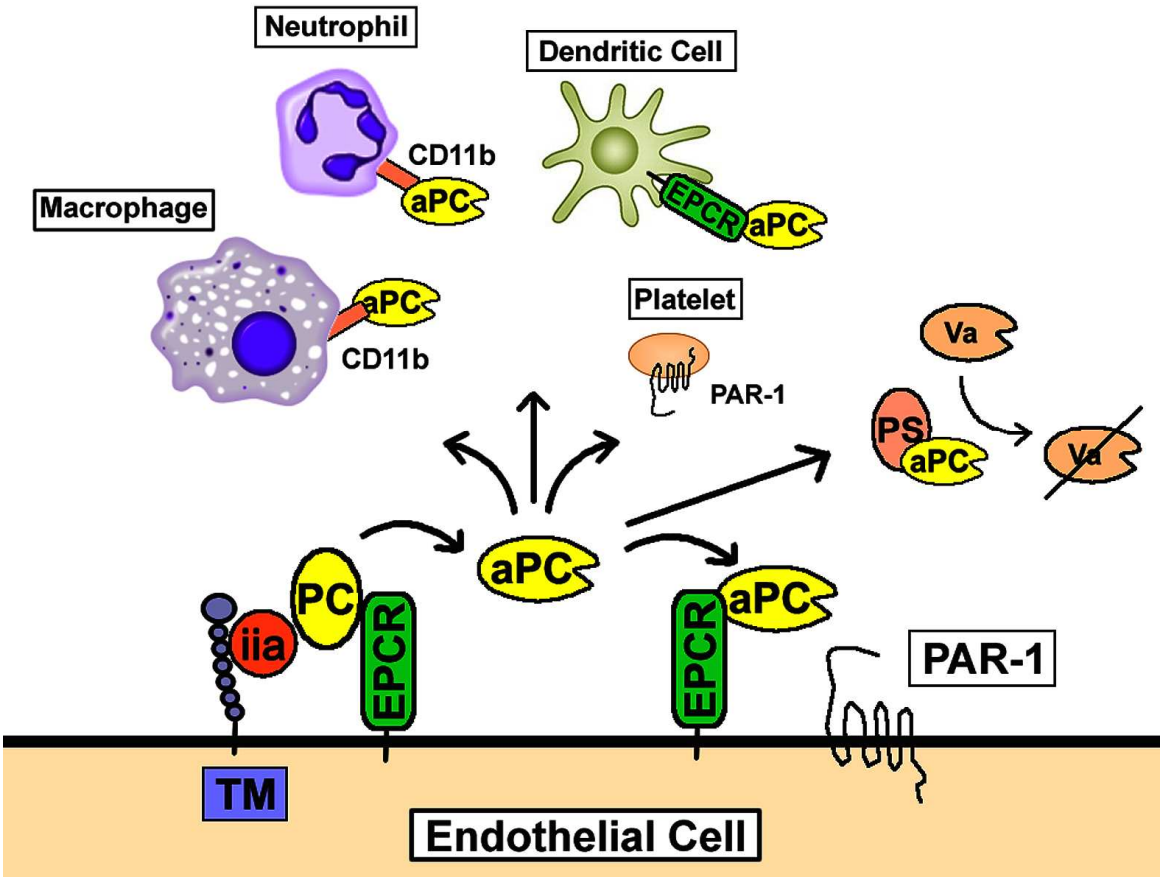

Figure 1.1. The Protein C Pathway

Protein C bound to EPCR is activated at the endothelial membrane by the thrombin-TM complex. Resultant APC may remain bound to endothelial EPCR, activating PAR-1 and other receptors, or it may exert a variety of other effects, amongst them inhibition of the coagulation cascade (via Protein S-dependent cleavage of Factors Va and VIIIa) and modulation of immune cell (neutrophil, macrophage, and dendritic cell) functions.

actions not seen with rhAPC, due to the increased generation of thrombin and activation of the thrombin-activatable fibrinolysis inhibitor (TAFI). In addition to blocking the efficient activation of plasmin, TAFI inhibits bradykinin and the anaphylatoxins C3a and C5a[119], both of which contribute to the systemic inflammatory response. Although these genetic modifications may address some of the limitations of rhAPC[120], the modified drugs still face significant pharmacokinetic challenges and their ability to succeed in the clinical realm has yet to be determined.

Another strategy for augmenting the protein C pathway is the infusion of soluble forms of TM. Unlike infusion of an activated zymogen, soluble TM (sTM) reproduces some of the "on demand" nature of the endogenous protein C pathway, generating a biological effect primarily at sites of thrombin generation[121]. Genetic modifications have been made to sTM to separate the function of its domains, prolong circulation time, and prevent inactivation by reactive oxidant species[93,122,123]. While preliminary studies in animal models and early stage human clinical trials have demonstrated beneficial effects[124–126], sTM and its derivatives fail to reproduce a key aspect of the protein C pathway, its localization to the endothelial membrane. Although improper localization in this case may not be as significant as it is with siRNA or other biotherapeutics, it does prevent the interaction of recombinant TM with a key cofactor, the endothelial protein C receptor (EPCR).

Endothelial targeted biotherapeutics

Endothelial targeting of recombinant TM was first reported by our laboratory in 2008[127]. To anchor sTM to the luminal membrane, its natural location and (presumably) site of optimal activity, it was fused to a PECAM-1-specific single chain antibody fragment, 390 scFv. The 390 scFv/TM fusion protein was found to bind to immobilized PECAM-1 *in vitro* and to lung ECs following IV injection. Mice treated with 390 scFv/TM were protected from both

ischemic and inflammatory lung injury, without the bleeding side effects seen with equipotent doses of recombinant mouse APC[127].

While the ability of endothelial-anchored 390 scFv/TM to partner with endogenous EPCR was not tested in these initial experiments, studies conducted in the field of biomaterials suggested that this would be an important question. Material scientists have long taken an interest in the protein C pathway as a potential means of preventing the activation of the immune system and coagulation cascade on implantable medical devices[128]. TM has been immobilized on polyurethane, PEG-modified glass, and even liposomes[129–131]. In 2006, one group reported *in vitro* flow studies utilizing a membrane-mimetic material, which had been functionalized with phospholipids and TM. The rate of APC generation was measured following the perfusion of thrombin and PC. At relatively low TM surface density, increases in TM surface content accelerated APC production. Beyond a certain critical TM density, however, a plateau was reached and further increases in TM surface content had no effect[132]. This finding was attributed to a limitation in protein C availability at the surface, presumably due to the absence of EPCR. Subsequent efforts achieved higher rates of APC generation via co-immobilization of TM and EPCR, but the effect was only seen if the recombinant proteins were in close proximity (< 10nm). Random, unordered distribution of TM and EPCR was not effective[133]. This potentially stringent requirement for proximity between TM and EPCR gave rise to several important questions regarding the potential partnering of EC-anchored 390 scFv/TM and endogenous EPCR.

IV. Scope of the Dissertation

As indicated above, the primary goal of targeting recombinant TM to the endothelial membrane has been to optimize its activity by allowing for partnering with endogenous cofactors. As of 2009, it remained unknown to what extent 390 scFv/TM was able to take advantage of its localization. There were three

questions, in particular, which we wanted to answer, and which form the basis of this dissertation:

1) Is thrombin bound to membrane-anchored scFv/TM capable of interacting with PC bound to EPCR?

There were two reasons for concern that partnering between scFv/TM and EPCR might not be possible. The first was related to the design of the 390 scFv/TM fusion protein, which was constructed with the scFv moiety on the N-terminal end and the sTM moiety on the C-terminal end (figure 1.2a). While this design was chosen for technical reasons (prior data suggested that 390 scFv may not bind to PECAM-1 if a large cargo protein like TM was fused to its N-terminus), it left the sTM moiety in an "inverted" conformation. The N-terminal lectin domain of TM is typically the most distal to the membrane, with the six EGF-like domains, including the thrombin-binding site (EGF-like domains 5 and 6), more proximal. In contrast, the lectin domain in the fusion is adjacent to the scFv and the EGF domains may be further from the membrane, depending on the exact conformation the protein takes after binding to PECAM-1 (figure 1.2b).

The second, and somewhat related, reason for concern was that the combination of the scFv moiety and PECAM-1 might introduce too much distance between recombinant TM and the surface membrane to allow access to PC and EPCR (Figure 1.2b). Some separation from the plasmalemma is known to be required for full activity of the thrombin/TM complex, which sits approximately 65Å from the cell surface[134]. Specifically, this was studied in a series of experiments, in which the Ser/Thr rich region of TM (which is positioned immediately adjacent to the membrane) was replaced by polypeptides of varying length. Decreasing the size of this spacer progressively diminished thrombin binding and protein C activation, suggesting that the active site is optimally held at a certain distance from the membrane[135]. Nonetheless, the interposition of

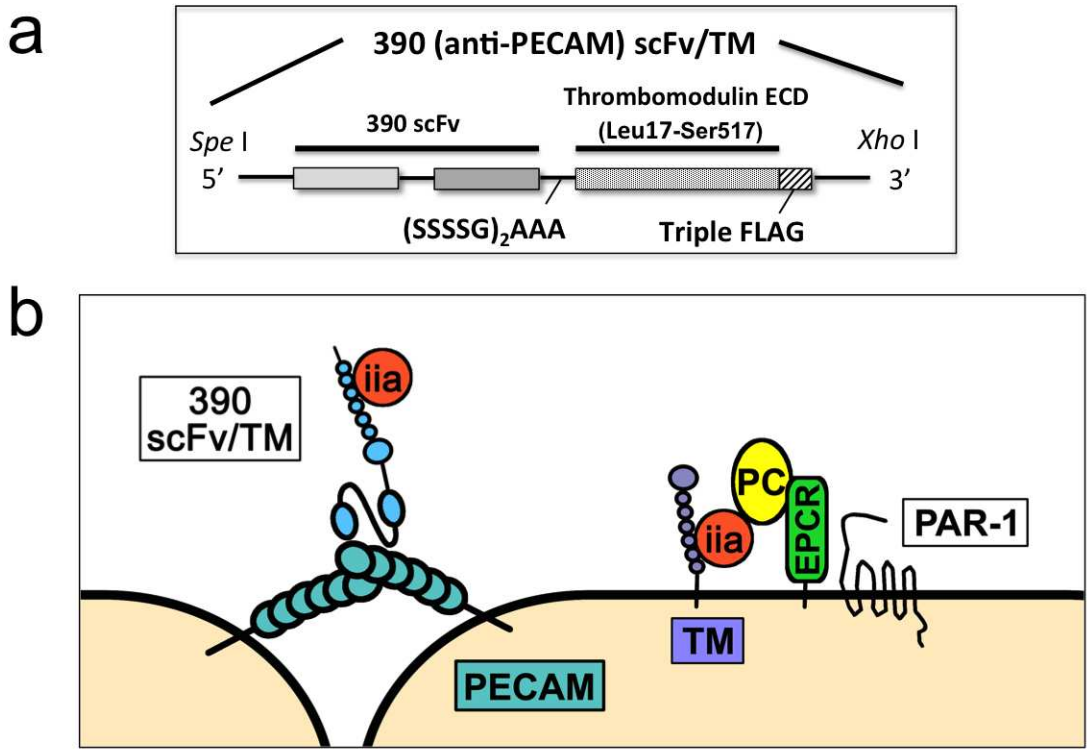

Figure 1.2. Schematic depiction of 390 scFv/TM molecular design and positioning vs. endogenous TM

(a) sTM moiety was placed on 3', or C-terminal, end. (b) The "inverted" conformation of the sTM moiety, its distance from the plasmalemma, and its localization to cell-cell junctions could all impair partnering with endogenous EPCR.

PECAM-1 and the 390 scFv might introduce a significantly greater distance than 65Å, and the effect of this displacement on partnering with EPCR was unknown.

2) Assuming the thrombin-scFv/TM complex is physically capable of interacting with PC-EPCR, do differences in the distribution of PECAM-1 and EPCR along the EC membrane prevent effective enzymatic partnering?

PECAM-1 on ECs is predominantly localized to cell-cell junctions[136,137], whereas endogenous TM and EPCR are believed to be concentrated in lipid rafts in the endothelial apical plasmalemma[96,138]. Based the results of the previously described experiments involving co-immobilization of TM and EPCR on artificial surfaces, there was concern that PECAM-anchored TM might have insufficient proximity to allow effective partnering with EPCR (figure 1.2b).

Chapter 2 details our experimental approach to these first two questions. We describe an assay for measuring the activation of PC by cell membrane-bound TM fusion proteins. We use this method to show that 390 scFv/TM is capable of partnering with EPCR, at least while anchored to the membrane of non-endothelial cells, engineered to overexpress mouse PECAM-1 and EPCR. In contrast, experiments on mouse ECs indicate that PECAM-anchored 390 scFv/TM is largely unable to partner with EPCR, at least in comparison to endogenous TM.

3) What approaches can be designed to allow or improve enzymatic partnering between EC-anchored scFv/TM and EPCR (without compromising therapeutic delivery)?

In the light of the results presented in Chapter 2, two strategies were developed for enhancing enzymatic partnering between endothelial-targeted TM and EPCR. The implementation and validation of these approaches are discussed at length in Chapters 3 and 4.

CHAPTER TWO: PECAM-BOUND scFv/TM – MEASUREMENT OF PROTEIN C ACTIVATION AND PARTERING WITH EPCR

I. INTRODUCTION

As discussed in Chapter 1, vascular immunotargeting of drugs involves conjugation or recombinant fusion to specific affinity ligands of determinants on the luminal surface of ECs. Although in the past it has been thought of as a strategy for controlling and altering pharmacokinetics, its application to biotherapeutics is primarily intended to precisely localize drugs and allow optimal interaction with endogenous partners. Indeed, the primary justification for targeting recombinant TM to ECs, reported by our lab in 2008, was not one of pharmacokinetics[127]. Other means exist for achieving prolonged circulation of sTM, including subcutaneous injection, chemical modification (e.g. PEGylation), genetic alteration (e.g. solulin), and attachment to blood cells[139–141]. While these therapeutics are systemic and cannot be directed to one organ in particular, the fact that sTM activates PC only at sites of thrombin generation "localizes" its effect to sites of inflammation or thrombosis.

Given that endothelial targeting of TM was primarily motivated by potential partnering with EPCR and other endogenous cofactors, our group had great interest in determining if such interaction was possible. To address these questions, we developed an assay for measuring the activation of protein C by cell-bound 390 scFv/TM and utilized this method to determine the extent of partnering with EPCR.

II. RESULTS

Studies on Non-Endothelial REN Cells

The human mesothelioma cell line REN is a useful model system, with no expression of mouse PECAM, ICAM, TM, or EPCR at baseline. REN-PECAM

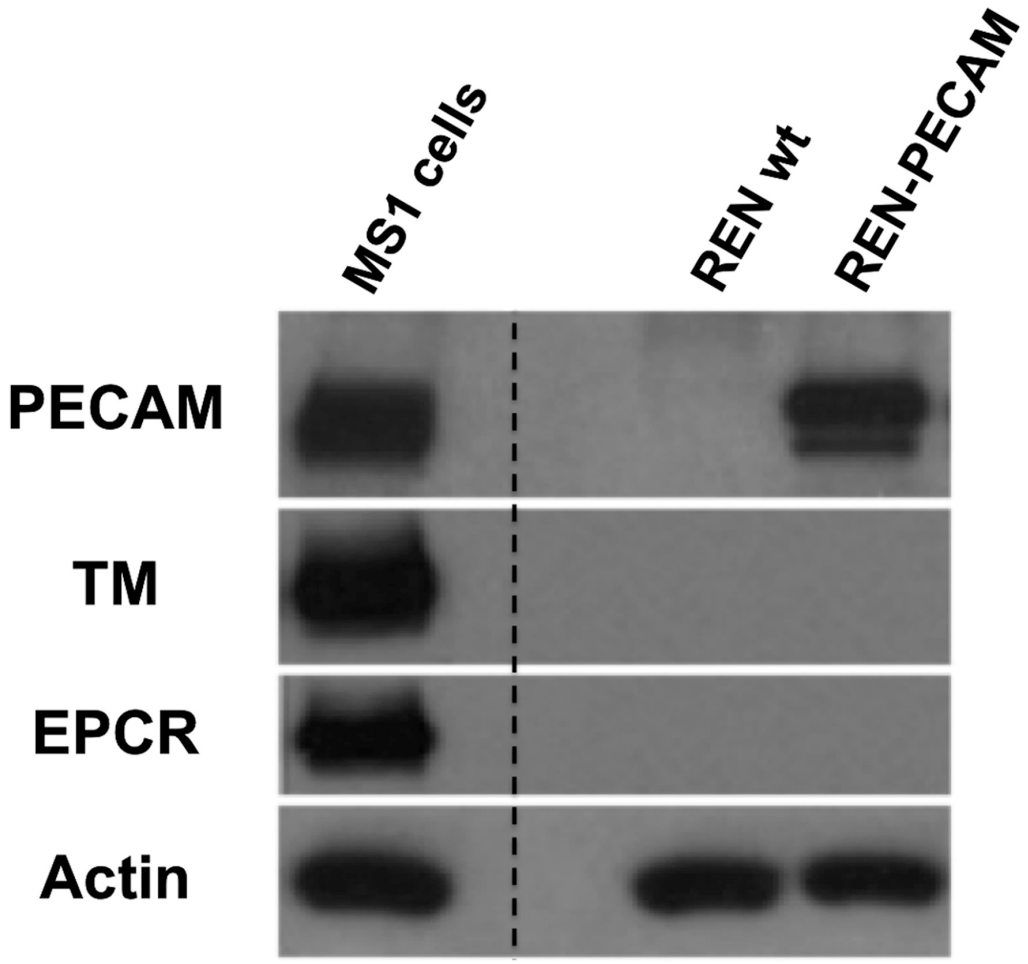

Figure 2.1. Non-endothelial REN cell system
Western blot demonstrating expression of mouse endothelial proteins on REN cells (wt = wild type) and stably transfected REN-PECAM cells, with MS1 mouse endothelial cells included for comparison.

cells, which stably express mouse PECAM-1, have been utilized in our laboratory extensively (Figure 2.1)[142,143].

Binding and functional activity of 390 scFv/TM on PECAM-expressing REN cells

Both 390 scFv and 390 scFv/TM fusion protein demonstrated nanomolar affinity to REN-PECAM cells. Little or no non-specific binding was seen to wild type REN cells (Figure 2.2a,b). For the next series of experiments, we developed an assay for measuring the activation of protein C by TM fusion proteins bound to the surface of REN cells. 390 scFv/TM demonstrated dose-dependent, thrombin-mediated activation of protein C on REN-PECAM cells, but not on wild type REN cells (Figure 2.3). Recombinant sTM was used as an additional control and showed no activity on either cell type.

EPCR expression potentiates the functional activity of 390 scFv/TM bound to REN-PECAM cells

Having determined the baseline rate of protein C activation by REN cell-bound 390 scFv/TM, we next assessed its ability to partner with EPCR in the membrane. To achieve this, EPCR expression was induced on REN-PECAM cells, producing the stable cell line REN-PECAM-EPCR. Expression of EPCR was confirmed by western blotting (Figure 2.4). Expression of EPCR expression resulted in ~4-fold enhancement of thrombin-mediated APC generation by 390 scFv/TM (Figure 2.5a). To confirm that this effect was dependent on EPCR, we utilized a monoclonal antibody that blocks the binding of PC to murine EPCR and thereby inhibits its ability to accelerate APC production by the thrombin-TM complex[69]. Treatment with this antibody resulted in approximately 75% reduction in APC generation (Figure 2.5b).

Studies on Mouse Endothelial Cells

EPCR expression on MS1 cells vs. REN-PECAM-EPCR cells

While transfected REN cells are convenient for studying TM fusion

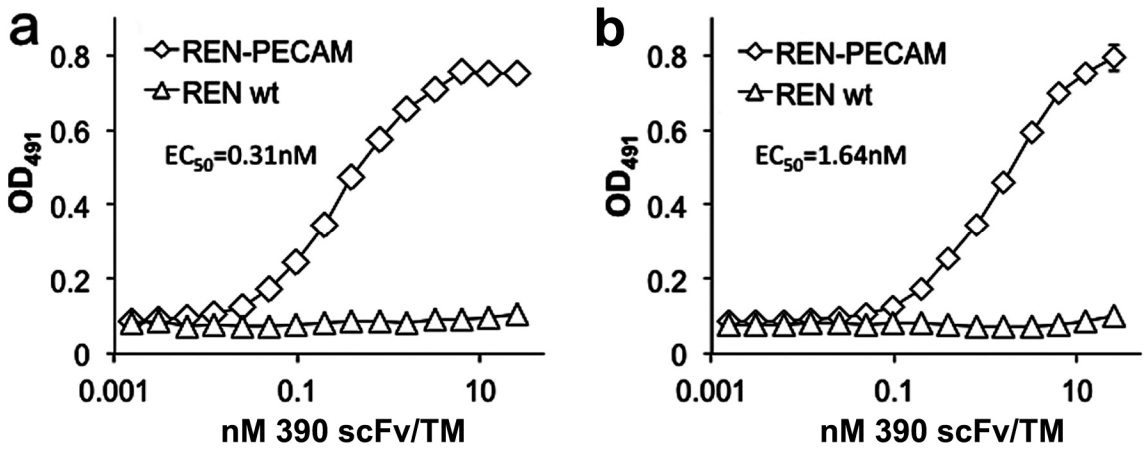

Figure 2.2. Binding of 390 scFv and scFv/TM to REN-PECAM cells
Cell based ELISAs show binding of (a) 390 scFv and (b) 390 scFv/TM fusion protein to PECAM expressing REN cells. No significant binding is seen to wild type REN cells. Experiments were done in triplicate (each point shown represents three wells). SD are shown but too small to be seen in most cases. EC50 is shown for each curve.

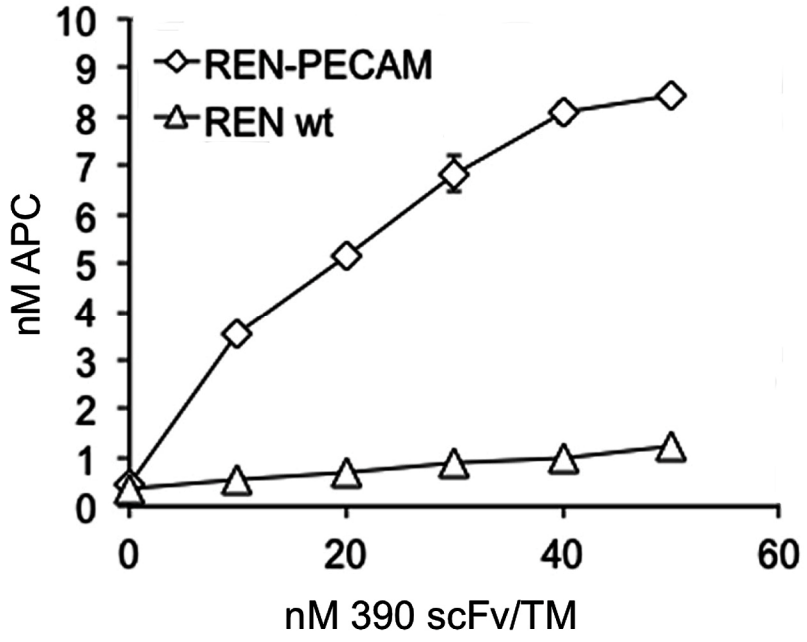

Figure 2.3. APC generation by 390 scFv/TM on REN-PECAM cells
390 scFv/TM activates protein C while bound to PECAM-expressing cells. Minimal APC is generated on wild type REN cells, presumably due to lack of binding. All experiments were done in triplicate. Data shown are mean ± SD.

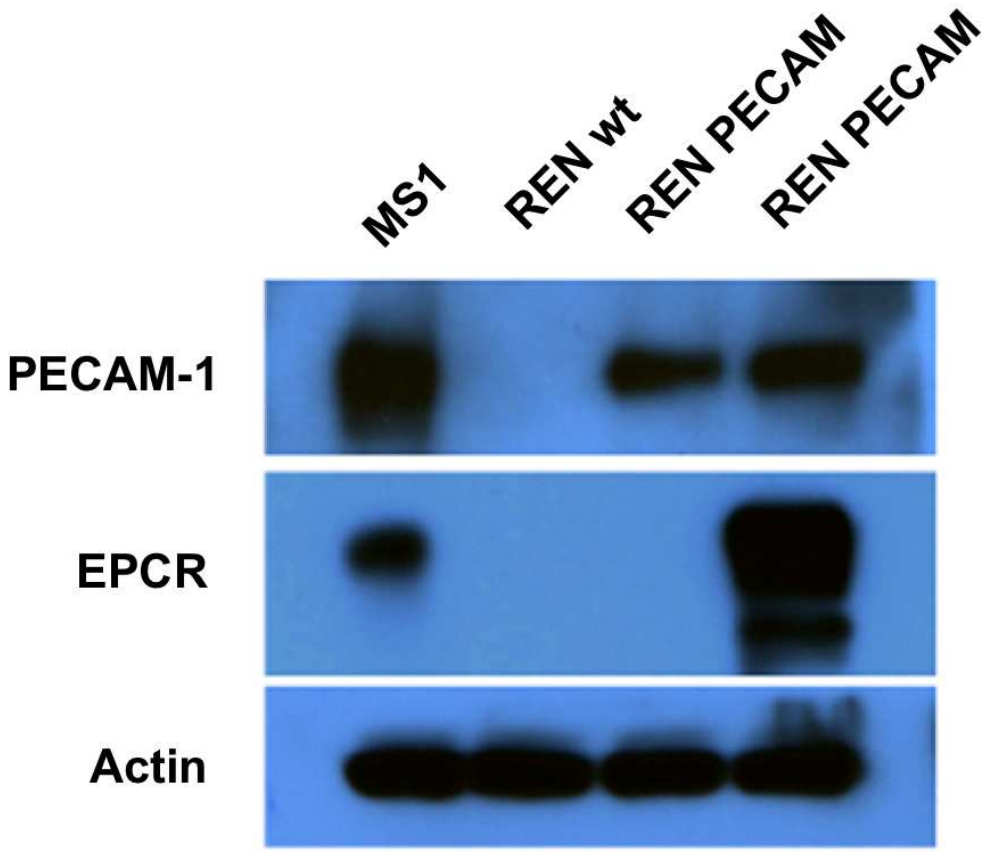

Figure 2.4. Creation of REN cells stably expressing PECAM and EPCR
Western blot of REN-PECAM-EPCR cells, which stably overexpress mouse EPCR. REN wt, REN-PECAM, and MS1 endothelial cells included as comparison.

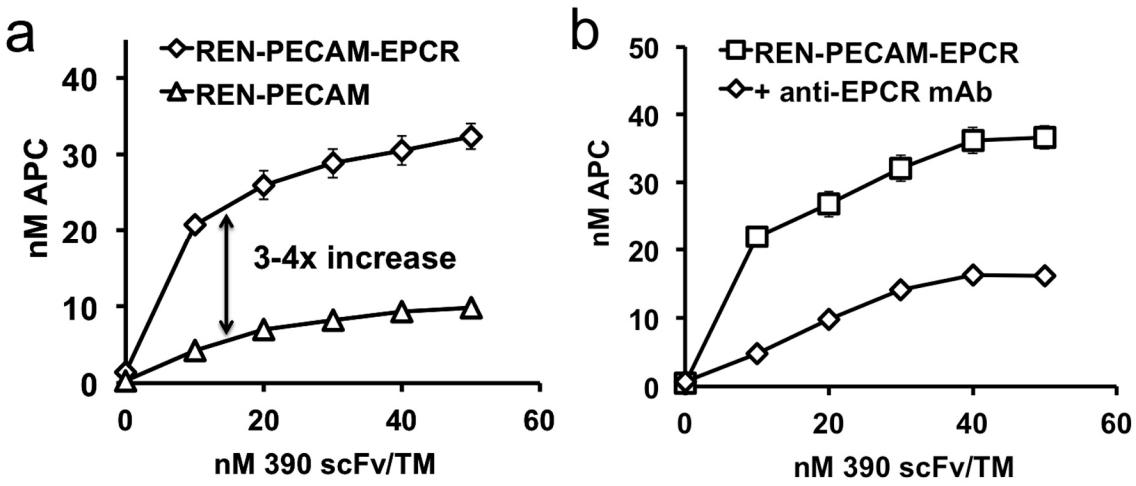

Figure 2.5. APC generation by 390 scFv/TM on REN-PECAM-EPCR vs. REN-PECAM cells

(a) A ~4-fold increase in APC generation is seen when 390 scFv/TM is anchored to REN-PECAM-EPCR cells, as compared to EPCR-negative counterparts. Differences between groups were highly significant ($p < 0.001$) at all (non-zero) doses of 390 scFv/TM fusion protein. (b) Cells treated with anti-EPCR mAb1560, which blocks protein C binding to EPCR, show ~75% reduction in APC generation. Differences between groups were highly significant ($p < 0.001$) at all (non-zero) doses of fusion protein. All experiments were done in triplicate. Data shown are mean ± SD, error bars too small to be seen at some points.

proteins, they clearly represent an artificial system, in which the surface expression and distribution of PECAM, ICAM, and EPCR do not necessarily reflect what is present on endothelial cells. For example, radioimmunoassays performed using ^{125}I-labeled anti-EPCR revealed that the number of binding sites on REN-PECAM-EPCR cells is an order of magnitude higher than on MS1 mouse endothelial cells (Figure 2.6).

Binding of 390 scFv/TM to MS1 endothelial cells

390 scFv/TM demonstrated specific binding to PECAM-1, as evidenced by near complete inhibition of binding by a 10-fold excess of parental 390 mAb (Figure 2.7). Calculated affinity constants were similar to those seen in previous experiments using REN-PECAM cells.

Suppression of endogenous TM on MS1 cells

Measuring the activity of 390 scFv/TM while bound to MS1 cells proved to be substantially more complicated than on REN cells, due to high level of expression of endogenous TM. These cells express endogenous TM at high level in a stable fashion resistant to agents that typically suppress its level in endothelium (e.g., TNF and other cytokines). To measure fusion protein-specific APC generation on endothelial cells, we experimented with several methods of suppressing the activity of endogenous TM. The first of these methods utilized mouse TM-specific siRNA. Although western blotting demonstrated robust suppression of TM levels, relatively high levels of lipid transfecting reagent were required (Figure 2.8a). The cells were damaged in this process and inevitably lifted off gelatinized 24 well plates during the repeated washes of the APC generation assay. We subsequently transfected MS1 cells with a TM-specific shRNA vector containing the puromycin resistance gene. Stably transfected cells were selected and maintained in puromycin. Unfortunately, western blotting demonstrated no difference in the expression of mouse TM in shRNA-transfected vs. wild type cells (Figure 2.8b).

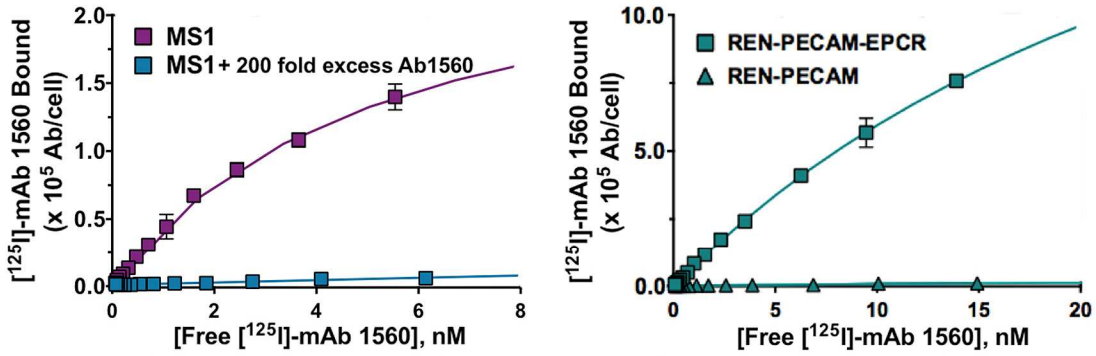

Cells	K_d (nM)	B_{max} (Ab/cell)
MS1	5.3	2.7×10^5
REN-PECAM-EPCR	32.4	2.5×10^6

Figure 2.6. Quantification of EPCR on ECs vs. REN-PECAM-EPCR cells
(a) Radioimmunoassays of ^{125}I-labeled anti-EPCR antibody (mAb1560). (b) Summary of anti-EPCR binding parameters on each cell type. Radioimmunoassays were done in quadruplicate (i.e. each data point represents 4 wells of cells). Data shown are mean ± SD.

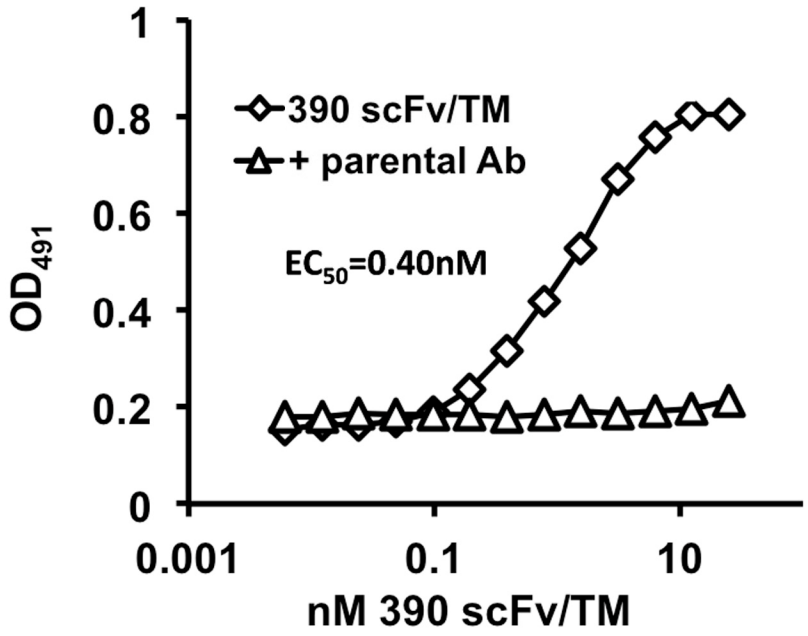

Figure 2.7. Binding of 390 scFv/TM to MS1 mouse ECs
Specificity is demonstrated by inhibition of binding by 10-fold excess of parental 390 mAb. All experiments were done in triplicate (i.e. each data point represents 3 wells of cells). Data shown are mean ± SD, error bars too small to be seen at some points.

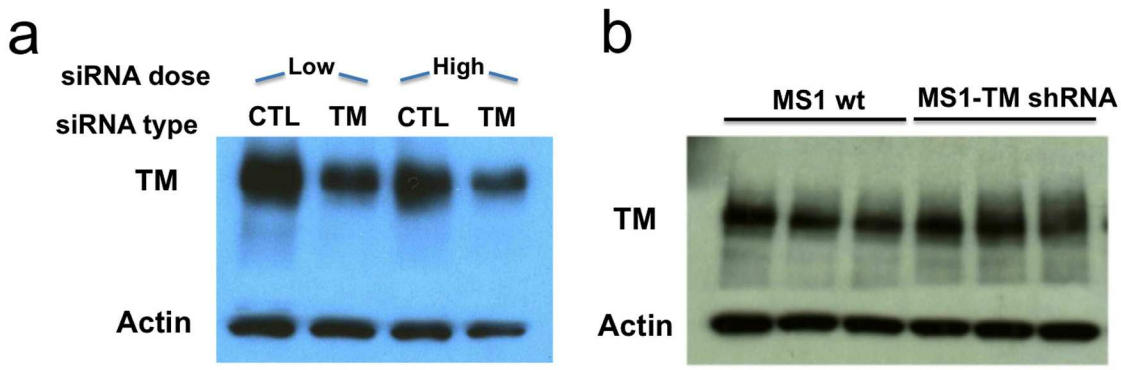

Figure 2.8. Attempts to knockdown endogenous TM on MS1 cells
(a) Mouse TM specific siRNA effectively suppressed TM, especially at high doses. Unfortunately, cell toxicity made APC generation assays technically impossible. (b) Stable transfection of a mouse TM specific shRNA did not result in effective knockdown, despite antibiotic selection.

Isolation of lung microvascular endothelial cells from TM$^{pro/pro}$ mice

TM$^{pro/pro}$ mice are homozygous for a single amino acid mutation, Glu404→Pro, in the interdomain loop between the fourth and fifth EGF-like domains of TM. This mutation results in a 75% reduction in the level of expression of TM in lung homogenates, a ~100-fold reduction in thrombin binding, and a ~1000-fold reduction in the rate of APC generation[144]. We reasoned that TM$^{pro/pro}$ ECs would provide an ideal system for testing activation of protein C by EC-bound 390 scFv/TM. Accordingly, lung endothelial cells were isolated from TM$^{pro/pro}$ mice. The cells were grown to passage 4 (Figure 2.9a) and tested for the binding of 390 scFv/TM. Unfortunately, no binding was seen on TM$^{pro/pro}$ ECs, in contrast to MS1 cells (Figure 2.9b).

Blockade of endogenous TM on MS1 cells

Another strategy employed to suppress the activity of endogenous TM was that of antibody blockade. A variety of anti-mouse TM (mTM) antibodies were screened for their ability to block thrombin binding and APC generation, with PPACK-inactivated thrombin used as a positive control. While several anti-mTM mAbs had no effect, a polyclonal anti-mTM antibody was able to fully inhibit APC generation (Figure 2.10a). Unlike PPACK-thrombin, the polyclonal antibody had a sustained effect after washing (Figure 2.10b). Sustained blockade of 60-70% of endogenous TM activity, provided by anti-TM antibody, enabled measurement of dose responsive, 390 scFv/TM-dependent protein C activation (Figure 2.10c).

Functional activity of EC-bound 390 scFv/TM and lack of EPCR partnering

We employed anti-mTM antibody blockade to assess protein C activation by 390 scFv/TM anchored to MS1 cells. Since the expression of PECAM-1 on ECs is more than an order of magnitude higher than that of TM (10^6 copies/cell vs. $4x10^4$ copies/cell)[145,146], we expected that saturating concentrations of 390 scFv/TM (e.g. 40nM based on enzyme-linked Immunosorbent assays, ELISAs)

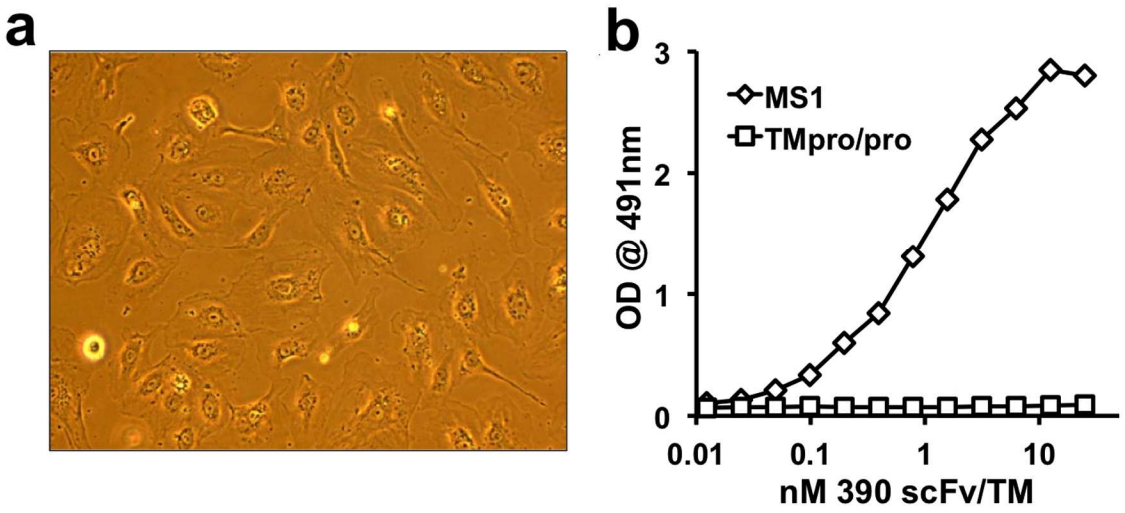

Figure 2.9. Isolation and culture of lung ECs from $TM^{pro/pro}$ mice
(a) Phase contrast image of isolated ECs. (b) Cell-based ELISA demonstrated binding of 390 scFv/TM to MS1 cells, but not isolated $TM^{pro/pro}$ cells.

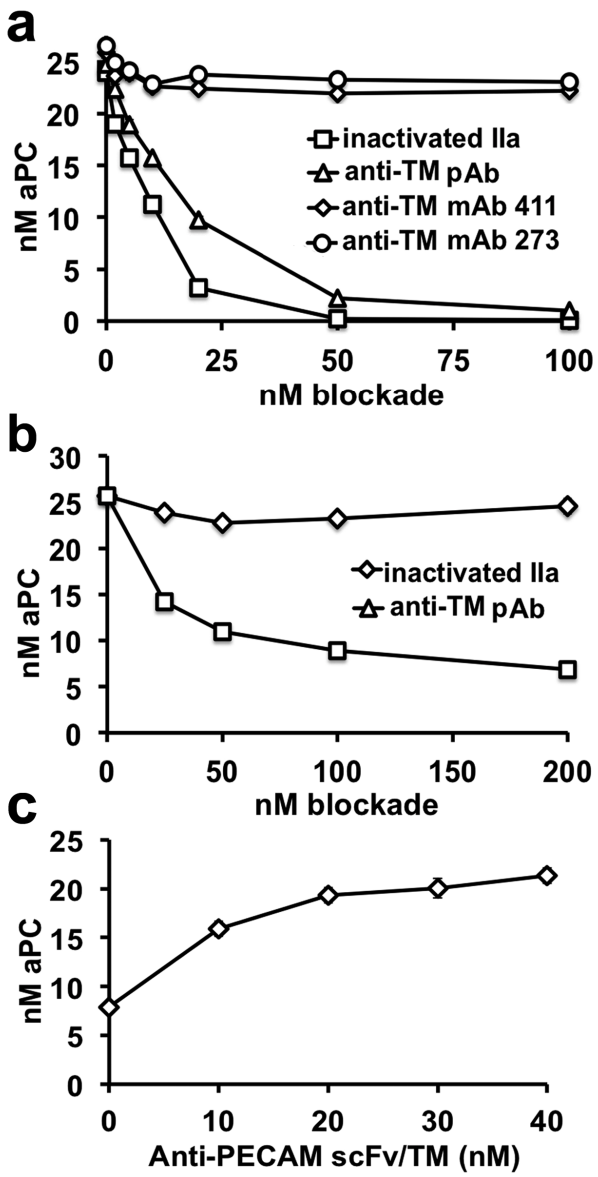

Figure 2.10. APC generation on MS1 cells following blockade of endogenous TM

(a) Blockade of endogenous TM with PPACK-inactivated thrombin and polyclonal anti-TM prevents thrombin-dependent APC generation. Monoclonal anti-TM antibodies, clone 411 and clone 273 (generously provided by Dr. Stephen J. Kennel, University of Tennessee, Knoxville, TN) did not inhibit APC generation. (b) Antibody blockade, but not inactivated IIa, had a sustained blocking effect when cells were washed prior to addition of thrombin and protein C. (c) Antibody blockade of endogenous TM enabled measurement of dose responsive, fusion protein-dependent protein C activation. All experiments were done in triplicate. Data shown are mean ± SD, error bars too small to be seen at some points.

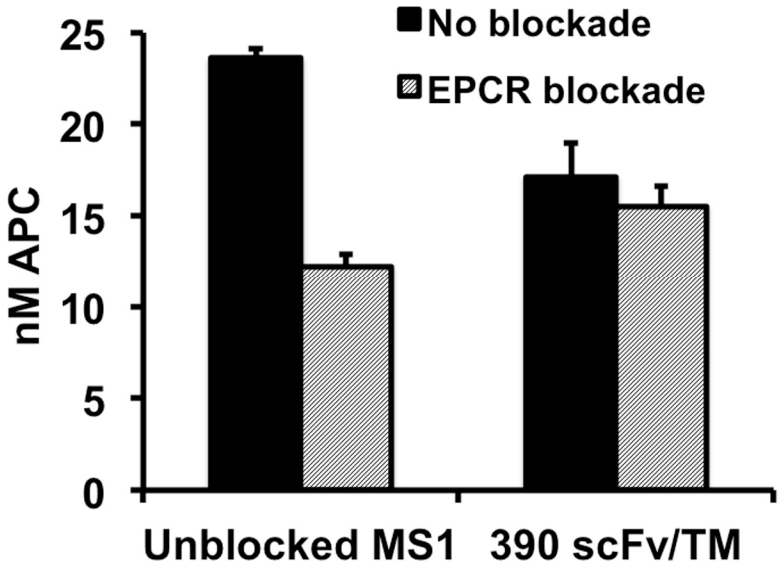

Figure 2.11. APC generation by 390 scFv/TM on MS1 cells
MS1 cells blocked with anti-mTM antibody and treated with 390 scFv/TM unexpectedly showed less activation of PC than unblocked MS1 cells (which reflect the activity of endogenous TM). One potential explanation is the finding that APC generation by 390 scFv/TM is not significantly affected by blockade of EPCR ($p = 0.32$), unlike unblocked MS1 cells ($p << 0.001$), indicating ineffective partnering of the fusion protein with this key co-factor. Experiments were done in triplicate (i.e. n=3). Data shown are mean ± SD.

would result in substantially higher levels of APC than unblocked MS1 cells. When we compared unblocked MS1 cells to antibody-blocked cells treated with 40nM of 390 scFv/TM, however, we found that the latter actually generated significantly less APC (Figure 2.11).

To assess the role of EPCR in this result, we utilized EPCR blocking antibody and found that treatment of MS1 cells with the anti-EPCR antibody resulted in approximately 50% reduction in thrombin-dependent activation of protein C by endogenous TM. In contrast, there was no significant effect on the activation of protein C by 390 scFv/TM (Figure 2.11).

III. CONCLUSIONS

Several significant conclusions can be drawn from the *in vitro* data presented in this chapter. First, experiments using the non-endothelial REN cell system clearly demonstrate that partnering between TM fusion proteins and EPCR is at least possible. In this system, in which EPCR is marked overexpressed (~10-fold more copies per REN-PECAM-EPCR cell than MS1 cell), PECAM-anchored 390 scFv/TM is able bind thrombin and access PC bound to EPCR. This is conclusively demonstrated by both the 4-fold increase in APC generation seen on REN-PECAM-EPCR cells, as well as the near complete reversal of this effect following EPCR blockade with mAb1560. This antibody has been well characterized and is known to inhibit approximately 70% of protein C binding to mouse EPCR, eliminating to substantial extent, but not completely, its ability to accelerate the activation of protein C[69]. Our results were quite consistent with these figures, demonstrating a 75% reduction in 390 scFv/TM-dependent APC generation following antibody blockade (Figure 2.5b).

The other main finding is the apparent inability of PECAM-bound 390 scFv/TM to partner with EPCR on MS1 cells. Two pieces of evidence suggest that 390 scFv/TM differs substantially from endogenous TM in terms

of its partnering with endogenous co-factors. First, anti-mTM blocked MS1 cells treated with a saturating concentration of 390 scFv/TM generate only ~70% as much APC than unblocked MS1 cells (Figure 2.11). Since PECAM-1 is typically expressed at much higher levels per EC than TM (~20 fold difference has been reported for HUVECs), this observation indicates a huge difference in the amount of APC generated per TM molecule. Since 390 scFv/TM and sTM demonstrate similar rates of APC generation in fluid-phase assays[127], there was no reason to suspect a difference in thrombin binding or catalytic efficiency. Instead, we suspected that our data might be explained by a difference in partnering with EPCR. Indeed, blockade of EPCR using mAb1560 had essentially no effect on APC generation by 390 scFv/TM, whereas a highly significant 50% reduction was seen on unblocked MS1 cells (Figure 2.11). Together, these data strongly suggest that PECAM-anchored 390 scFv/TM is unable to effectively partner with endogenous EPCR, at least with respect to protein C activation.

IV. MATERIALS AND METHODS

Cell lines and animals

MS1 cells were purchased from ATCC (Manassas, VA) and maintained in DMEM with 10% FBS and 1X antibiotic-antimycotic (Life technologies, Grand Island, NY). $TM^{pro/pro}$ mice were a generous gift from Dr. Helmut Weiler at the Blood Center of Wisconsin.

Antibodies and other reagents

Purified anti-PECAM (390) antibody was obtained from BioLegend (San Diego, CA). Anti-mTM polyclonal antibody (AF3894) and anti-EPCR polyclonal antibody (AF2749) were purchased from R&D systems (Minneapolis, MN). Anti-EPCR blocking antibody, mAb1560, was supplied by the Esmon laboratory. Collagenase A and HRP-conjugated Anti-FLAG (M2-HRP) antibody were obtained from Sigma Aldrich (St Louis, MO). PPACK-inactivated thrombin was a

generous gift of Sriram Krishnaswamy. Bovine thrombin was purchased from Sigma. Human protein C zymogen was obtained from Haematologic Technologies (Essex Junction, VT). APC substrate S-2366 was purchased from Diapharma (West Chester, OH). Mouse TM-specific siRNA (sc-36687), control siRNA (sc-37007), siRNA transfection reagent (sc-29528), and siRNA transfection media (sc-36868) were purchased from Santa Cruz Biotechnology (Santa Cruz, CA). FITC-conjugated Anti-ICAM-2 antibody, clone 3C4, was from Southern Biotech (Birmingham, AL).

Generation of REN-PECAM-EPCR stable cell line

A vector containing the entire coding sequence of mouse EPCR and a portion of the 5' and 3' UTRs (nt 171-1413) was obtained from the Esmon laboratory[147]. The EPCR cDNA was excised using XbaI and EcoRI and ligated into the pcDNA3.1/Zeo(-) vector (Life Technologies, Grand Island, NY). Since REN-PECAM cells already stably express the Geneticin resistance gene, this expression vector (which confers resistance to the antibiotic Zeocin) was utilized. Cells were transfected with Lipofectamine 2000 and REN-PECAM-EPCR cells were selected in media with Geneticin and 250 µg/mL of Zeocin.

Live cell ELISA Assays

ELISAs were performed on live cells as previously described[142], although in the experiments reported here, cell monolayers were incubated with increasing concentrations of scFv or scFv/TM fusion protein rather than whole antibodies. Since all fusion proteins carry a C-terminal triple FLAG tag, anti-FLAG (M2)-peroxidase (HRP) conjugate was used as a detection antibody. In experiments involving MS1 endothelial cells, specific binding of 390 scFv/TM was assessed by co-incubation with 10-fold excess of parental 390 mAb. ELISA binding data was analyzed and binding parameters (EC_{50}) were determined using PRISM 6.0 software (GraphPad, San Diego, CA)[142].

Protein C Activation Assays

Generation of APC by scFv/TM fusion was assayed following the incubation of confluent REN cell or MS1 monolayers with 390 scFv/TM fusion protein. Cells were washed x 3 with media to remove non-specifically bound protein, prior to the addition of 1 nM thrombin and 100 nM protein C. In all cases, protein C activation occurred at 37℃ in assay buff er (20 mM Tris, 100 mM NaCl, 1 mM $CaCl_2$, 0.1% (w/v) bovine serum albumin (BSA), pH 7.5) and the reaction was stopped by addition of an excess of hirudin. In experiments involving MS1 cells, the monolayer was first treated with 200nM anti-mTM antibody to block endogenous TM and then washed x 3 prior to incubation with scFv/TM fusion protein. In experiments involving EPCR blockade, cells were incubated with 300nM of anti-EPCR antibody (Ab1560) for 15 minutes prior to the addition of protein C and thrombin. This antibody has been well characterized and is known to inhibit approximately 70% of protein C binding, eliminating to a substantial extent the ability of EPCR to accelerate the activation of protein C by the thrombin-TM complex[69].

Radioimmunoassays (RIAs) using ^{125}I-labeled Antibodies

Anti-EPCR antibody (mAb1560) was directly radioiodinated with [^{125}I]NaI (Perkin Elmer, Waltham, MA) and purified using Zeba desalting spin columns (ThermoScientific). Radiolabeling efficiency was > 75% and free iodine was < 5%, post-purification. RIAs were performed and binding parameters (K_d, B_{max}) determined as previously reported[142].

siRNA knockdown of mouse TM

MS1 cells were transfected with a pool of three mouse TM-specific siRNA or control siRNA per manufacturer protocol. Specific siRNA sequences were not made available by the manufacturer. Cells were plated and allowed to grow until they were approximately 75% confluent. 10 pmol of siRNA were mixed with transfection reagent and allowed to sit for 30 minutes at room temperature prior

to addition to each well of cells. Cells were exposed for 7 hours, after which they were gently washed and incubated with antibiotic-free growth media. 48 hours later, cells were lysed for analysis of TM expression by western blot.

shRNA knockdown of mouse TM

MS1 cells were transfected with a pool of three mouse TM-specific shRNAs using Lipofectamine 2000 (as with siRNA, sequences proprietary to manufacturer). Cells were selected using 4 μg/mL puromycin, a concentration found to kill 100% of wild type MS1 cells.

Isolation of $TM^{pro/pro}$ lung endothelial cells

Animal studies were carried out in accordance with the Guide for the Care and Use of Laboratory Animals as adopted by the NIH, under protocols (803320 and 804349) approved by University of Pennsylvania IACUC. The genotype of $TM^{pro/pro}$ mice was verified using genomic DNA obtained from mouse tail tips. Lung endothelial cells were isolated as previously described[148]. Briefly, neonatal pups (7-14 days old) were anaesthetized with ketamine and xylazine and given an intramuscular injection of 25 μL of heparin (1000U/mL). The thoracic cavity was entered and 5 mL of ice cold DMEM was injected into the pulmonary circulation via the right ventricle. 1 mL of collagenase A (1.0 mg/mL) was instilled through the trachea into the lungs, which were then tied off. The lungs were removed and incubated with 5 mL of collagenase A for 30 min at 37℃. 30 mL of sterile PBS was added and the tube was shaken. The resulting tissue/cell suspension was passed through a 70μm filter, centrifuged, resuspended in complete DMEM, and plated onto gelatinized T75 flasks. The cells were grown in M199 medium for 2 days, trypsinized, and subjected to FACS sorting using anti-ICAM-2 antibody (clone 3C4). The sorted cells were pooled, plated at $3x10^5$ cells/mL in a T25 flask, and split 1:2 at each passage.

Data analysis and statistics

Results are expressed as mean ± SD unless otherwise noted. Significant differences between means were determined using Student's t-test or one-way ANOVA followed by appropriate multiple comparison (Tukey) test. For experiments involving the comparison of multiple dose response curves (e.g. APC generation by 390 scFv/TM on REN-PECAM vs. REN-PECAM-EPCR cells), two-way ANOVAs were performed. $P<0.05$ was considered statistically significant.

CHAPTER THREE: OPTIMIZATION OF PARTNERING WITH ENDOGENOUS EPCR

I. INTRODUCTION

Having reached the conclusion that 390 scFv/TM anchored to PECAM on ECs likely does not partner efficiently with endogenous EPCR, our attention turned to potential strategies for enhancing interaction between endothelial targeted TM and this key co-factor. Another cell adhesion molecule, ICAM-1, has been shown to localize to apical membrane microdomains on ECs, and to cluster in lipid rafts following cytokine stimulation, leukocyte adhesion, and/or binding of anti-ICAM-1 antibodies[149]. Since EPCR, PAR1, and to some extent, TM, are also believed to localize to these membrane microdomains[96], we hypothesized that anchoring TM to ICAM-1 might allow for enhanced proximity and improved partnering with endogenous co-factors and signaling pathways.

II. RESULTS

PECAM-1 vs. ICAM-1

Relative proximity of PECAM-1 and ICAM-1 to EPCR

To assess the relative proximity of EPCR to PECAM-1 and ICAM-1, mouse MS1 endothelial cells were stained for each antigen and imaged using a fluorescence microscope (Figure 3.1a). 390 mAb, the parental antibody of the 390 scFv/TM fusion, was used to stain PECAM-1. YN1/1.7.4 (hereafter referred to as YN1) was used to stain ICAM-1. This mAb has been extensively studied in our laboratory and blocks leukocyte LFA-1 interaction[150]. In agreement with previous reports, most PECAM-1 staining occurred at cell-cell borders[136], with minimal overlap with EPCR. In contrast, there was overlap of staining for ICAM-1 and that for EPCR (Figure 3.1a).

Binding of anti-ICAM and anti-PECAM mAbs to MS1 cells

Next, we studied the binding to MS1 cells of ^{125}I-labeled YN1 and 390

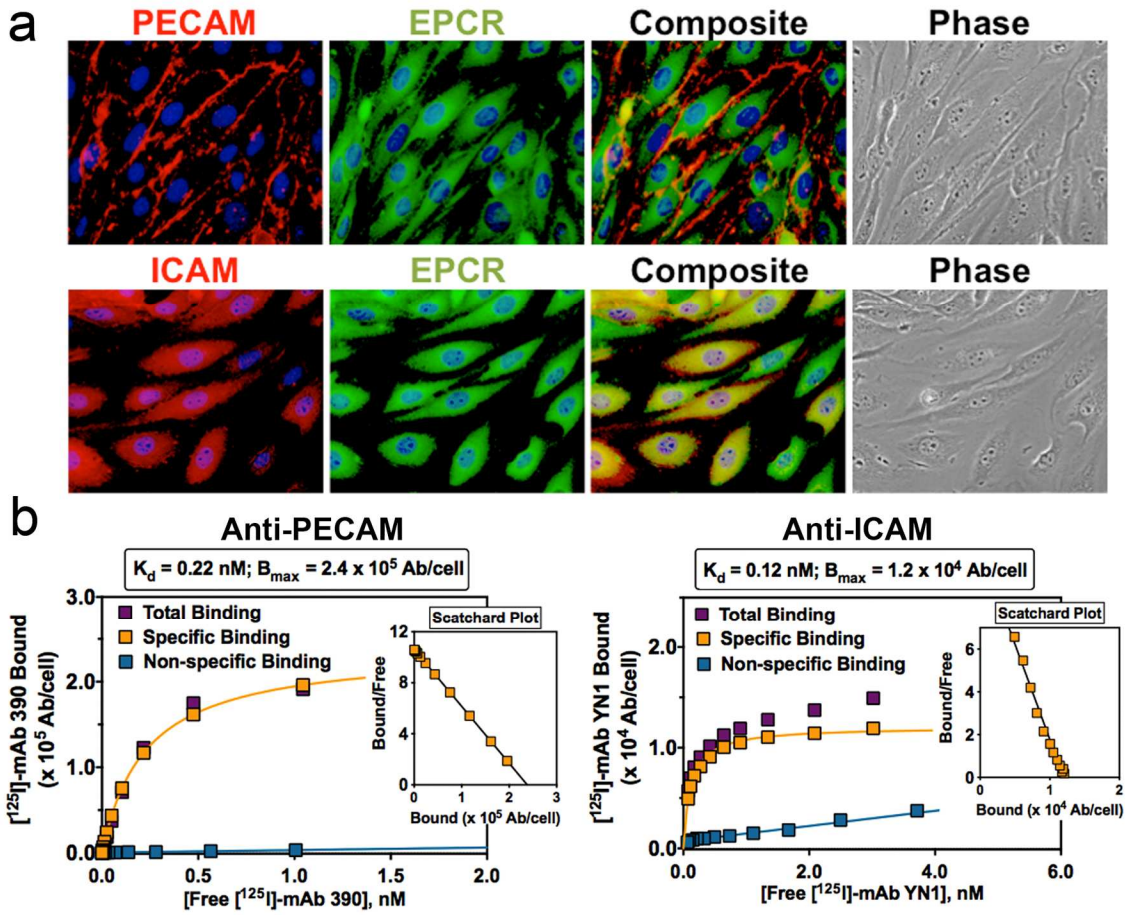

Figure 3.1. Localization of PECAM-1, ICAM-1, and EPCR on mouse endothelial cells

(a) Immunofluorescence images demonstrate superior co-localization of ICAM-1 and EPCR, as compared to PECAM-1 and EPCR. (b) Radioimmunoassay data using ^{125}I-labeled anti-PECAM (390 mAb) and anti-ICAM (YN1 mAb) to determine affinity and number of binding sites per endothelial cell. Radioimmunoassays done in quadruplicate (i.e. each point represents four wells of cells), data shown are mean ± SD, some error bars too small to be seen.

mAbs. The antibodies had similar subnanomolar affinities (K_d of approx. 0.12 and 0.22nM, respectively), although PECAM-1 provided ~20-fold more binding sites than ICAM-1 (approximately 240,000/cell vs. 12,000/cell, respectively), reflecting a substantial difference in the level of cell surface expression of these molecules (Figure 3.1b). Interestingly, according to these data, MS1 have a slightly lower number of anti-PECAM binding sites than human umbilical vein endothelial cells (HUVECs, ~10^6 binding sites per cell[145]), which may reflect innate differences between these cell lines. MS1s are a transformed cell line, whereas HUVECs are primary ECs. Moreover, MS1s are smaller than HUVEC, so their number of PECAM copies per cell surface area may be fairly similar.

Construction of an ICAM-targeted scFv/TM Fusion Protein

Cloning of YN1 scFv and fusion to sTM

Using a previously reported PCR-based technique, we next cloned an anti-ICAM-1 scFv from the YN1 hybridoma[151]. Whereas cloning of the V_H cDNA was straightforward, the typical approach produced only the previously reported Y3-Ag 1.2.3 myeloma V_L sequence[152] (i.e. the myeloma used to make the YN1 hybridoma). As a result, mass spectrometry was used to identify an 8 amino acid peptide unique to the ICAM-specific V_L, which was then used to produce a full length V_L cDNA (Figure 3.2). The V_H and V_L cDNAs were assembled into a complete anti-ICAM-1 YN1 scFv, which was fused to the extracellular domain of TM. The YN1 scFv/TM construct was designed to be identical to 390 scFv/TM, with the scFv moiety on the 5' end (Figure 3.3a). The purity of YN1 scFv and YN1 scFv/TM is shown by gel electrophoresis (Figure 3.3b).

Functional activity of 390 scFv/TM, YN1 scFv/TM, and sTM in solution

To ensure that activity of the TM moiety in YN1 scFv/TM was intact, we measured APC generation in a fluid-phase assay. Both YN1 scFv/TM and 390 scFv/TM fusion proteins were nearly identical to soluble TM in their ability to stimulate thrombin-mediated activation of protein C (Figure 3.4).

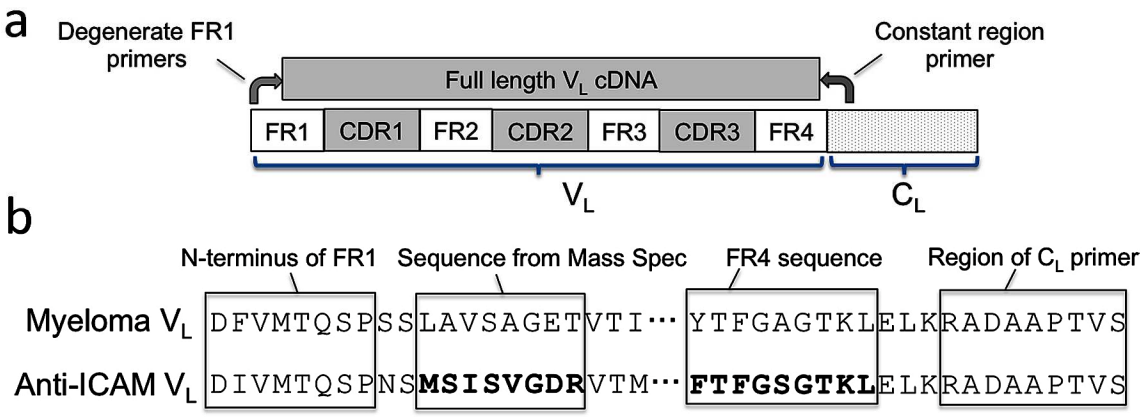

Figure 3.2. Cloning of anti-ICAM V_H and V_L cDNAs

(a) A PCR-based approach to cloning of variable heavy and light chain regions (V_H and V_L) utilizes degenerate 5' primers corresponding to the beginning of the 1st framework region (FR1) and a 3' primer corresponding to the start of the constant region[151]. (b) In the case of the YN1 hybridoma, the V_H domain was readily cloned, but the typical approach amplified only the myeloma-derived V_L, which is nearly identical to the anti-ICAM V_L at the N-terminus of FR1. Mass spectrometry was used to identify an 8 amino acid sequence unique to the anti-ICAM V_L. This sequence allowed the majority of the V_L to be cloned. A 9 amino acid sequence in FR4 was paired with the original 5' primers to identify the residues at the N-terminus of the anti-ICAM V_L.

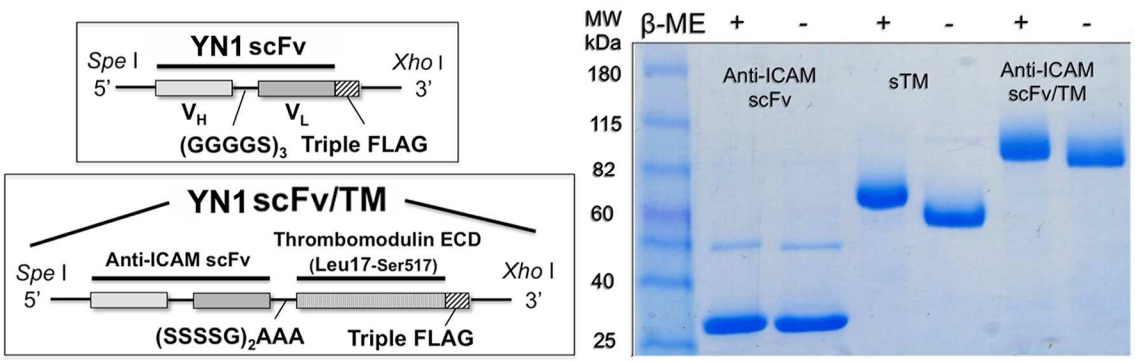

Figure 3.3. Design and synthesis of YN1 scFv and scFv/TM
(a) Assembly of V_H and V_L sequences into scFv and scFv/TM constructs. (b) SDS PAGE gel electrophoresis of YN1 scFv, soluble TM, and YN1 scFv/TM fusion protein under reducing and non-reducing conditions.

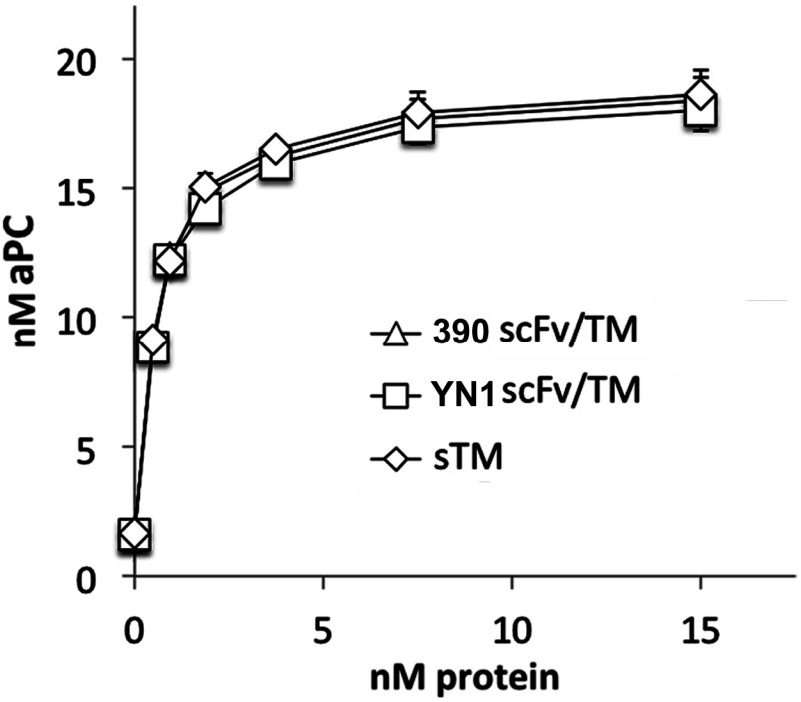

Figure 3.4. Fluid-phase APC generation

Thrombin-dependent activation of protein C was measured in solution and compared to soluble TM (sTM). The proteins were mixed with 0.5 nM thrombin and a large excess of protein C (1 μM). The reaction was stopped after 15min by addition of hirudin. The fusion proteins performed identically to sTM over a range of concentrations.

Creation of ICAM-1 expressing REN cells

As discussed in Chapter 2, the human mesothelioma cell line REN is a useful model system, with no expression of mouse PECAM, ICAM, TM, or EPCR at baseline (see Figure 2.1). Although wild type REN cells do express low levels of human ICAM-1[153], they were found to have no detectable cross-reactivity with YN1 mAb by flow cytometry and cell-based ELISA (data not shown). As a result, we created a new stably transfected cell line, REN-mICAM cells, which express high levels of mouse ICAM-1.

Binding and functional activity of YN1 scFv/TM on ICAM-expressing REN cells

Both YN1 scFv and YN1 scFv/TM demonstrated nanomolar affinity to REN-ICAM cells, with no non-specific binding seen on wild type REN cells (Figure 3.5a,b). YN1 scFv/TM demonstrated dose-dependent, thrombin-mediated activation of protein C on REN-ICAM cells, but not on wild type REN cells (Figure 3.6a). Recombinant sTM showed no activity on either cell type.

EPCR expression potentiates the functional activity of YN1 scFv/TM on REN-ICAM cells

We next assessed the ability of ICAM-anchored YN1 scFv/TM to partner with EPCR in the artificial REN cell system. As had been done for REN-PECAM cells, EPCR expression was induced on REN-ICAM cells, producing the stable cell line REN-ICAM-EPCR. As was seen with 390 scFv/TM, EPCR expression resulted in ~4-fold enhancement of thrombin-mediated APC generation by YN1 scFv/TM (Figure 3.6b). In summary, while bound to their corresponding anchors on non-endothelial REN cells, PECAM and ICAM-targeted scFv/TM fusion proteins demonstrated roughly equivalent functional activity and similar capacity to partner with cellular EPCR, at least with respect to thrombin-dependent APC generation.

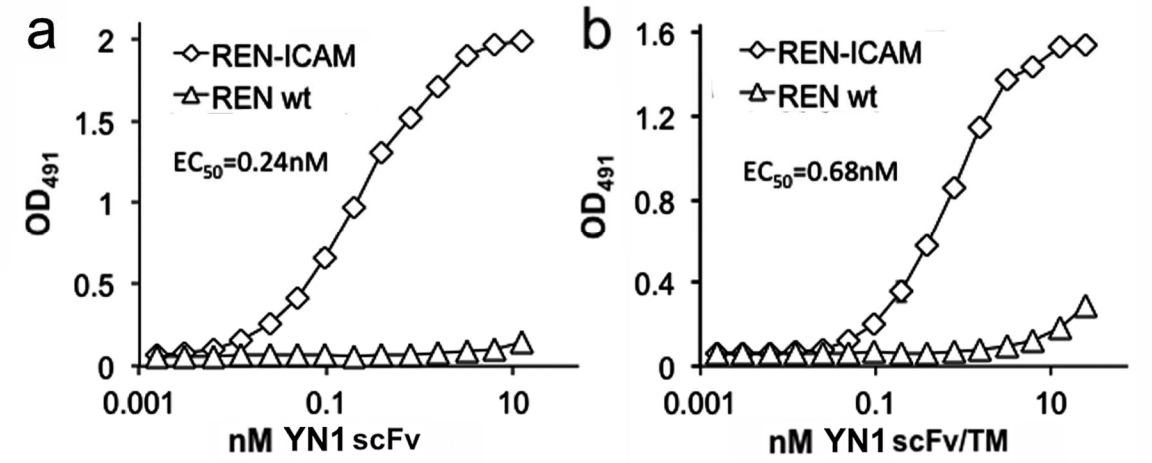

Figure 3.5. Binding of YN1 scFv and scFv/TM to REN-ICAM cells

Cell based ELISAs show binding of (a) YN1 scFv and (b) YN1 scFv/TM fusion protein to ICAM expressing REN cells. No significant binding is seen to wild type REN cells. Experiments were done in triplicate (i.e. each point shown represents three wells of cells). Data shown are mean ± SD, although error bars are too small to be seen in most cases. EC_{50} is shown for each curve.

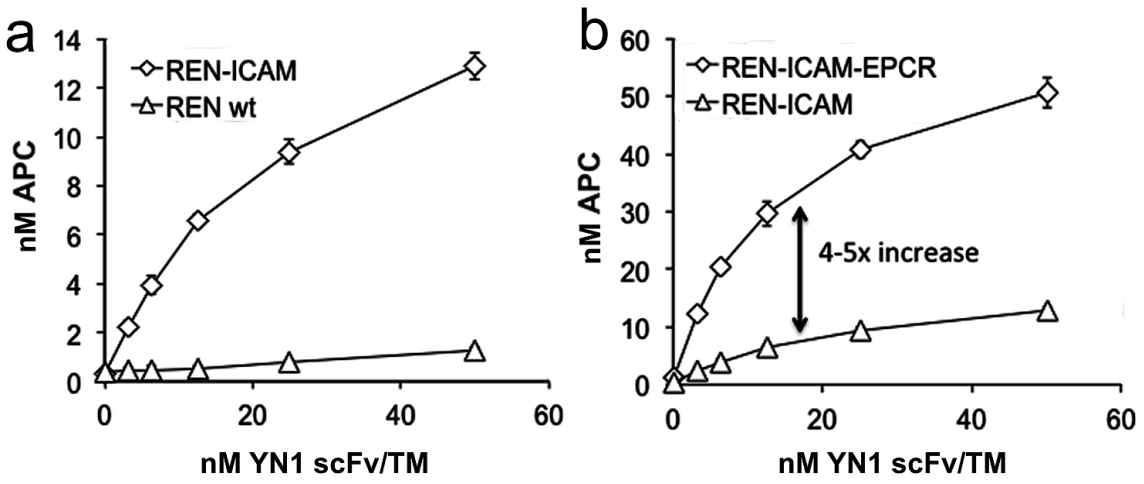

Figure 3.6. APC generation by YN1 scFv/TM on REN-ICAM cells with and without EPCR expression

(a) YN1 scFv/TM activates protein C while bound to ICAM-expressing cells. Minimal APC is generated on wild type REN cells, presumably due to lack of binding. (b) A ~4-fold increase in APC generation is seen when YN1 scFv/TM is anchored to REN-ICAM-EPCR cells, as compared to EPCR-negative counterparts. Differences between groups were highly significant ($p < 0.001$) at all (non-zero) doses of YN1 scFv/TM fusion protein. All experiments were done in triplicate (i.e. each point shown represents three wells of cells). Data shown are mean ± SD, although error bars are too small to be seen in some cases.

Studies on Mouse Endothelial Cells

Binding of YN1 scFv/TM to quiescent and TNF-stimulated endothelial cells

The binding of YN1 scFv/TM was tested on MS1 cells. Unlike most endothelial cells (e.g., HUVEC), quiescent MS1 cells express significant levels of ICAM-1, although they demonstrate a similar ~1.5-fold increase in response to TNF or other cytokine stimulation. YN1 scFv/TM demonstrated ICAM-specific binding to MS1 cells, as evidenced by near complete inhibition of binding by a 10-fold excess of parental antibody (Figure 3.7). Likewise, stimulation of the cells with mouse TNF demonstrated a small but significant increase in fusion protein binding. Calculated affinity constants were similar to those seen in REN-ICAM cell experiments.

Functional activity of EC-bound 390 scFv/TM and lack of EPCR partnering

We employed anti-mTM antibody blockade (described in Chapter 2) to assess protein C activation by YN1 scFv/TM anchored to MS1 cells. APC generation was compared to unblocked MS1 cells and antibody blocked MS1 cells treated with 40nM 390 scFv/TM. As with 390 scFv/TM, a high concentration of YN1 scFv/TM was used (40nM), in order to saturate available binding sites. The maximum numbers of PECAM- and ICAM-binding sites were known from our radioimmunoassays (Figure 3.1b). Despite a 20-fold difference in binding sites, only a ~1.5 fold difference was seen in the level of APC generation (Figure 3.8a). We assessed the role of EPCR using the mAb1560 blocking antibody and found that YN1 scFv/TM-treated MS1 cells showed a 50% reduction in protein C activation, similar to unblocked MS1s and in contrast to 390 scFv/TM-treated cells (Figure 3.8a).

In order to directly compare the activity of EC-bound YN1 scFv/TM and 390 scFv/TM, APC generation was normalized to the number of binding sites per cell. This analysis revealed that YN1 scFv/TM has ~15-fold greater functional activity then 390 scFv/TM, while anchored to MS1 cells (Figure 3.8b).

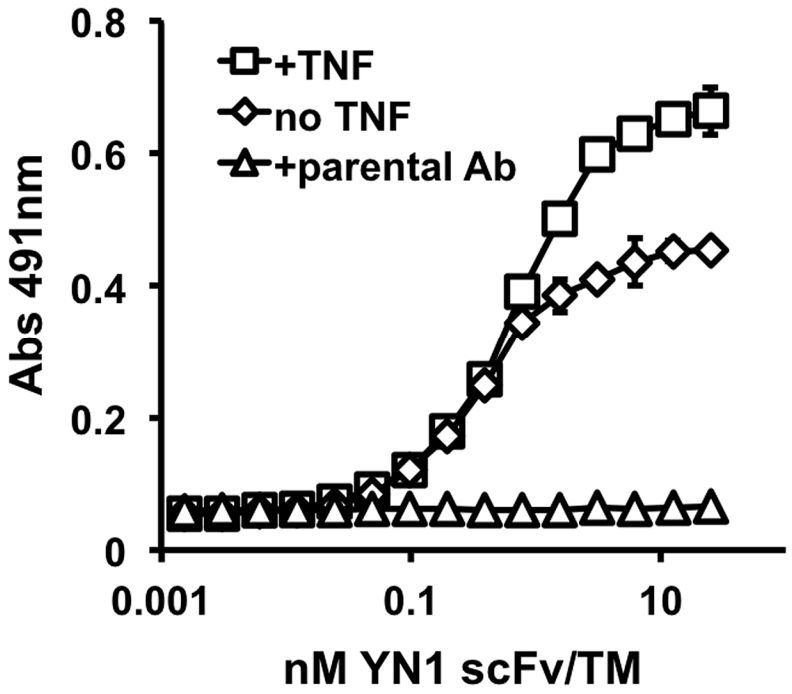

Figure 3.7. Binding of YN1 scFv/TM to quiescent and activated MS1 cells
Specificity is demonstrated by inhibition of binding by 10-fold excess of parental 390 mAb. All experiments were done in triplicate (i.e. each point shown represents three wells of cells). Data shown are mean ± SD, although error bars are too small to be seen in some cases.

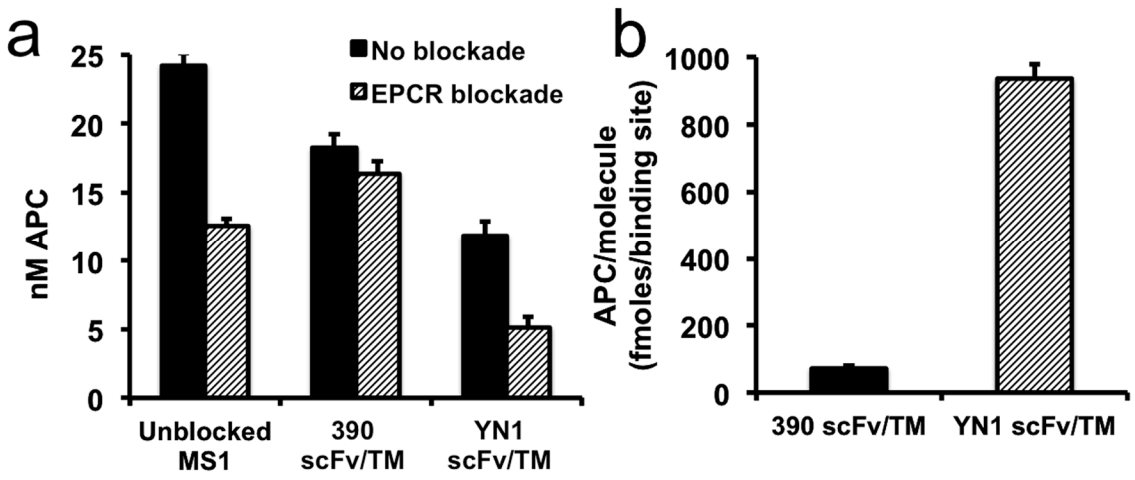

Figure 3.8. APC generation by PECAM- vs. ICAM-anchored scFv/TM on antibody blocked MS1 cells

(a) Despite a 20-fold difference in the number of PECAM vs. ICAM binding sites, antibody-blocked MS1 cells treated with 390 scFv/TM generate only ~1.5-fold more APC than those treated with YN1 scFv/TM. Moreover, APC generation by YN1 scFv/TM, but not 390 scFv/TM, is affected by blockade of EPCR ($p < 0.001$). The 50% reduction is similar to what is seen with unblocked MS1 cells (reflecting the activity of endogenous TM). (b) Normalization of APC generation to number of binding sites shows that functional activity of YN1 scFv/TM is ~15-fold greater than 390 scFv/TM ($p << 0.001$). Experiments done in triplicate. Data shown are mean ± SD.

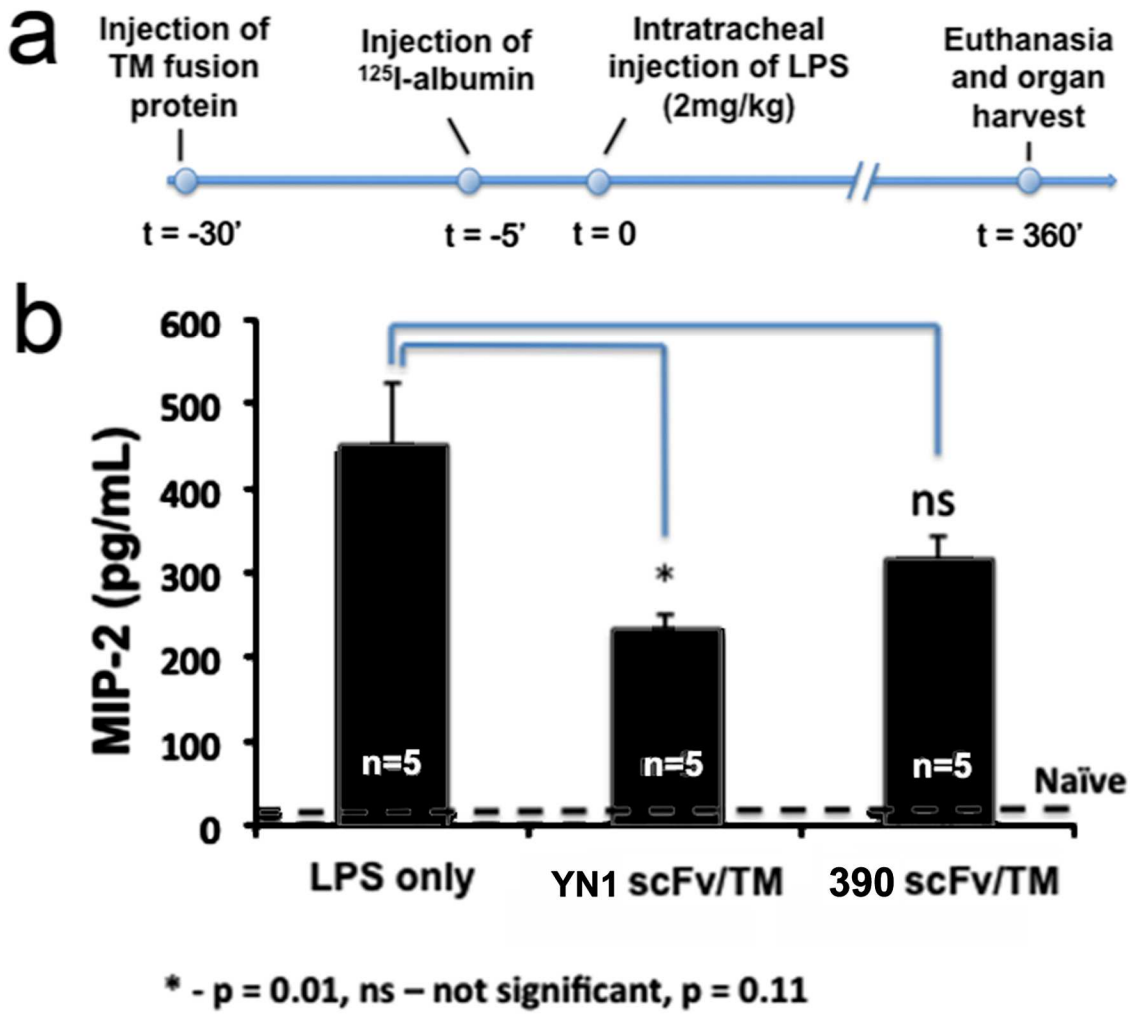

Figure 3.9. YN1 scFv/TM reduces MIP-2 in a mouse model of lung injury
(a) Timeline of intratracheal LPS lung injury model. In experiments assessing endothelial barrier dysfunction, a tracer amount of ^{125}I-labeled albumin was injected 5 minutes prior to LPS administration. (b) Concentration of the critical neutrophil chemokine, MIP-2, in bronchoalveolar lavage (BAL) fluid. Data shown are mean ± SD, with number of animals as shown.

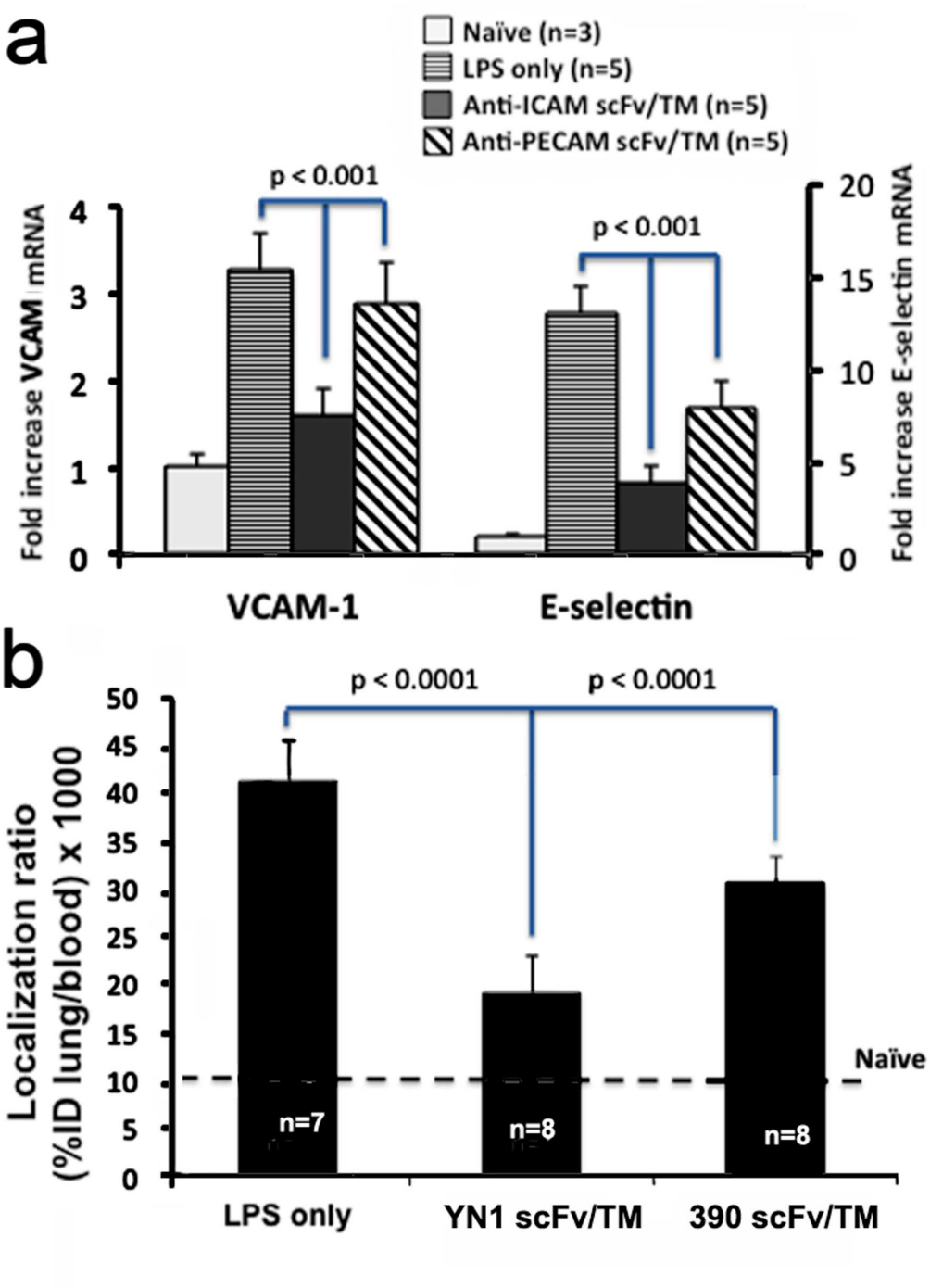

Figure 3.10. YN1 scFv/TM reduces inflammatory marker expression and endothelial barrier dysfunction in mouse lung injury model

(a) mRNA transcript levels of pro-inflammatory cell adhesion molecules, VCAM-1 and E-selectin, in lung homogenate. (b) Endothelial barrier dysfunction, as measured by leakage of ^{125}I-labeled albumin from blood into lung interstitium and/or alveolar space. All data shown are mean ± SD, with number of animals as shown.

In vivo Experiments

Endothelial protective effects of YN1 scFv/TM and 390 scFv/TM in a mouse model of acute lung injury

Anti-inflammatory effects of YN1 scFv/TM and 390 scFv/TM were then compared in a model of lung inflammation, in which mice receive an intratracheal (IT) injection of endotoxin[154]. The fusion proteins, or PBS vehicle, were injected intravenously 30 minutes prior to LPS challenge (Figure 3.9a). Relevant indices of lung inflammation and injury were measured, including the level of MIP-2 in bronchoalveolar lavage fluid (Figure 3.9b), expression of cell adhesion molecules VCAM-1 and E-selectin in lung tissue homogenate (Figure 3.10a), and extravascular leakage of radiolabeled albumin injected intravenously and detected in the lungs (Figure 3.10b). While both YN1 scFv/TM and 390 scFv/TM showed evidence of protection, the ICAM-targeted fusion protein was more effective in all cases.

III. CONCLUSIONS

The data presented in this chapter support the notion that the ability of endothelial targeted scFv/TM fusion proteins to interact with endogenous EPCR depends on which surface determinant is targeted, and that this variable may have significant therapeutic implications, with YN1 scFv/TM fusion demonstrating more potent protective effects *in vivo*. Our data, along with prior reports regarding the distribution of ICAM and PECAM on the endothelial membrane[136,137,149], suggest that the proximity of the TM fusion to EPCR may be the critical factor. Figure 3.11 shows a simplified model of an endothelial cell with the TM fusion proteins bound to their target ligands. The figure accurately depicts the fusion proteins binding the domains of PECAM-1 and ICAM-1 which lie furthest from the plasma membrane, consistent with the location of their target epitopes[142,150]. The schematic highlights the proposed difference in proximity to the EPCR/Protein C complex, which may account for our experimental observations.

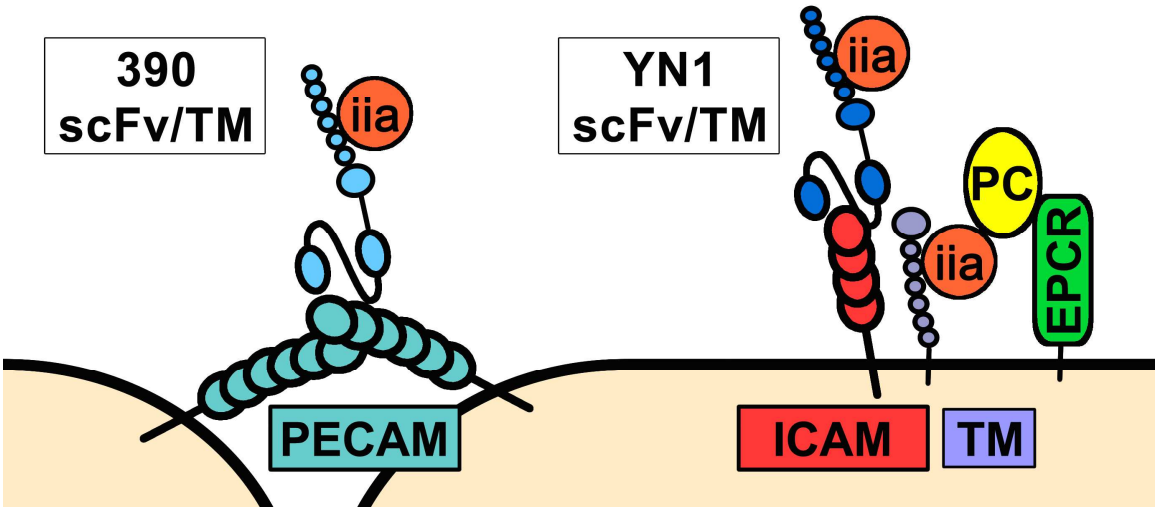

Figure 3.11. Schematic representation of TM fusion proteins anchored to the endothelial plasmalemma

The proximity of ICAM-targeted scFv/TM to endogenous EPCR/Protein C may account for its enhanced activity *in vitro* and *in vivo*.

It is worth noting that these results align with the general notion that anchoring agents to distinct determinants on the same target cell may produce distinct outcomes, due to the differing functions, location, surface density, and trafficking of these surface molecules. For example, our laboratory previously reported that binding of the H_2O_2-producing enzyme, glucose oxidase (GOX), to endothelial cells induced varying degrees of vascular damage, depending on whether PECAM or TM was chosen as the surface target[155]. The variation in outcome in those experiments was attributed to the substantially different function of these two surface molecules and the consequences of their blockade by GOX conjugates. In contrast, it is difficult to attribute the current results to any functional difference between ICAM and PECAM, two closely related proteins which both support leukocyte adhesion, pro-inflammatory signaling, and uptake of antibody conjugates via a similar endocytic mechanism[156,157]. For this reason, we believe that the most logical explanation for our current experimental results is the distinct localization of ICAM and PECAM on the endothelial membrane and their differing capacity to allow interaction of anchored scFv/TM with EPCR.

In summary, our first approach for enhancing partnering of endothelial-targeted TM and EPCR involved the rational selection of an endothelial determinant, ICAM-1, based on knowledge of its membrane distribution. We constructed and synthesized a recombinant ICAM-targeted scFv/TM fusion protein. In comparing its function to that of PECAM-targeted scFv/TM, we found evidence of superior functional activity on ECs, partnering with endogenous EPCR, and enhanced protective effects in a mouse model of lung injury. Together, these results suggest that delivery of recombinant TM to the endothelial membrane in a way that mimics its natural distribution and optimizes interaction with endogenous co-factors is more effective. These findings underscore the complexity of targeting biotherapeutics to the plasmalemma, and suggest that precision on a nanometer scale is necessary for optimal biotherapeutic effect.

IV. MATERIALS AND METHODS

Cell lines

YN1 hybridoma and MS1 cells were purchased from ATCC (Manassas, VA). YN1 cells were cultured in RPMI 1640 supplemented with 10% (v/v) fetal bovine serum (FBS). MS1 cells were maintained in DMEM with 10% FBS and 1X antibiotic-antimycotic (Life technologies, Grand Island, NY).

Antibodies and other reagents

Purified anti-PECAM (390) and anti-ICAM (YN1) antibodies were obtained from BioLegend (San Diego, CA). Anti-TM polyclonal antibody (AF3894) and anti-EPCR polyclonal antibody (AF2749) were purchased from R&D systems (Minneapolis, MN). Anti-EPCR blocking antibody, mAb1560, was supplied by the Esmon laboratory. HRP-conjugated Anti-FLAG (M2-HRP) antibody was obtained from Sigma Aldrich (St Louis, MO). Alexa Fluor-labeled secondary antibodies were purchased from Life Technologies (Grand Island, NY). Bovine thrombin, LPS (serotype B4), and mouse TNF were purchased from Sigma. Human protein C zymogen was obtained from Haematologic Technologies (Essex Junction, VT). APC substrate S-2366 was purchased from Diapharma (West Chester, OH).

Endothelial cell immunofluorescence staining

MS1 cell monolayers were grown in 8 well µ-slides (Ibidi, Verona, WI) and fixed for 20 minutes at room temperature (RT) with Histochoice (Amresco, Solon, OH). In some cases, cells were treated with 10 ng/mL mouse TNF for 8 hours prior to fixation. After three washes, cells were blocked with 3% (w/v) BSA in HBSS for 1 hour at RT. Cells were stained with either anti-PECAM (390, 15 µg/mL) or anti-ICAM (YN1, 1 µg/mL) mAbs, in addition to polyclonal goat anti-mouse EPCR (0.5 µg/mL) for 2 hours at RT. Cells were washed three times with 0.1% Tween in HBSS and then stained with Alexa Fluor 594 anti-rat (1:200) and Alexa Fluor 488 anti-goat (1:1000). After 1 hour incubation, cells were washed

four times with 0.1% Tween in HBSS and once in PBS. ProLong Gold Antifade reagent with DAPI (Life technologies, Grand Island, NY), and a coverslip was applied and cells were allowed to dry overnight prior to immunofluorescence imaging.

Cloning of anti-ICAM V_L and V_H cDNAs

Total cellular RNA was isolated from YN1 hybridoma cells using the RNeasy kit (Qiagen, Valencia, CA). Combined reverse transcription and PCR was performed using SuperScript One Step RT-PCR kit (Life Technologies, Grand Island, NY) and previously reported FR1 region primers[151]. Mass spectrometry to identify an 8-aa sequence unique to the ICAM-specific VL was done by the Core Facility at the University of Pennsylvania using purified YN1 antibody that had been run on a denaturing SDS PAGE gel and excised. Degenerate PCR primers were synthesized based on this sequence and used to produce a full length V_L distinct from the known Y3-Ag 1.2.3 myeloma V_L sequence[152].

Assembly and expression of anti-ICAM scFv and anti-ICAM scFv/TM constructs

Completed anti-ICAM V_L and V_H cDNAs were assembled into constructs encoding anti-ICAM scFv and the anti-ICAM scFv/TM fusion protein. In each case, V_H and V_L sequences were separated by a $(GGGGS)_3$ linker, and a triple FLAG tag was appended to the 3' end (C terminus) for purposes of purification and detection. The YN1 scFv moiety was separated from the extracellular domain of TM (amino acids Leu17-Ser517) by an $(SSSSG)_2$AAA linker. Both proteins were expressed in S2 cells and purified using a C-terminal triple FLAG tag. Purity was assessed using SDS-PAGE.

Generation of REN-derived Stable Cell Lines

REN-mICAM cells. A full-length cDNA for mouse ICAM-1 was purchased from Thermo Scientific (Rockford, IL). The clone was sequenced and found to

contain the entire coding sequence of mouse ICAM-1 and a portion of the 5' and 3' UTRs (nt 46-2440) between EcoRI and XbaI restriction enzyme sites. The clone was excised and ligated into the pcDNA3 mammalian expression vector, and transfected into REN cells using Lipofectamine 2000 (Life Technologies, Grand Island, NY). Stably expressing cells were selected in media containing 200 µg/mL of Geneticin (Life Technologies, Grand Island, NY).

REN-mICAM-mEPCR cells. A vector containing the entire coding sequence of mouse EPCR and a portion of the 5' and 3' UTRs (nt 171-1413) was obtained from the Esmon laboratory[147]. The EPCR cDNA was excised using XbaI and EcoRI and ligated into the pcDNA3.1/Zeo(-) vector (Life Technologies, Grand Island, NY). Since REN-ICAM cells already stably express the Geneticin resistance gene, this expression vector (which confers resistance to the antibiotic Zeocin) was utilized. Cells were transfected with Lipofectamine 2000 and REN-ICAM-EPCR cells were selected in media with Geneticin and 250 µg/mL of Zeocin.

Live Cell ELISA Assays

Enzyme-linked Immunosorbent Assays (ELISAs) were performed on live cells as described in Chapter 2. ELISA binding data was analyzed and binding parameters (EC_{50}) were determined using PRISM 6.0 software (GraphPad, San Diego, CA)[142].

RIAs using ^{125}I-labeled antibodies

390 and YN1 mAbs were directly radioiodinated with [^{125}I]NaI (Perkin Elmer, Waltham, MA) and purified using Zeba desalting spin columns (ThermoScientific). In all cases, radiolabeling efficiency was > 75% and free iodine was < 5%, post-purification. RIAs were performed and binding parameters (K_d, B_{max}) determined as previously reported[142].

Protein C activation assays

Generation of APC by cell-bound scFv/TM fusion was assayed as described in Chapter 2. For fluid-phase APC generation experiments, sTM, 390 scFv/TM, and YN1 scFv/TM were each mixed with 0.5nM thrombin and 1 μM protein C in a micro-Eppendorf tube. In all cases, protein C activation occurred at 37℃ in assay buffer (20 mM Tris, 100 mM NaCl, 1 mM $CaCl_2$, 0.1% (w/v) BSA, pH 7.5) and the reaction was stopped by addition of an excess of hirudin. As described in Chapter 2, MS1 cell monolayers were first treated with anti-TM antibody to block endogenous TM and then washed x 3 prior to incubation with scFv/TM fusion protein. The amount of APC generated by cell-bound fusions in these experiments was normalized to the number of binding sites per cell, as determined in MS1 RIAs (approximately 240,000/cell for PECAM-1 and 12,000/cell for ICAM-1). Antibody blockade of EPCR was performed as described in Chapter 2, using 300nM of anti-EPCR antibody (Ab1560) for 15 minutes prior to the addition of protein C and thrombin.

IT LPS model

Animal studies were carried out in accordance with the Guide for the Care and Use of Laboratory Animals as adopted by the NIH, under protocols (803320 and 804349) approved by University of Pennsylvania IACUC. C57BL/6 male mice weighing 20-30 gm were anaesthetized and placed in a supine position. Acute lung injury was induced via IT injection of 2 mg/kg of endotoxin in a volume of 100 μL of PBS. Endotoxin injection was followed immediately by injection of 150 μL of air, to ensure even distribution of LPS throughout all distal airspaces. In relevant experiments, anti-PECAM scFv/TM, anti-ICAM scFv/TM, or PBS vehicle and ^{125}I-labeled albumin were injected intravenously prior to LPS administration as shown. 6 hours after induction of lung injury, blood was withdrawn from the inferior vena cava and animals were euthanized.

In experiments involving tracing of ^{125}I-labeled albumin, a catheter was placed in the pulmonary artery and the pulmonary circulation was gently flushed

with PBS prior to the harvesting of organs. The amount of radioactivity in the blood and lungs was measured using a Wizard^2 2470 gamma counter (PerkinElmer, Waltham, MA). The localization ratio of ^{125}I-albumin (calculated as (% injected dose present in lung/g of lung tissue)/blood level) was used as a surrogate for pulmonary edema.

In other experiments, bronchoalveolar lavage was performed via a 19-gauge stainless steel catheter (Harvard Apparatus, Holliston, MA) placed in the trachea and secured via a 5-0 silk suture. Each animal was lavaged twice with 0.8 mL of ice-cold PBS. The lavages were pooled and MIP-2 was quantified using a Quantikine ELISA kit (R&D systems, Minneapolis, MN). For quantification of VCAM-1 and E-selectin mRNA, lungs were homogenized with steel beads (Sigma) and a Tissue Lyser II (Qiagen). Total RNA was isolated with RNeasy kit and cDNA was synthesized using the Transcriptor 1st Strand cDNA Synthesis Kit (Roche Applied Science, Indianapolis, IN). qPCR was performed using the FastStart DNA MasterPLUS kit (SYBR green) and a Lightcycler 1.5 carousel-based system (Roche Applied Science). Validated Quantitect primers for mouse VCAM-1, E-selectin, and actin (housekeeping control) were utilized (Qiagen, Valencia, CA).

Data analysis and statistics

Results are expressed as mean ± SD unless otherwise noted. Significant differences between means were determined using Student's t-test or one-way ANOVA followed by appropriate multiple comparison (Tukey) test. For experiments involving the comparison of multiple dose response curves (e.g. APC generation by YN1 scFv/TM on REN-ICAM vs. REN-ICAM-EPCR cells), two-way ANOVAs were performed. $P<0.05$ was considered statistically significant.

CHAPTER FOUR: DUAL TARGETING OF TM AND EPCR FUSION PROTEINS TO THE ENDOTHELIUM

I. INTRODUCTION

Although anchoring TM to ICAM-1 appears to improve partnering with endogenous EPCR, PECAM-1 has desirable features from the standpoint of vascular immunotargeting[48]. Its constitutive, stable, and high level of expression throughout the vasculature makes it the preferred choice for targeting of prophylactic agents, e.g., prior to a predictable vascular insult like cardiopulmonary bypass or organ transplantation. Likewise, PECAM-1 differs from other pan-endothelial determinants (e.g., angiotensin converting enzyme, or ACE), in that it is relatively poorly internalized by ECs, allowing for surface targeting of TM fusion proteins. Finally, anchoring of scFv/TM to PECAM-1 is unlikely to be deleterious, and if anything, would be expected to have an anti-inflammatory effect due to inhibition of transendothelial leukocyte migration[158,159].

As a result, we wanted to explore the possibility of utilizing PECAM-1 as a surface determinant for dual targeting of recombinant scFv/TM and scFv/EPCR. By anchoring both proteins to PECAM-1, we hypothesized that we would achieve sufficient proximity to allow enzymatic partnering. Another reason for choosing PECAM-1 as the surface determinant was our discovery of the "collaborative enhancement" phenomenon, in which paired antibodies to adjacent, distinct epitopes on PECAM-1 increase each other's binding to the endothelium *in vitro* and *in vivo*[142]. Based on this mechanism, we hypothesized that scFv/TM and scFv/EPCR fusion proteins directed to paired PECAM-1 epitopes would enhance – rather than competitively inhibit – each other's binding. Altogether, dual targeting of these therapeutic fusion proteins would have the capacity to accelerate protein C activation via two distinct mechanisms: 1. collaborative enhancement of binding and 2. enzymatic partnering of the TM and EPCR moieties.

II. RESULTS

Construction of a PECAM-targeted scFv/EPCR Fusion Protein

Cloning of Mec13 scFv and fusion to mouse EPCR

Previous studies in our laboratory demonstrated that mAbs 390 and Mec13.3 (hereafter referred to as Mec13), which bind to distinct, but adjacent, epitopes located in the extracellular Ig-domain 2 of mouse PECAM-1[160], enhance each others binding (Figure 4.1a). This phenomenon of "collaborative enhancement" exists in both transfected (i.e. REN-PECAM) cells and mouse endothelial cells (Figure 4.1b) and also contributes to enhanced endothelial binding of antibodies *in vivo* (Figure 4.1c)[142].

To take advantage of collaborative enhancement with 390 scFv/TM, we wanted to design the scFv/EPCR fusion protein using an antibody fragment derived from the Mec13 hybridoma. As in the cloning of the YN1 scFv described in Chapter 3, the Mec13 V_H cDNA was easily identified using degenerate framework region 1 (FR1) primers. Once again, however, this approach produced only a non-functional, myeloma-derived V_L cDNA, with an in frame stop codon in the FR1 region (Figure 4.2a). As a result, the Mec13 light chain was sequenced using the N-terminal Edman technique. The first 7 amino acids of the FR1 region were identified and used to clone of a full length V_L cDNA (Figure 4.2a). The V_H and V_L cDNAs were assembled into a complete anti-PECAM-1 Mec13 scFv, which was fused to the extracellular domain of EPCR. The scFv moiety was positioned on the 3' end, to keep the protein C binding site of EPCR (located on the N-terminal end) freely accessible (Figure 4.2b). Recombinant soluble mouse EPCR (sEPCR) was synthesized as well. The purity of each protein is shown by gel electrophoresis (Figure 4.2c).

Binding of Mec13 scFv/EPCR to REN-PECAM cells and immobilized Protein C

Both Mec13 scFv and the Mec13 scFv/EPCR bound to REN-PECAM-

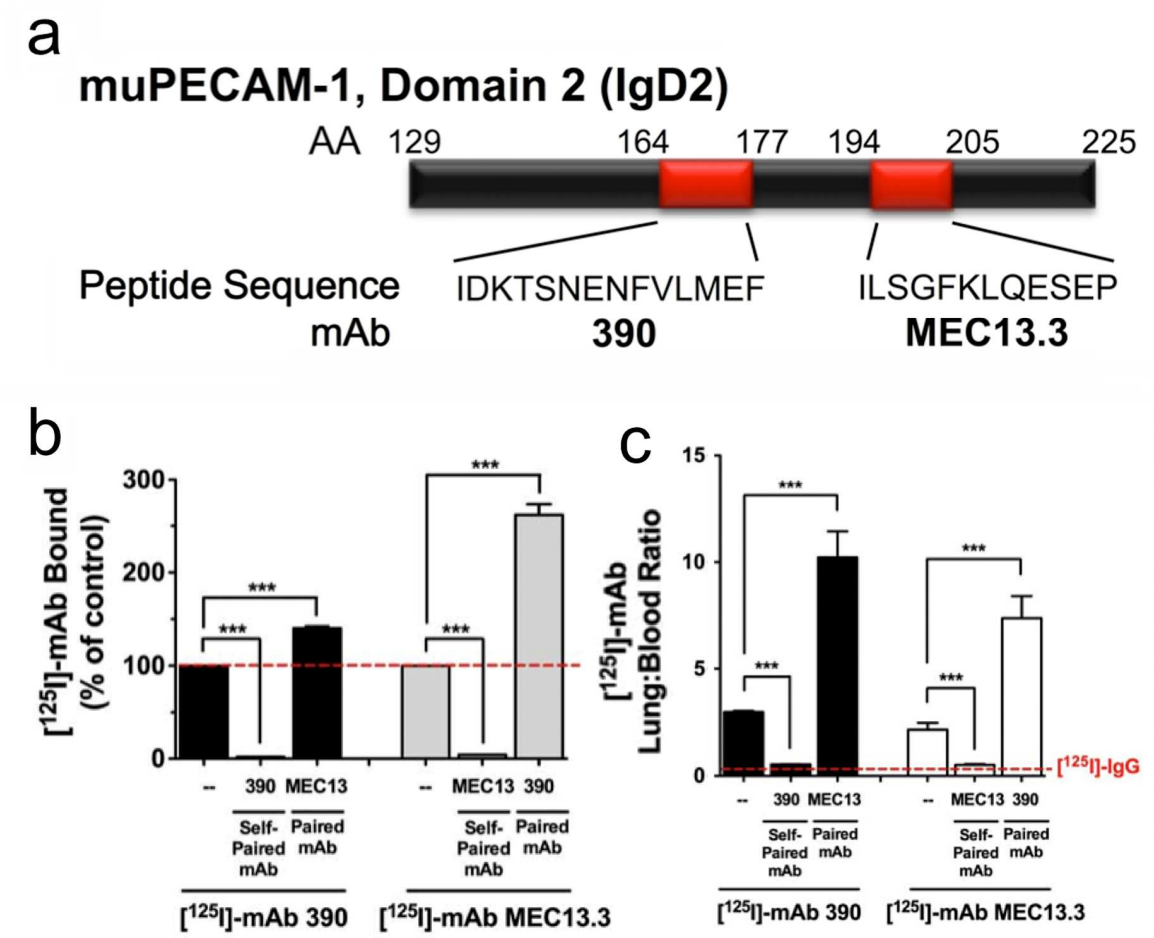

Figure 4.1. Collaborative enhancement of mAb binding to PECAM-1
(a) Amino acid location of epitopes for mAbs 390 and MEC13 on Ig-domain 2 (IgD2) of mouse PECAM-1 (b) Collaborative binding studies of mAbs 390 and MEC13 on REN-PECAM cells. Whereas unlabeled self-paired mAb 390 and mAb MEC13 competitively inhibit binding of [^{125}I]-mAb390 and [^{125}I]-mAb MEC13 to REN-PECAM cells, mAb pairs [^{125}I]-mAb 390/MEC13.3 and [^{125}I]-mAb MEC13.3/390 enhance binding by 1.5 fold and 2.7 fold, respectively. (c) *In vivo* endothelial targeting of [^{125}I]-mAb to PECAM-1 is enhanced by paired anti-PECAM-1 mAb. Lung:blood ratio for [^{125}I]-mAb 390/mAb MEC13 and [^{125}I]-mAb MEC13.3/mAb 390 pairs increases 3.4 fold. The dotted red line is the lung:blood ratio of [^{125}I]-IgG at 30 minutes. Data is reported as the standard error of the mean of n = 4–5 animals (***, P = 0.001). (All data reproduced from Chacko A-M et al. PLoS One 2012, reference 142)

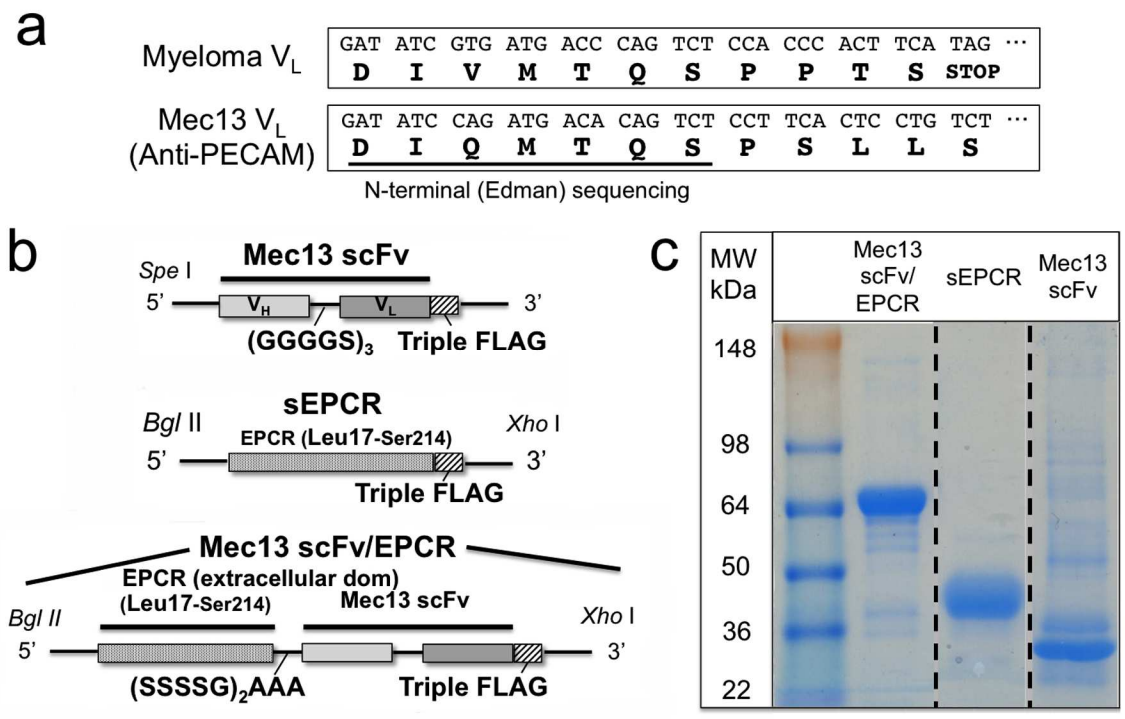

Figure 4.2. Cloning, assembly, and purification of Mec13 scFv, sEPCR, and Mec13 scFv/EPCR fusion protein

(a) The Mec13 V_L and the myeloma-derived V_L are nearly identical at the N-terminus of FR1 region. N-terminal (Edman) sequencing was used to identify a one amino acid difference (Gln vs. Val), which ultimately enabled amplification of a full length Mec V_L cDNA. (b) Assembly of V_H and V_L sequences into Mec13 scFv and Mec13 scFv/EPCR constructs. An sEPCR construct was also made (c) Purity of recombinant proteins as shown by SDS PAGE.

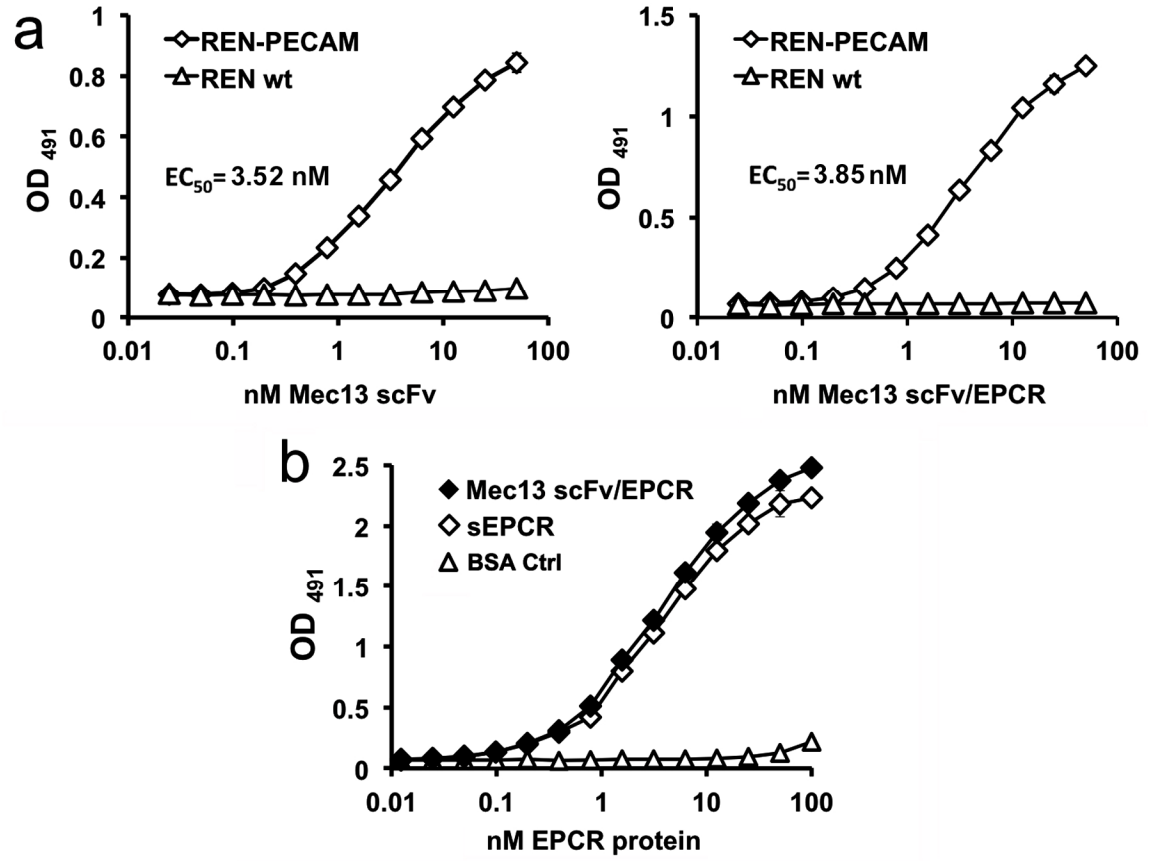

Figure 4.3. Function of scFv and EPCR moieties of Mec13 scFv/EPCR fusion protein

(a) Cell based ELISAs show that binding of Mec13 scFv/EPCR fusion protein to PECAM expressing REN cells is similar to that of Mec13 scFv. No significant binding is seen to wild type REN cells. (b) Mec13 scFv/EPCR fusion protein binds immobilized protein C in nearly identical manner as sEPCR. Empty triangles (△) indicate non-specific binding of Mec13 scFv/EPCR to BSA-coated wells. All experiments were done in triplicate (each point shown represents three wells), with SD shown.

cells, but not wild type REN cells (Figure 4.3a). Having confirmed the function of the scFv moiety, the function of the EPCR moiety was tested by comparing the binding of Mec13 scFv/EPCR and sEPCR to immobilized protein C. Both proteins showed equal binding, with no non-specific binding to albumin-coated wells (Figure 4.3b).

Functional Activity of Mec13 scFv/EPCR

Creation of TM expressing REN wt and REN-PECAM cells

To assess the ability of Mec13 scFv/EPCR to augment protein C activation by TM/thrombin complex on the cell surface, we generated a series of transfected REN cells stably expressing mouse TM and/or PECAM-1 on their surface. Thrombin-dependent protein C activation was measured on REN-PECAM-TM cells, which stably express both mouse PECAM-1 and TM (Figure 4.4a), and compared to APC generation on REN-TM and REN-PECAM cells. As expected, REN-TM and REN-PECAM-TM cells, but not TM-lacking cells (REN and REN-PECAM) exerted thrombin dependent activation of protein C (Figure 4.4b).

Mec13 scFv/EPCR enhances APC generation on REN-PECAM-TM cells

Mec13 scFv/EPCR stimulated thrombin-dependent production of APC by REN-PECAM-TM, but not REN-TM cells (Figure 4.4c). This indicates that the EPCR fusion protein is able to partner with TM in the cell membrane while bound to PECAM. No such effect was seen with Mec13 scFv or sEPCR (Figure 4.4d), confirming the need for both functional moieties in the fusion protein to bind to target cells and partner with TM in the plasma membrane.

Dual Targeting of Mec13 scFv/EPCR and 390 scFv/TM to REN Cells

Mec13 scFv/EPCR and 390 scFv/TM demonstrate collaborative enhancement

Collaborative enhancement of binding was originally described with paired

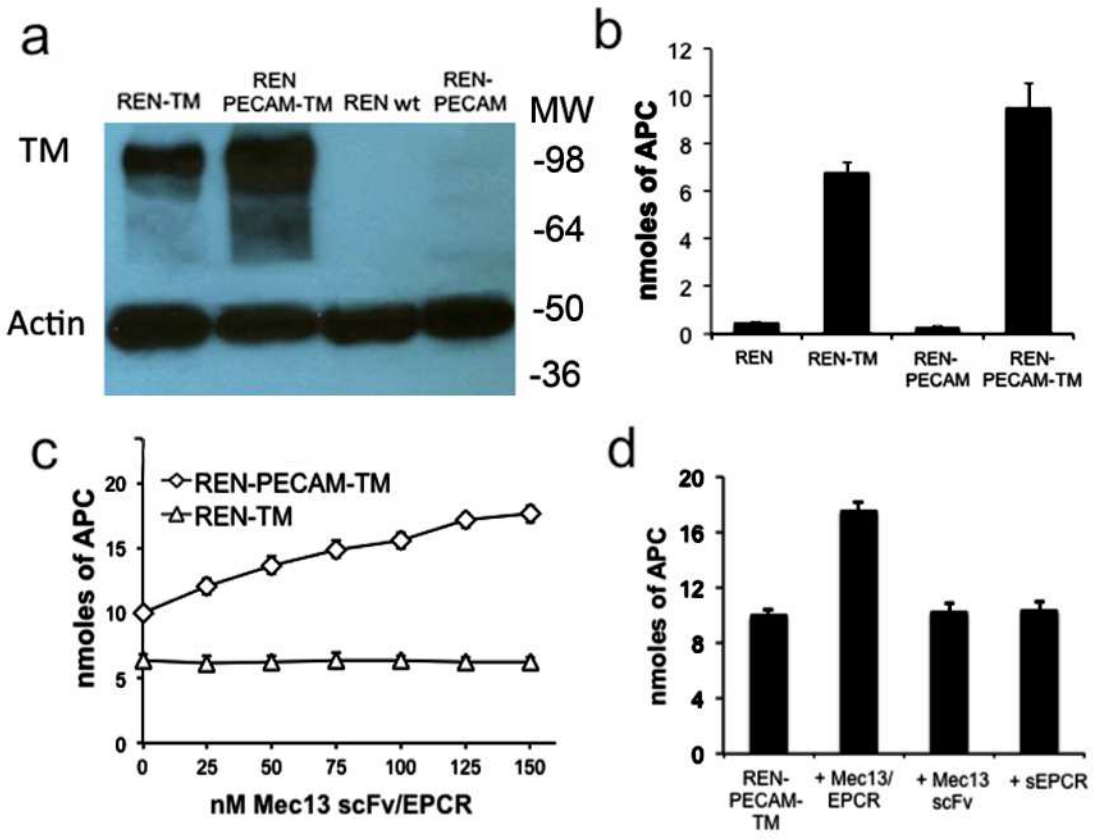

Figure 4.4. Functional activity of Mec13 scFv/EPCR fusion protein
(a) Western blotting confirms expression of mouse TM on REN-PECAM-TM and REN-TM cells. (b) APC generation assay on REN-PECAM-TM and REN-TM cells confirms surface localization and functional activity of expressed TM. (c) Mec13/EPCR enhances protein C activation by surface expressed TM on REN-PECAM-TM cells. No effect is seen on REN-TM cells, to which the fusion does not bind. (d) Mec13 scFv and sEPCR (each 150 nM) have no effect on APC generation on REN-PECAM-TM cells.

antibodies to PECAM-1 (Figure 4.1). We were interested to determine if TM and EPCR fusion proteins directed to the same paired epitopes would demonstrate the same phenomenon. Indeed, both Mec13 scFv and Mec13 scFv/EPCR increased the binding of 390 scFv/TM to REN-PECAM cells (Figure 4.5a). Likewise, 390 scFv and 390 scFv/TM increased the binding of Mec13 scFv/EPCR to these cells (Figure 4.5b).

Mec13 scFv/EPCR enhances protein C activation by 390 scFv/TM on REN-PECAM cells

We next studied the activation of protein C on REN-PECAM cells following dual targeting of scFv/TM and scFv/EPCR fusion proteins. Mec13 scFv/EPCR demonstrated a dose-dependent enhancement of thrombin-dependent APC generation in cells also treated with 390 scFv/TM, with nearly ~5-fold increase seen at the highest dose (Figure 4.6a).

In theory, both enhanced binding and functional partnering between the TM and EPCR moieties may contribute to the 5-fold increase observed. We conducted several experiments to determine the relative contribution of each effect. First, Mec13 scFv (lacking the EPCR moiety) was used to estimate the "binding effect" and provided ~2-fold stimulation of APC production by 390 scFv/TM (Figure 4.6b). Conversely, we estimated the contribution of enzymatic partnering (the "EPCR effect") by using mAb1560 to block the interaction of EPCR and murine protein C. In REN-PECAM cells treated with Mec13 scFv/EPCR and 390 scFv/TM, blockade of EPCR reduced APC generation by ~2-fold to almost exactly the level seen in cells co-treated with TM fusion protein and Mec13 scFv (Figure 4.6b). Taken together, these data reveal two distinct mechanisms, which make roughly equivalent contributions to the net effect of Mec13 scFv/EPCR on the generation of APC by 390 scFv/TM.

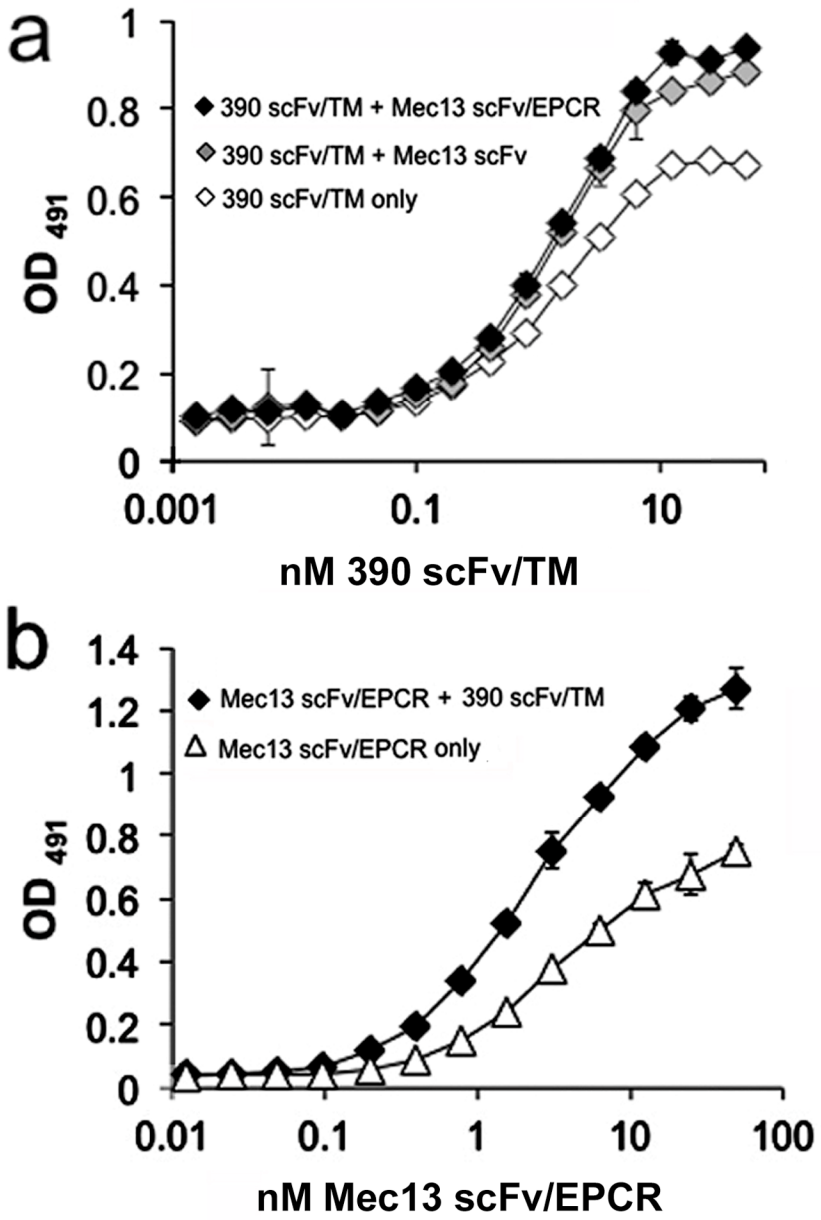

Figure 4.5. Mec13 scFv/EPCR and 390 scFv/TM fusion proteins demonstrate collaborative enhancement of binding

(a) In agreement with experiments done using intact antibodies, Mec13 scFv and Mec13 scFv/EPCR enhance the binding of 390 scFv/TM and (b) 390 scFv/TM enhances the binding of Mec13 scFv/EPCR to REN-PECAM cells. Experiments were done in triplicate (each point shown represents three wells), with SD shown.

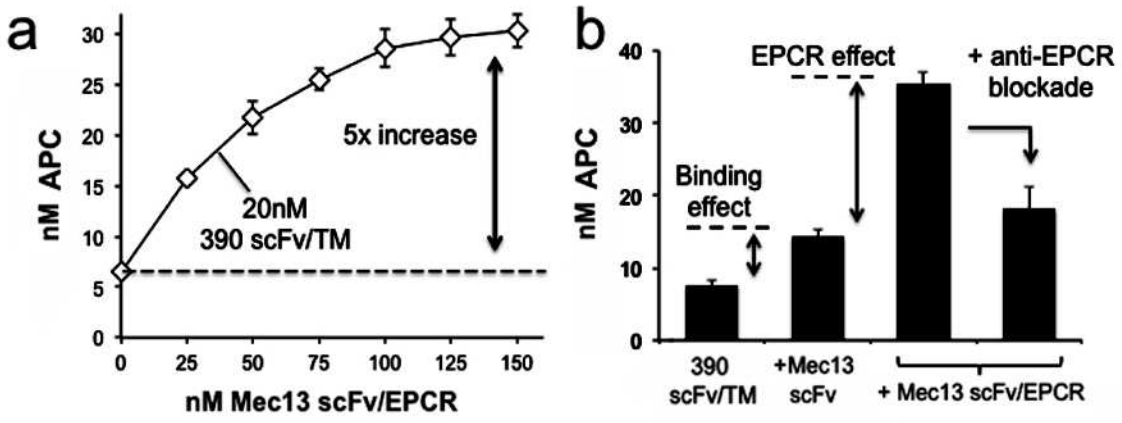

Figure 4.6. Mec13 scFv/EPCR enhances APC generation by 390 scFv/TM via two distinct mechanisms

(a) Co-treatment of REN-PECAM cells with Mec13 scFv/EPCR produces a dose dependent increase in APC generation by surface bound 390 scFv/TM. (b) Additional experiments suggest that two distinct effects contribute to the action of Mec13 scFv/EPCR fusion protein: 1. an increase in 390 scFv/TM binding and 2. partnering of cell bound TM and EPCR. The binding effect, demonstrated by co-treatment of cells with 390 scFv/TM and Mec13 scFv (150 nM), is significant ($p = 0.004$). Likewise, co-treatment with 390 scFv/TM and Mec13 scFv/EPCR results in significantly greater APC generation ($p < 0.001$ compared to all other groups) and is demonstrated to be EPCR-dependent via the use of an anti-EPCR monoclonal antibody. All experiments were done in triplicate. Data shown are mean ± SD.

Dual Targeting on Mouse Endothelial Cells

Mec13 scFv/EPCR enhances protein C activation by 390 scFv/TM on MS1 cells

Using the anti-mTM antibody blockade technique described in Chapter 2, we measured protein C activation by 390 scFv/TM anchored to MS1 cells, with and without addition of Mec13 scFv/EPCR. Similar to what had been seen on REN-PECAM cells, Mec13 scFv/EPCR increased protein C activation by 390 scFv/TM. Likewise, use of Mec13 scFv and EPCR blocking mAb revealed a similar contribution of two distinct mechanisms by which the EPCR fusion protein exerts its effect: collaborative enhancement of binding and enzymatic partnering (Figure 4.7).

Construction and characterization of YN1 scFv/EPCR

We next sought to determine if anchoring TM and EPCR to different surface molecules would achieve effects similar to what was seen with Mec13 scFv/EPCR and 390 scFv/TM. To test this, we designed and synthesized an anti-ICAM YN1 scFv/EPCR fusion protein (Figure 4.8a). We confirmed its binding to ICAM-expressing cells and its effect on APC generation by TM in a series of experiments similar to those described above. In this case we utilized REN-ICAM-TM cells, instead of REN-PECAM-TM cells (Figure 4.8b). Anti-ICAM scFv/EPCR bound REN-ICAM-TM cells, but not REN-TM cells (Figure 4.8c), and enhanced protein C activation by membrane TM (Figure 4.8d). Therefore, anti-ICAM scFv/EPCR displayed binding and functional activity, including TM partnering, similar to Mec13 scFv/EPCR.

YN1 scFv/EPCR does not enhance protein C activation by 390 scFv/TM

We utilized YN1 scFv/EPCR and 390 scFv/TM fusion proteins to test anchoring TM and EPCR to different surface molecules. In contrast to Mec13 scFv/EPCR, no enhancement of protein C activation was seen with YN1 scFv/EPCR fusion protein, nor was there any effect of the EPCR blockade

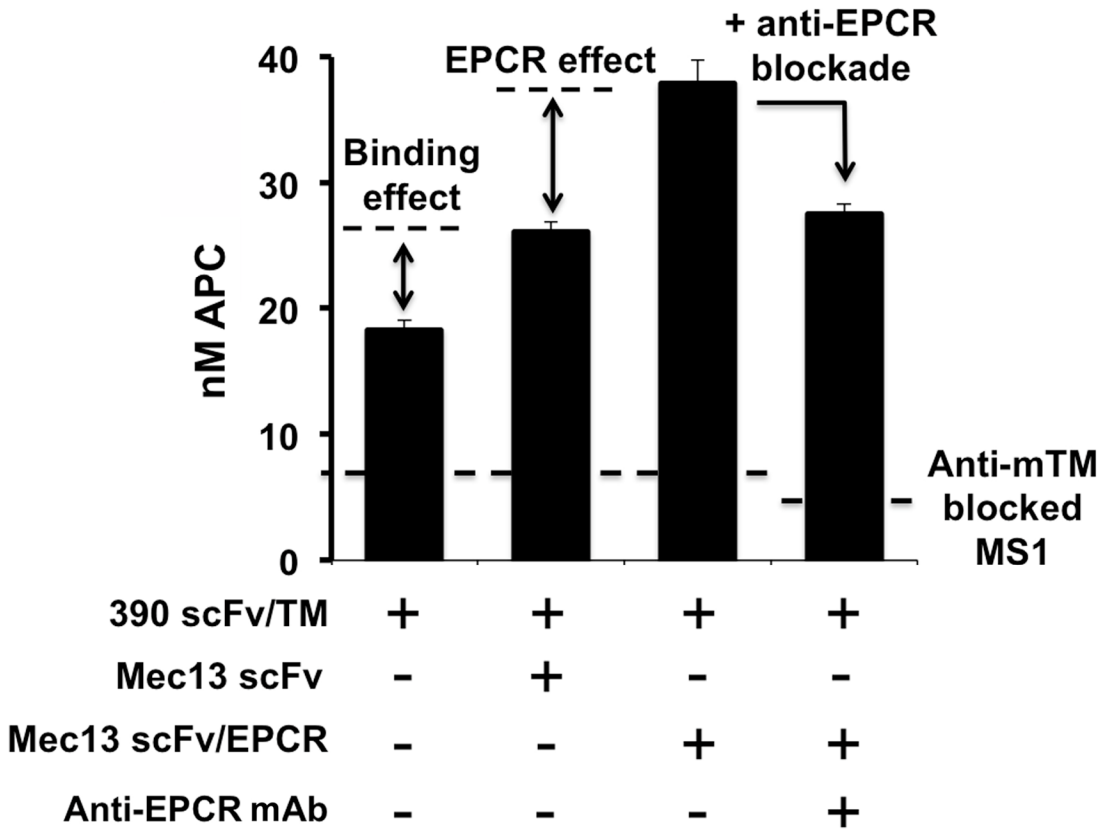

Figure 4.7. Mec13 scFv/EPCR enhances APC generation by 390 scFv/TM on antibody blocked MS1 cells

(a) APC generation by 390 scFv/TM was assayed on anti-mTM blocked MS1 cells. The residual activity of endogenous TM is indicated by the dotted line. Mec13 scFv/EPCR (100 nM) enhances APC generation by cell bound 390 scFv/TM. As seen in REN-PECAM cell experiments, two independent mechanisms can be discerned: a binding effect ($p < 0.001$ compared to 390 scFv/TM alone) and an EPCR-dependent effect ($p < 0.001$ compared to all other groups). Of note, EPCR blockade slightly reduces the residual activity of endogenous TM, as indicated by the lower dotted line. Experiments were done in triplicate. Data shown are mean ± SD.

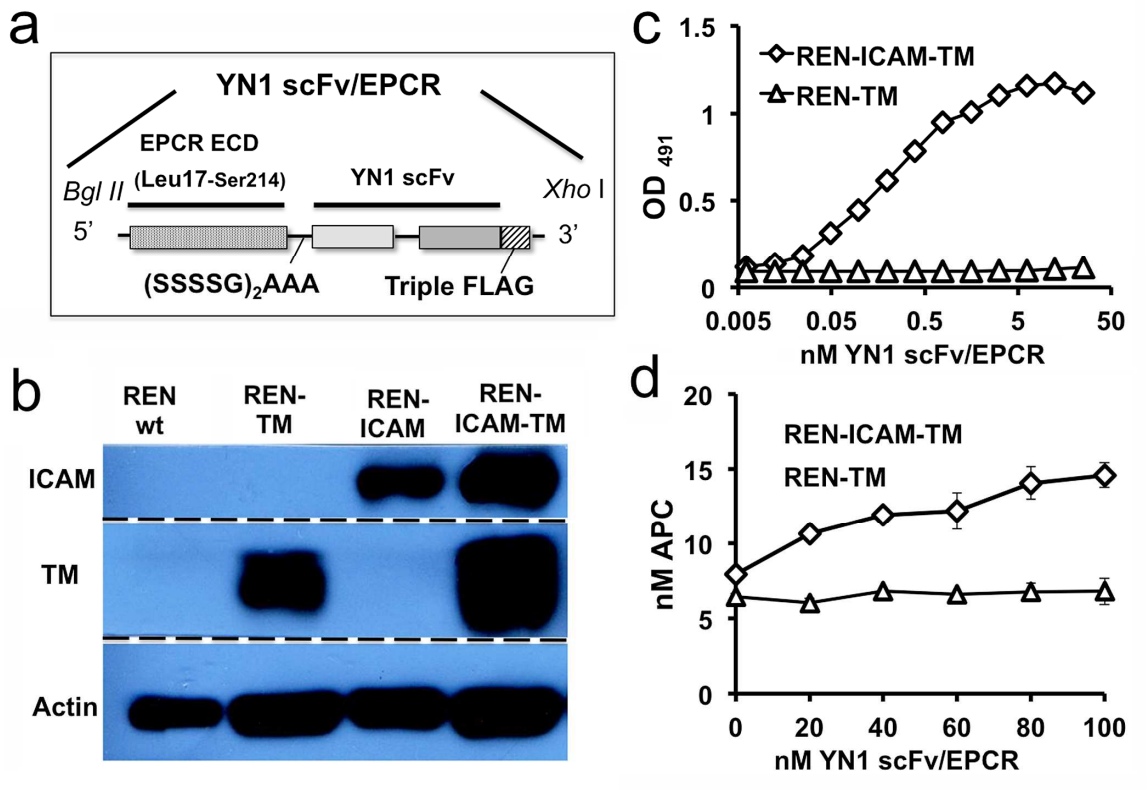

Figure 4.8. Construction and characterization of YN1 scFv/EPCR
(a) Molecular design of YN1 scFv/EPCR (b) Western blot of REN-ICAM-TM cells demonstrates expression of mouse ICAM-1 and TM. (c) Cell-based ELISA confirms binding of anti-ICAM/TM to REN-ICAM-TM but not REN-TM cells. (d) YN1 scFv/EPCR enhances activation of protein C by surface expressed TM when bound to REN-ICAM-TM cells. ELISA and APC generation experiments done in triplicate, data shown are mean ± SD.

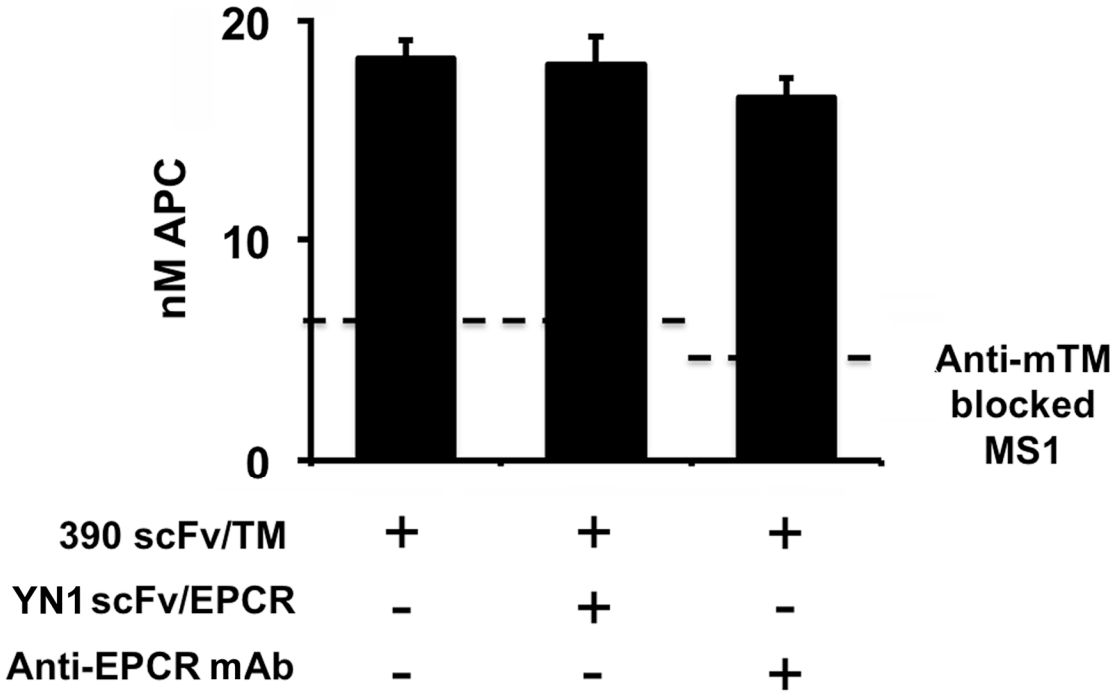

Figure 4.9. YN1 scFv/EPCR does not enhance protein C activation by 390 scFv/TM on MS1 cells

Anchoring TM and EPCR to different endothelial surface determinants on MS1 cells (PECAM-1 and ICAM-1, respectively), does not enhance APC generation ($p = 0.75$). Antibody blockade of EPCR has no effect, other than a small reduction in the residual activity of endogenous TM. Experiments were done in triplicate; data shown are mean ± SD.

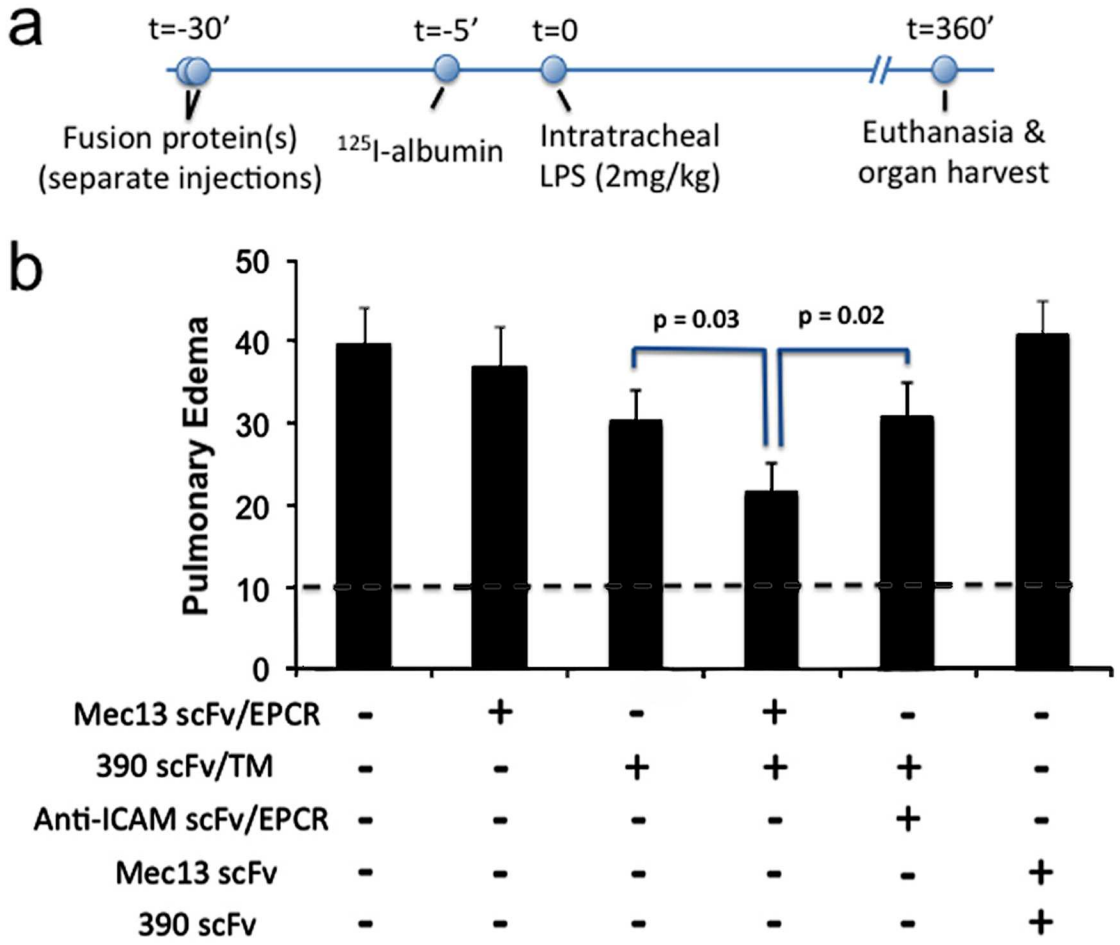

Figure 4.10. Dual targeting of Mec13 scFv/EPCR and 390 scFv/TM reduces pulmonary edema in a mouse model of lung injury

(a) Timeline of intratracheal LPS lung injury model. (b) Pulmonary edema, as determined by leakage of ^{125}I-labeled albumin from the blood into lung interstitium and/or alveolar space, is reduced by pre-treatment with 390 scFv/TM. Co-administration of Mec13 scFv/EPCR, but not anti-ICAM scFv/EPCR, significantly enhances protection. Pre-treatment with Mec13 scFv/EPCR alone and co-administration of Mec13 and 390 scFvs have no effect. Data shown are mean ± SD, with n=4-5 mice in each group. Dotted line indicates level of albumin leakage seen in control animals that did not receive LPS.

antibody (Figure 4.9).

In vivo Experiments

Dual targeting of fusion proteins in a mouse model of acute lung injury

Dual targeting of Mec13 scFv/EPCR and 390 scFv/TM was then tested in a mouse model of lung inflammation/injury and compared to treatment with the TM fusion protein alone. Pulmonary edema induced by LPS endotoxin challenge was measured by uptake of IV injected ^{125}I-labeled albumin. Fusion proteins, or PBS vehicle, were injected IV 30 minutes prior to LPS challenge (Figure 4.10a). Dual targeting of Mec13 scFv/EPCR and 390 scFv/TM maximally effectively reduced pulmonary edema, with a significant improvement compared to treatment with the TM fusion protein alone. Administration of Mec13 scFv/EPCR alone had no effect, nor did sequential injection of Mec13 and 390 scFvs. The latter was done as a control to ensure that the effects on barrier function were not simply the result of the two antibody fragments binding to PECAM-1. Finally, co-treatment with 390 scFv/TM and YN1 scFv/EPCR resulted in no additional protection, consistent with our observations on MS1 cells (Figure 4.10b).

III. CONCLUSIONS

This chapter describes an alternate strategy for replicating the enzymatic partnering seen with endogenous TM and EPCR, namely dual targeting of both recombinant molecules to the same endothelial surface determinant. As hypothesized, our *in vitro* experiments indicate two distinct mechanisms by which the Mec13 scFv/EPCR enhances the activity of 390 scFv/TM: 1. increased binding and 2. enzymatic partnering (Figure 4.11).

Interestingly, we find that anchoring TM and EPCR to different endothelial determinants has no effect. This result is consistent with the experiments described in Chapter 1, in which TM and EPCR were co-immobilized on polyurethane. In those studies, EPCR was found to have an effect only when

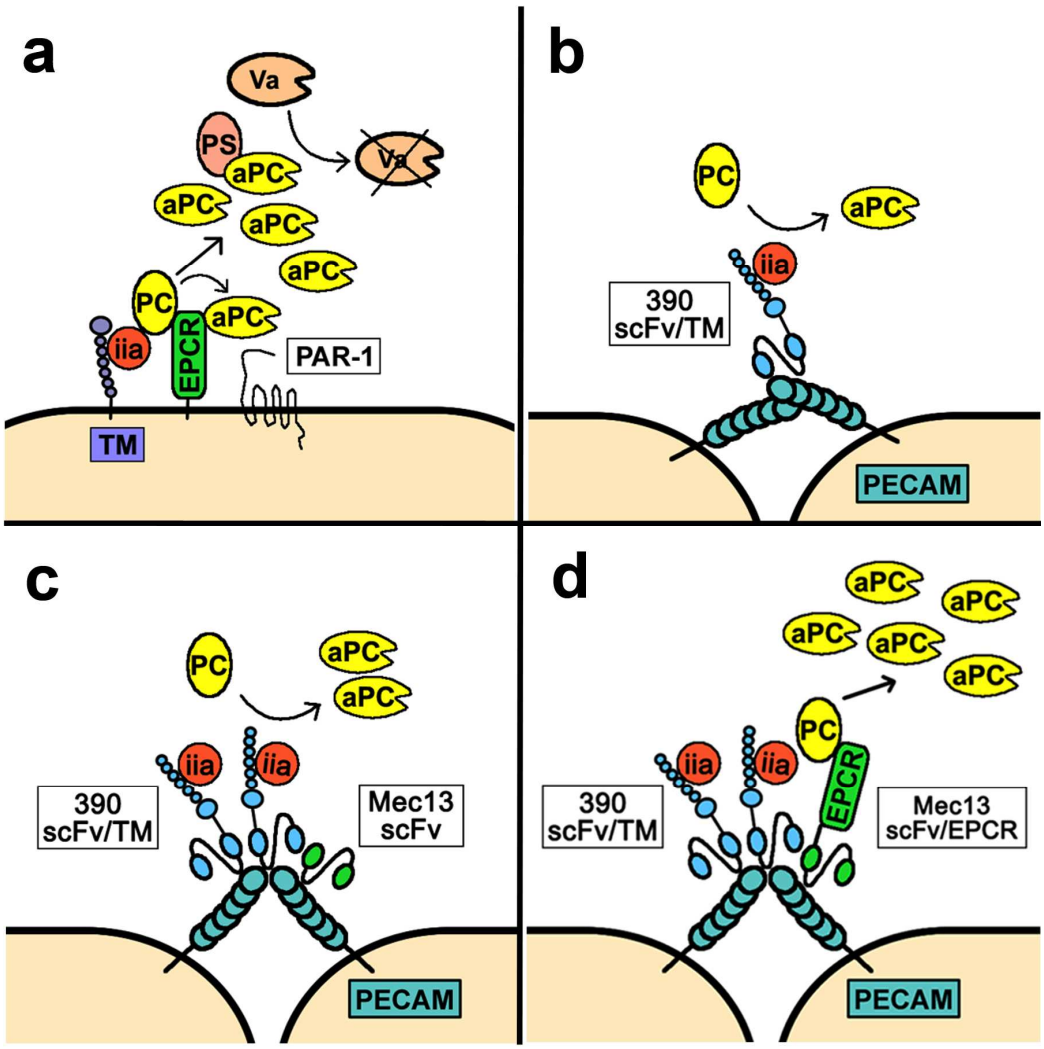

Figure 4.11. Schematic model of dual targeting of scFv/TM and scFv/EPCR to increase APC production

(a) Normal function of thrombin, TM, EPCR, and PC on the endothelial cell membrane. Endothelial TM binds thrombin (Factor IIa) and activates protein C. This process is accelerated by the key co-factor, EPCR, which optimally positions PC for cleavage. APC can signal to endothelial cells while bound to EPCR or can bind to protein S and exert anti-coagulant effects, such as the cleavage of Factor Va. (b) APC generation by surface bound 390 scFv/TM fusion protein. TM fusion protein anchored to PECAM-1 generates APC, but is unable to partner with endogenous EPCR. (c) Mec13 scFv increases binding of 390 scFv/TM to PECAM-1 via "collaborative enhancement" mechanism. Increased binding results in an ~2 fold increase in APC production. (d) Dual targeting of 390 scFv/TM and Mec13 scFv/EPCR. The combination of enhanced binding and enzymatic partnering between TM and EPCR further increases APC production, to levels roughly equal to endogenous TM/EPCR.

the two recombinant proteins were kept in close proximity (< 10 nm)[133], and not with a random, unordered distribution. Although our experiments on mouse ECs do not establish a clear cutoff value, it seems likely that some critical distance exists, beyond which endothelial-anchored TM and EPCR are no longer sufficiently close to partner efficiently. These results also support the notion that PECAM-anchored TM may be unable to partner with endogenous EPCR due to insufficient proximity along the membrane surface.

Apart from its mechanistic significance, dual targeting of TM and EPCR fusion proteins to paired PECAM-1 epitopes demonstrates enhanced protection *in vivo* and could represent a plausible strategy for mitigating acute endothelial dysfunction in a variety of settings.

IV. MATERIALS AND METHODS

Cell lines

Lysate from the Mec13.3 hybridoma (herein referred to as Mec13) was a generous gift of Dr. Annunciata Vecchi. MS1 cells were purchased from ATCC (Manassas, VA) and maintained in DMEM with 10% FBS and 1% antibiotic-antimycotic (Life technologies, Grand Island, NY).

Antibodies and other reagents

Anti-TM polyclonal antibody (AF3894) was purchased from R&D systems (Minneapolis, MN). A second anti-TM polyclonal antibody, used in Western blotting (sc-7097) was purchased from Santa Cruz Biotechnology (Santa Cruz, CA). The anti-EPCR blocking mAb 1560, was supplied by the Esmon laboratory. HRP-conjugated Anti-FLAG (M2-HRP) antibody was obtained from Sigma Aldrich (St Louis, MO). HRP-conjugated anti-goat secondary antibody (sc-2056) was from Santa Cruz Biotechnology. Purified recombinant human protein C was a generous gift of Dr. Sriram Krishnaswamy. Bovine thrombin and lipopolysaccharide (LPS, serotype B4) were purchased from Sigma. APC substrate, S-2366, was purchased from Diapharma (West Chester, OH).

Cloning of Mec13 V_L and V_H cDNAs

Mec13.3 cell lysate in Trizol was extracted with chloroform and phases were separated by centrifugation. The aqueous phase was removed, mixed with ethanol, and total RNA was purified using the RNeasy kit (Qiagen, Valencia, CA). Combined reverse transcription and PCR was performed using SuperScript One Step RT-PCR kit (Life Technologies, Grand Island, NY). Mec13 light chain was purified on reducing SDS PAGE and sent for N-terminal (Edman) sequencing at the UC Davis Proteomics Core Facility. The 7 amino acids identified were used to design degenerate PCR primers.

Assembly and expression of Mec13 scFv, sEPCR, and Mec13/EPCR constructs

Completed Mec13 V_L and V_H cDNAs were assembled into a scFv construct, with V_H and V_L sequences separated by a $(GGGGS)_3$ linker and a triple FLAG tag appended to the 3' end (C-terminus) for purposes of purification and detection. The extracellular domain of mouse EPCR (sEPCR) was cloned by PCR from the full-length cDNA described in Chapter 2, and a C-terminal triple FLAG tag appended. Finally, the Mec13 scFv/EPCR fusion protein was constructed with mEPCR on the 5' end (N-terminus), separated from the Mec13 scFv by an $(SSSSG)_2$AAA linker. All proteins were expressed in S2 cells and purified using an anti-FLAG affinity column (Sigma Aldrich, St Louis, MO).

Generation of REN-derived stable cell lines

REN-PECAM-TM and REN-ICAM-TM cells. To make cells expressing both PECAM/TM and ICAM/TM, a mouse TM (mTM) cDNA (containing the entire coding sequence of mTM and a portion of the 5' and 3' UTRs, nt 87-3482) was purchased from Origene and cloned into the pcDNA3.1/Zeo(-) vector (Life Technologies, Grand Island, NY). Since REN-PECAM and REN-ICAM cells already stably express the Geneticin resistance gene, this expression vector (which confers resistance to the antibiotic Zeocin) was utilized. Each cell type

was transfected with Lipofectamine 2000 and selected in media with 250 μg/mL of Zeocin and 200 μg/mL of Geneticin.

Live cell ELISA assays

ELISAs were performed on live cells as described in Chapters 2 and 3. In ELISA experiments involving more than one recombinant protein, however, such as those aimed at measuring collaborative enhancement of binding, anti-FLAG-HRP could not be used, as each fusion protein carries a C-terminal triple FLAG tag. In these cases, detection was via either goat anti-mTM or goat anti-mEPCR polyclonal antibody, with an anti-goat-HRP secondary antibody. ELISA binding data was analyzed using PRISM 6.0 software (GraphPad, San Diego, CA).

Protein C ELISA

ELISAs were performed using the same protocol as above, except that instead of live cells, fusion proteins were bound to protein C immobilized on high-binding plastic wells. Briefly, wells were incubated overnight at 4℃ with a solution of 4 μg/mL recombinant human protein C in Tris buffered saline (TBS). Protein C solution was removed and the plate was blocked with 3% BSA solution for 2 hours. BSA-coated wells with no protein C were used as a control for non-specific binding.

Protein C activation assays

Generation of APC by scFv/TM fusion was assayed as described in Chapters 2 and 3. Briefly, cell monolayers were incubated with various combinations of TM and EPCR fusion proteins and washed three times with media prior to the addition of 1nM thrombin and 100nM protein C. In all cases, protein C activation occurred at 37 ℃ in assay buf fer (20 mM Tris, 100 mM NaCl, 1 mM $CaCl_2$, 0.1% (w/v) BSA, pH 7.5), and the reaction was stopped by addition of an excess of hirudin. Anti-mTM antibody blockade and EPCR blockade using mAb 1560 were performed as described in Chapter 2.

IT LPS model

Animal studies were carried out in accordance with the Guide for the Care and Use of Laboratory Animals as adopted by the NIH, under protocols (803320 and 804349) approved by University of Pennsylvania IACUC. The IT LPS model was performed as described in Chapter 3, with several exceptions. First, in some experiments, animals received more than one fusion protein, e.g., scFv/TM and scFv/EPCR. Proteins were injected IV in rapid succession, not mixed. Likewise, bronchoalveolar lavage was not performed in these experiments.

Data analysis and statistics

Results are expressed as mean ± SD unless otherwise noted. Significant differences between means were determined using Students t-test or one-way ANOVA followed by appropriate multiple comparison (Tukey) test. $P<0.05$ was considered statistically significant.

CHAPTER FIVE: DISCUSSION AND FUTURE DIRECTIONS

I. LIMITATIONS

The body of work described here is not without limitations. Of greatest concern is the issue touched upon in Chapter 1, namely that the 390 and YN1 scFv/TM fusion proteins are constructed with the N-terminal lectin domain of TM adjacent to the scFv moiety (Figure 1.2b). Although the data presented in subsequent chapters indicates that this "inverted" conformation does not entirely preclude the partnering of scFv/TM fusion proteins with endogenous surface partners (e.g., EPCR) or co-delivered fusion proteins (e.g., scFv/EPCR), it is likely to have some significant impact on the function of TM, and we have yet to investigate this possibility in detail. For example, we have only examined the functional activity of endothelial targeted TM fusion proteins with respect to APC generation. TM is well known to have numerous other functions, including the direct neutralization of cytokines via its N-terminal lectin domain and the activation of TAFI[122,161]. These activities may be altered or completely absent given the unnatural conformation of the TM moiety in the current generation of fusion proteins.

The use of MS1 cells, a transformed pancreatic-derived endothelial cell line, represents another significant technical limitation of the current body of work. Immortalized endothelial cells are likely to differ substantially from primary cultures and/or ECs *in vivo*, in particular with regard to the precise spatial relationships between endothelial surface molecules. Moreover, it is plausible that we have masked some of the significance of these issues via the use of reagents from several different species -- i.e., bovine thrombin and human PC zymogen, alongside mouse TM and EPCR.

Finally, the significance of our conclusions must be tempered by the preliminary nature of the work. We have yet to investigate any cytoprotective signaling through PAR1 or other receptors, which might be generated by endothelial targeted TM and EPCR fusion proteins. Since PAR1 is thought to

localize to the same apical membrane microdomains as EPCR[96], it is possible that PECAM-anchored TM will demonstrate weak cytoprotective signaling through this receptor. Furthermore, dual targeting of scFv/EPCR fusion protein to PECAM, which has a significant effect on APC generation, may have little or no impact on PAR1 signaling. On the other hand, it is possible that the requirement for molecular proximity may be less stringent in this case, as APC generated by TM and/or EPCR fusion proteins might diffuse along the endothelial surface, bind to endogenous EPCR, and signal through PAR1 in a paracrine manner. This intriguing issue clearly merits further investigation. Likewise, further characterization is warranted with regards to the *in vivo* protection offered by the fusion proteins. IT administration of LPS does not faithfully reproduce all of the pathological aspects of human lung injury[162]. Likewise, administration of fusion protein prior to LPS does not reflect a realistic clinical scenario. A rigorous appraisal of the benefit/risk ratio of TM and EPCR fusion proteins will need to be conducted in relevant animal models of human disease, with administration after the onset of injury. Moreover, we will need to directly test the importance of TM/EPCR partnering *in vivo*, before definitively concluding that this factor is responsible for any differences we observe in the therapeutic efficacy of various fusion proteins.

II. FUTURE DIRECTIONS

Design of Human PECAM and ICAM-targeted TM Fusion Proteins

To simultaneously address the various technical limitations discussed above, we have cloned two new scFvs, Ab62[163] and R6.5[164], which are specific for human PECAM-1 and ICAM-1, respectively (Figure 5.1a,b). We are in the process of assembling these into fusion proteins with human TM (hTM). Unlike the previous generation of mouse specific fusion proteins, we have designed the scFv/hTM fusion proteins in both available conformations (Figure 5.1c), including a more natural configuration with the lectin domain free at the N-terminus of the

molecule. This will allow us to test the significance of the “natural” vs. “inverted” conformations, not only on the various functions of hTM, but also its partnering with endogenous surface molecules. The widespread availability of high quality human primary ECs (e.g., HUVECs and human pulmonary microvascular endothelial cells, or HPMVECs), will resolve any artifacts related to the use of immortalized cells. Finally, hTM fusion proteins will be tested using human PC and thrombin, thus eliminating any issues related to species variation of reagents.

The use of human ECs will enable testing of signaling pathways and cell responses not possible with MS1 cells. In particular, HUVECs and HPMVECs both form tight monolayers and can be used for testing endothelial permeability. Since both thrombin and APC affect endothelial barrier function through PAR1[84], we plan to use permeability assays as an important means of testing the new hTM fusion proteins and their capacity to influence signaling through this receptor. Other responses known to depend on APC mediated signaling, e.g., the expression of cell-adhesion molecules, will also be examined.

Finally, the use of Ab62 scFv/hTM and R6.5 scFv/hTM fusion proteins should allow the study of other TM functions, including the potential neutralization of HMGB1, a damage-associated molecular pattern molecule (DAMP) and cytokine. HMGB1 is bound and sequestered by the N-terminal lectin domain of TM and infusion of recombinant sTM has been shown to reduce its plasma concentration in animal models of systemic inflammation[165,166]. The N-terminus of the lectin domain, which is exposed in both soluble and membrane-bound TM, may be inaccessible on the fusion proteins due to its positioning adjacent to the scFv moiety. Most importantly, these new scFv/TM fusion proteins will allow pre-clinical development in primates and, ultimately, testing in human clinical trials if warranted.

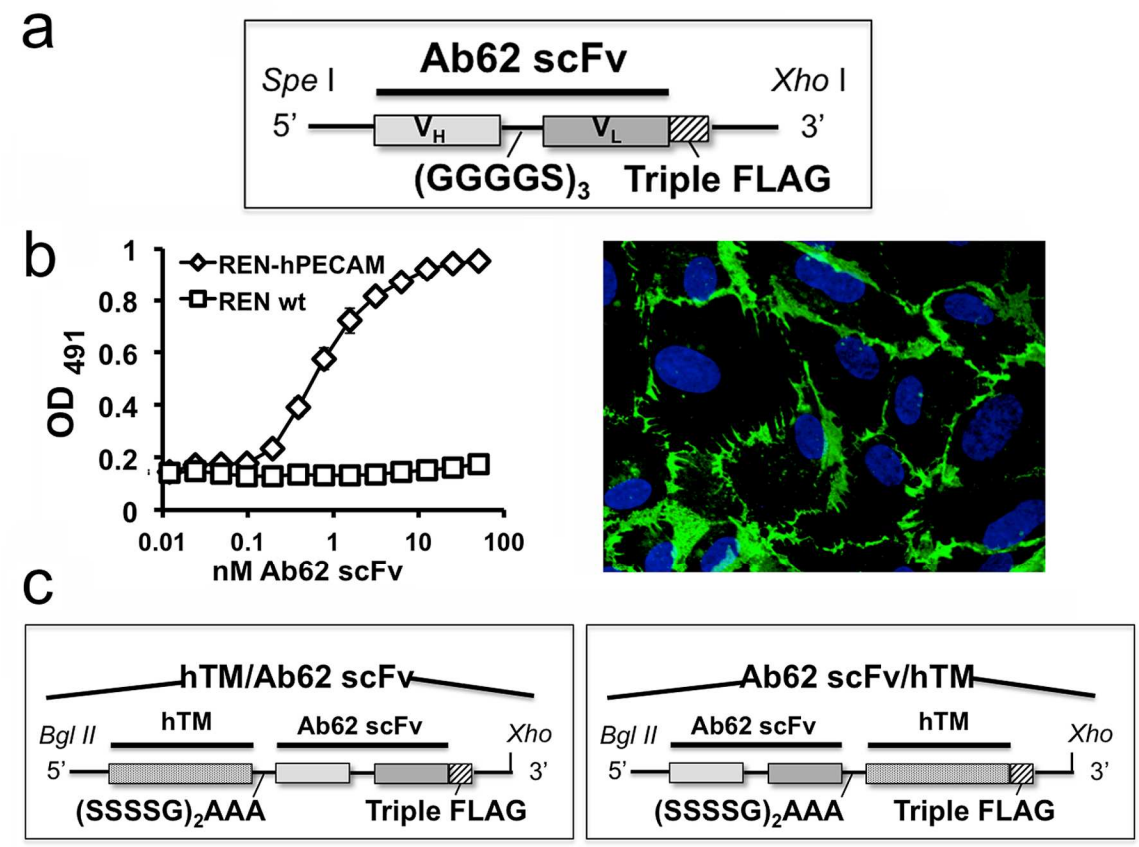

Figure 5.1. Human PECAM-1 Specific Ab62 scFv
(a) Molecular design of Ab62 scFv, (b) Ab62 scFv binds to human PECAM-1, as demonstrated by live cell ELISA (done with REN cells transfected with human PECAM-1) and immunofluorescence of HUVECs. Strong staining seen at cell-cell junctions is typical for PECAM-1. (c) Fusion of Ab62 scFv with human TM in both conformations, for testing of lectin and EGF domain function.

Strategies to Define and Improve Endothelial Targeting

One aspect of the endothelial targeted TM fusion proteins that remains poorly characterized is their ability to target the endothelium *in vivo*. Although initial experiments indicated that 390 scFv/TM effectively targets the lung following intravenous injection[127], subsequent efforts have failed to confirm thisresult. Likewise, the biodistribution of YN1 scFv/TM, which has been more rigorously characterized, indicates very weak targeting to lung endothelium. This result was somewhat unexpected, given the robust targeting of the parental mAb (Figure 5.2), and the fact that the scFv/TM fusion proteins are large enough to escape the rapid renal clearance seen with free scFvs.

There are multiple possible explanations for these findings. First, the scFv/TM fusion proteins are monovalent, and the decreased avidity, as compared to mAbs, could have a drastic effect on their ability to anchor themselves to the endothelium under the flow conditions present in the vasculature. Second, TM may mediate uptake or clearance of fusion proteins by the liver and spleen. Third, scFv/TM fusion proteins lack Fc domains and therefore are incapable of recycling through the neonatal Fc receptor (FcRn), which markedly prolongs the circulation time of mAbs[167]. Finally, there is some evidence that even bivalent engagement of ICAM-1 may induce internalization by ECs, meaning that some component of the lung biodistribution of YN1 mAb may reflect intracellular, rather than surface bound antibody[168]. Of note, this latter possibility differs from the others in that it would be a potential negative for endothelial targeting of TM, which requires surface localization.

To investigate these possibilities, we are in the process of designing and testing several new constructs. In particular, we are collaborating with the Tsourkas laboratory in the Department of Bioengineering to develop a means of site-specific conjugation of TM to anti-PECAM and anti-ICAM mAbs. Conventional mAb conjugation, which utilizes non-specific chemistry, is limited by poor efficiency, the possibility of impaired mAb or cargo (i.e. TM) function, and the inability to limit or precisely control conjugate size. The introduction of site

specific modifications on the mAb and TM moieties, however, allows the use of highly efficient click chemistry, results in predictable orientation of the components, and enables the incorporation of only one mAb and TM into each conjugate (Figure 5.3). Using this new technology, we plan to test the role of each of the above factors (avidity, TM clearance, FcRn recycling, and internalization) in determining biodistribution to the lung and other organs. Better understanding of these variables should allow the eventual design of TM therapeutics with improved endothelial targeting.

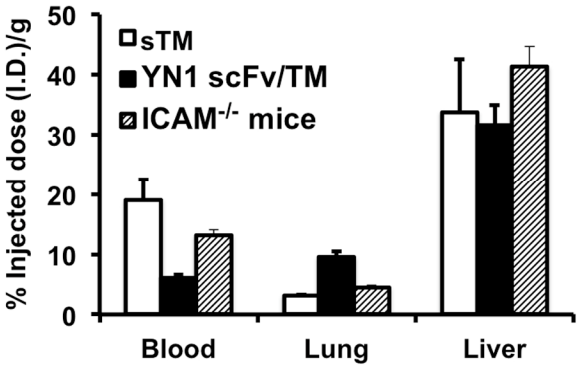

Protein	Lung biodistribution (%ID/g)
YN1 scFv/TM	9
YN1 mAb	81

Figure 5.2. Biodistribution of YN1 scFv/TM and YN1 mAb *in vivo*
(a) Biodistribution of YN1 scFv/TM at 30 min post-injection shows weak, but specific targeting to the lung, based on comparison to sTM and testing in ICAM$^{-/-}$ mice. (b) Lung targeting of YN1 scFv/TM is an order of magnitude weaker than parental mAb.

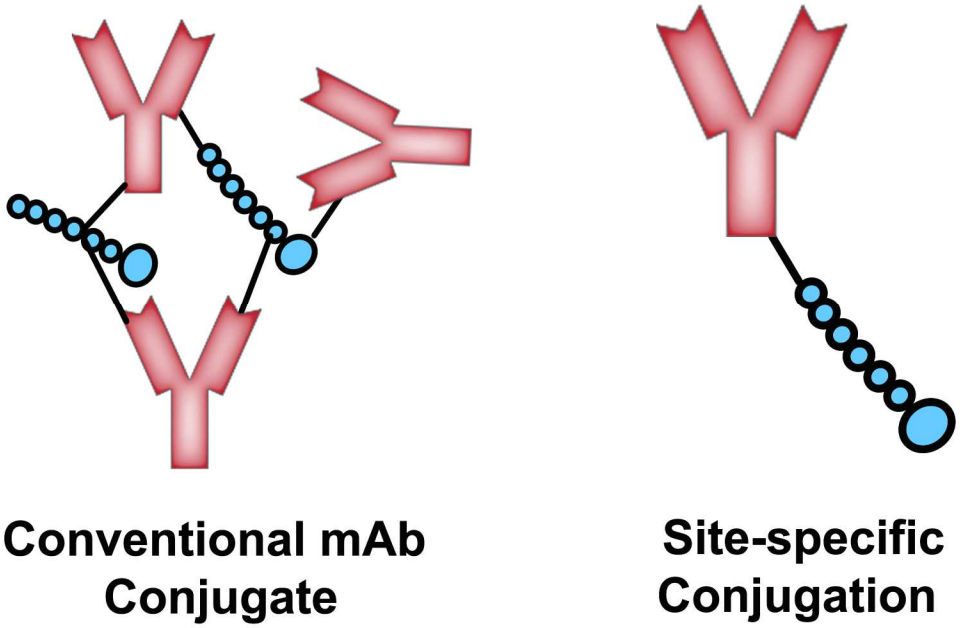

Figure 5.3. Design of site-specific mAb/sTM conjugates
Conventional bioconjugation is limited by potential disruption of mAb and sTM function, as well as inability to control the size of the resulting conjugate. Site-specific conjugation, in contrast, allows 1:1 incorporation with defined orientation of the individual components.

References:

1. Langer, R. Drug delivery and targeting. *Nature* **392,** 5–10 (1998).
2. Walker, D. K. The use of pharmacokinetic and pharmacodynamic data in the assessment of drug safety in early drug development. *Br. J. Clin. Pharmacol.* **58,** 601–608 (2004).
3. Arrowsmith, J. Trial watch: Phase II failures: 2008-2010. *Nat. Rev. Drug Discov.* **10,** 328–329 (2011).
4. Einarson, T. R. Drug-related hospital admissions. *Ann. Pharmacother.* **27,** 832–840 (1993).
5. Hughes, D. A., Bagust, A., Haycox, A. & Walley, T. The impact of non-compliance on the cost-effectiveness of pharmaceuticals: a review of the literature. *Health Econ.* **10,** 601–615 (2001).
6. Gregoriadis, G. Old drugs in new clothing. *Nature* **310,** 186–187 (1984).
7. Heymann, P. D. B. Zur Geschichte der Seitenkettentheorie Paul Ehrlichs. *Klin. Wochenschr.* **7,** 1257–1260 (1928).
8. Ehrlich, P. Partial Cell Functions. (1908). at <http://www.nobelprize.org/nobel_prizes/medicine/laureates/1908/ehrlich-lecture.html>
9. Strebhardt, K. & Ullrich, A. Paul Ehrlich's magic bullet concept: 100 years of progress. *Nat. Rev. Cancer* **8,** 473–480 (2008).
10. Muzykantov, V. & Torchilin, V. *Biomedical Aspects of Drug Targeting*. (Springer US, 2002).
11. FOLKMAN, J. & LONG, D. M. THE USE OF SILICONE RUBBER AS A CARRIER FOR PROLONGED DRUG THERAPY. *J. Surg. Res.* **4,** 139–142 (1964).
12. Segal, S. J. The Development of NORPLANT Implants. *Stud. Fam. Plann.* **14,** 159 (1983).
13. Fraser, I. S. *et al.* Norplant® Consensus Statement and Background Review. *Contraception* **57,** 1–9 (1998).
14. Ogawa, Y., Yamamoto, M., Okada, H., Yashiki, T. & Shimamoto, T. A new technique to efficiently entrap leuprolide acetate into microcapsules of polylactic acid or copoly(lactic/glycolic) acid. *Chem. Pharm. Bull. (Tokyo)* **36,** 1095–1103 (1988).
15. Crosignani, P. G., Luciano, A., Ray, A. & Bergqvist, A. Subcutaneous depot medroxyprogesterone acetate versus leuprolide acetate in the treatment of endometriosis-associated pain. *Hum. Reprod.* **21,** 248–256 (2006).
16. Badaru, A. *et al.* Sequential Comparisons of One-Month and Three-Month Depot Leuprolide Regimens in Central Precocious Puberty. *J. Clin. Endocrinol. Metab.* **91,** 1862–1867 (2006).
17. Bennett, M. R. In-Stent Stenosis: Pathology and Implications for the Development of Drug Eluting Stents. *Heart* **89,** 218–224 (2003).
18. Hwang, C.-W., Wu, D. & Edelman, E. R. Physiological Transport Forces Govern Drug Distribution for Stent-Based Delivery. *Circulation* **104,** 600–605 (2001).

19. Drachman, D. E. *et al.* Neointimal thickening after stent delivery of paclitaxel: change in composition and arrest of growth over six months. *J. Am. Coll. Cardiol.* **36,** 2325–2332 (2000).
20. Bangalore, S. *et al.* Short- and long-term outcomes with drug-eluting and bare-metal coronary stents: a mixed-treatment comparison analysis of 117 762 patient-years of follow-up from randomized trials. *Circulation* **125,** 2873–2891 (2012).
21. Allen, T. M. & Cullis, P. R. Drug Delivery Systems: Entering the Mainstream. *Science* **303,** 1818–1822 (2004).
22. Matsumura, Y. & Maeda, H. A New Concept for Macromolecular Therapeutics in Cancer Chemotherapy: Mechanism of Tumoritropic Accumulation of Proteins and the Antitumor Agent Smancs. *Cancer Res.* **46,** 6387–6392 (1986).
23. Greish, K. Enhanced permeability and retention of macromolecular drugs in solid tumors: A royal gate for targeted anticancer nanomedicines. *J. Drug Target.* **15,** 457–464 (2007).
24. Duncan, R. Polymer conjugates as anticancer nanomedicines. *Nat. Rev. Cancer* **6,** 688–701 (2006).
25. Barenholz, Y. Doxil®--the first FDA-approved nano-drug: lessons learned. *J. Control. Release Off. J. Control. Release Soc.* **160,** 117–134 (2012).
26. Gabizon, A. *et al.* Prolonged Circulation Time and Enhanced Accumulation in Malignant Exudates of Doxorubicin Encapsulated in Polyethylene-glycol Coated Liposomes. *Cancer Res.* **54,** 987–992 (1994).
27. O'Brien, M. E. R. *et al.* Reduced cardiotoxicity and comparable efficacy in a phase III trial of pegylated liposomal doxorubicin HCl (CAELYX^{TM}/Doxil®) versus conventional doxorubicin for first-line treatment of metastatic breast cancer. *Ann. Oncol.* **15,** 440–449 (2004).
28. Solomon, R. & Gabizon, A. A. Clinical Pharmacology of Liposomal Anthracyclines: Focus on Pegylated Liposomal Doxorubicin. *Clin. Lymphoma Myeloma* **8,** 21–32 (2008).
29. Adler-Moore, J. & Proffitt, R. T. AmBisome: liposomal formulation, structure, mechanism of action and pre-clinical experience. *J. Antimicrob. Chemother.* **49 Suppl 1,** 21–30 (2002).
30. Adler-moore, J. P. & Proffitt, R. T. Development, Characterization, Efficacy and Mode of Action of Ambisome, A Unilamellar Liposomal Formulation of Amphotericin B. *J. Liposome Res.* **3,** 429–450 (1993).
31. Walsh, T. J. *et al.* Liposomal Amphotericin B for Empirical Therapy in Patients with Persistent Fever and Neutropenia. *N. Engl. J. Med.* **340,** 764–771 (1999).
32. Walsh, T. J. *et al.* Caspofungin versus liposomal amphotericin B for empirical antifungal therapy in patients with persistent fever and neutropenia. *N. Engl. J. Med.* **351,** 1391–1402 (2004).
33. FDA approval of generic version of cancer drug Doxil is expected to help resolve shortage. *FDA NEWS RELEASE* at

<http://www.fda.gov/newsevents/newsroom/pressannouncements/ucm337872.htm>
34. Greineder, C., Howard, M. D., Carnemolla, R., Cines, D. B. & Muzykantov, V. Advanced drug delivery systems for anti-thrombotic agents. *Blood* blood–2013–03–453498 (2013). doi:10.1182/blood-2013-03-453498
35. Duncan, R. The dawning era of polymer therapeutics. *Nat. Rev. Drug Discov.* **2,** 347–360 (2003).
36. De Duve, C. *et al.* Commentary. Lysosomotropic agents. *Biochem. Pharmacol.* **23,** 2495–2531 (1974).
37. Chipman, S. D., Oldham, F. B., Pezzoni, G. & Singer, J. W. Biological and clinical characterization of paclitaxel poliglumex (PPX, CT-2103), a macromolecular polymer-drug conjugate. *Int. J. Nanomedicine* **1,** 375–383 (2006).
38. Gao, W., Chan, J. & Farokhzad, O. C. pH-responsive Nanoparticles for Drug Delivery. *Mol. Pharm.* **7,** 1913–1920 (2010).
39. Vasey, P. A. *et al.* Phase I clinical and pharmacokinetic study of PK1 [N-(2-hydroxypropyl)methacrylamide copolymer doxorubicin]: first member of a new class of chemotherapeutic agents-drug-polymer conjugates. Cancer Research Campaign Phase I/II Committee. *Clin. Cancer Res. Off. J. Am. Assoc. Cancer Res.* **5,** 83–94 (1999).
40. Xia, W. & Low, P. S. Folate-Targeted Therapies for Cancer. *J. Med. Chem.* **53,** 6811–6824 (2010).
41. Leamon, C. P., Pastan, I. & Low, P. S. Cytotoxicity of folate-Pseudomonas exotoxin conjugates toward tumor cells. Contribution of translocation domain. *J. Biol. Chem.* **268,** 24847–24854 (1993).
42. Yang, J., Chen, H., Vlahov, I. R., Cheng, J.-X. & Low, P. S. Evaluation of disulfide reduction during receptor-mediated endocytosis by using FRET imaging. *Proc. Natl. Acad. Sci.* **103,** 13872–13877 (2006).
43. Low, P. S. & Kularatne, S. A. Folate-targeted therapeutic and imaging agents for cancer. *Curr. Opin. Chem. Biol.* **13,** 256–262 (2009).
44. Zhong, X., Neumann, P., Corbo, M. & Loh, E. in *Drug Discov. Dev. - Present Future* (Kapetanovi, I.) (InTech, 2011). at <http://www.intechopen.com/books/drug-discovery-and-development-present-and-future/recent-advances-in-biotherapeutics-drug-discovery-and-development>
45. Top 100 Drugs for 2013 by Sales. at <http://www.drugs.com/stats/top100/2013/sales>
46. Bonin-Debs, A. L., Boche, I., Gille, H. & Brinkmann, U. Development of secreted proteins as biotherapeutic agents. *Expert Opin. Biol. Ther.* **4,** 551–558 (2004).
47. Lanthier, M., Behrman, R. & Nardinelli, C. Economic issues with follow-on protein products. *Nat. Rev. Drug Discov.* **7,** 733–737 (2008).
48. Muzykantov, V. R. Targeted Drug Delivery to Endothelial Adhesion Molecules. *ISRN Vasc. Med.* **2013,** 1–27 (2013).

49. Wang, J., Lu, Z., Wientjes, M. G. & Au, J. L.-S. Delivery of siRNA Therapeutics: Barriers and Carriers. *AAPS J.* **12,** 492–503 (2010).
50. Ledford, H. Drug giants turn their backs on RNA interference. *Nat. News* **468,** 487–487 (2010).
51. Tissue plasminogen activator for acute ischemic stroke. The National Institute of Neurological Disorders and Stroke rt-PA Stroke Study Group. *N. Engl. J. Med.* **333,** 1581–1587 (1995).
52. Adeoye, O., Hornung, R., Khatri, P. & Kleindorfer, D. Recombinant Tissue-Type Plasminogen Activator Use for Ischemic Stroke in the United States A Doubling of Treatment Rates Over the Course of 5 Years. *Stroke* **42,** 1952–1955 (2011).
53. Weintraub, M. I. Thrombolysis (tissue plasminogen activator) in stroke: a medicolegal quagmire. *Stroke J. Cereb. Circ.* **37,** 1917–1922 (2006).
54. Chandler, W. L. *et al.* Clearance of Tissue Plasminogen Activator (TPA) and TPA/Plasminogen Activator Inhibitor Type 1 (PAI-1) Complex Relationship to Elevated TPA Antigen in Patients With High PAI-1 Activity Levels. *Circulation* **96,** 761–768 (1997).
55. Dellas, C. & Loskutoff, D. J. Historical analysis of PAI-1 from its discovery to its potential role in cell motility and disease. *Thromb. Haemost.* **93,** 631–640 (2005).
56. Ploneda Perilla, A. S. & Schneck, M. J. Unanswered Questions in Thrombolytic Therapy for Acute Ischemic Stroke. *Neurol. Clin.* **31,** 677–704 (2013).
57. Rosamond, W. *et al.* Heart Disease and Stroke Statistics—2008 Update A Report From the American Heart Association Statistics Committee and Stroke Statistics Subcommittee. *Circulation* **117,** e25–e146 (2008).
58. Remick, D. G. Cytokine therapeutics for the treatment of sepsis: why has nothing worked? *Curr. Pharm. Des.* **9,** 75–82 (2003).
59. Kumar, G. *et al.* Nationwide trends of severe sepsis in the 21st century (2000-2007). *Chest* **140,** 1223–1231 (2011).
60. Rea, T. D., Eisenberg, M. S., Becker, L. J., Murray, J. A. & Hearne, T. Temporal trends in sudden cardiac arrest: a 25-year emergency medical services perspective. *Circulation* **107,** 2780–2785 (2003).
61. Aird, W. C. The role of the endothelium in severe sepsis and multiple organ dysfunction syndrome. *Blood* **101,** 3765–3777 (2003).
62. Finigan, J. H. The coagulation system and pulmonary endothelial function in acute lung injury. *Microvasc. Res.* **77,** 35–38 (2009).
63. Neumar, R. W. *et al.* Post–Cardiac Arrest Syndrome Epidemiology, Pathophysiology, Treatment, and Prognostication. *Circulation* **118,** 2452–2483 (2008).
64. Cines, D. B. *et al.* Endothelial Cells in Physiology and in the Pathophysiology of Vascular Disorders. *Blood* **91,** 3527–3561 (1998).
65. Pober, J. S., Min, W. & Bradley, J. R. Mechanisms of Endothelial Dysfunction, Injury, and Death. *Annu. Rev. Pathol. Mech. Dis.* **4,** 71–95 (2009).

66. Pober, J. S. & Sessa, W. C. Evolving functions of endothelial cells in inflammation. *Nat. Rev. Immunol.* **7,** 803–815 (2007).
67. Davies, P. F. Flow-Mediated Endothelial Mechanotransduction. *Physiol. Rev.* **75,** 519–560 (1995).
68. Huang, Z. *et al.* Enlarged Infarcts in Endothelial Nitric Oxide Synthase Knockout Mice Are Attenuated by Nitro-l-Arginine. *J. Cereb. Blood Flow Metab.* **16,** 981–987 (1996).
69. Li, W. *et al.* Overexpressing endothelial cell protein C receptor alters the hemostatic balance and protects mice from endotoxin. *J. Thromb. Haemost.* **3,** 1351–1359 (2005).
70. Moreno, M. U. *et al.* The C242T CYBA polymorphism of NADPH oxidase is associated with essential hypertension. *J. Hypertens.* **24,** 1299–1306 (2006).
71. Barst, R. J. *et al.* A Comparison of Continuous Intravenous Epoprostenol (Prostacyclin) with Conventional Therapy for Primary Pulmonary Hypertension. *N. Engl. J. Med.* **334,** 296–301 (1996).
72. Murphy, E. A. *et al.* Nanoparticle-mediated drug delivery to tumor vasculature suppresses metastasis. *Proc. Natl. Acad. Sci. U. S. A.* **105,** 9343–9348 (2008).
73. Danilov, S. M. *et al.* Lung uptake of antibodies to endothelial antigens: key determinants of vascular immunotargeting. *Am. J. Physiol. Lung Cell. Mol. Physiol.* **280,** L1335–1347 (2001).
74. Muro, S. & Muzykantov, V. R. Targeting of antioxidant and anti-thrombotic drugs to endothelial cell adhesion molecules. *Curr. Pharm. Des.* **11,** 2383–2401 (2005).
75. Chrastina, A., Valadon, P., Massey, K. A. & Schnitzer, J. E. Lung vascular targeting using antibody to aminopeptidase P: CT-SPECT imaging, biodistribution and pharmacokinetic analysis. *J. Vasc. Res.* **47,** 531–543 (2010).
76. Kowalski, P. S. *et al.* Targeted siRNA delivery to diseased microvascular endothelial cells—Cellular and molecular concepts. *IUBMB Life* **63,** 648–658 (2011).
77. Esmon, C. T. The normal role of Activated Protein C in maintaining homeostasis and its relevance to critical illness. *Crit. Care Lond. Engl.* **5,** S7–12 (2001).
78. Marciniak, E. Coagulation inhibitor elicited by thrombin. *Science* **170,** 452–453 (1970).
79. Stenflo, J. A new vitamin K-dependent protein. Purification from bovine plasma and preliminary characterization. *J. Biol. Chem.* **251,** 355–363 (1976).
80. Kisiel, W. Human Plasma Protein C. *J. Clin. Invest.* **64,** 761–769 (1979).
81. Kisiel, W., Ericsson, L. H. & Davie, E. W. Proteolytic activation of protein C from bovine plasma. *Biochemistry (Mosc.)* **15,** 4893–4900 (1976).
82. Esmon, C. T. & Owen, W. G. The discovery of thrombomodulin. *J. Thromb. Haemost. JTH* **2,** 209–213 (2004).

83. Esmon, C. T. Thrombomodulin as a model of molecular mechanisms that modulate protease specificity and function at the vessel surface. *FASEB J.* **9,** 946–955 (1995).
84. Mosnier, L. O., Zlokovic, B. V. & Griffin, J. H. The cytoprotective protein C pathway. *Blood* **109,** 3161–3172 (2007).
85. Weiler, H. *et al.* Characterization of a Mouse Model for Thrombomodulin Deficiency. *Arterioscler. Thromb. Vasc. Biol.* **21,** 1531–1537 (2001).
86. Faust, S. N. *et al.* Dysfunction of endothelial protein C activation in severe meningococcal sepsis. *N. Engl. J. Med.* **345,** 408–416 (2001).
87. Sido, B. *et al.* Soluble thrombomodulin--a marker of reperfusion injury after orthotopic liver transplantation. *Transplantation* **60,** 462–466 (1995).
88. Laszik, Z. G., Zhou, X. J., Ferrell, G. L., Silva, F. G. & Esmon, C. T. Down-Regulation of Endothelial Expression of Endothelial Cell Protein C Receptor and Thrombomodulin in Coronary Atherosclerosis. *Am. J. Pathol.* **159,** 797–802 (2001).
89. Hafer-Macko, C. E., Ivey, F. M., Gyure, K. A., Sorkin, J. D. & Macko, R. F. Thrombomodulin deficiency in human diabetic nerve microvasculature. *Diabetes* **51,** 1957–1963 (2002).
90. Nawroth, P. P., Handley, D. A., Esmon, C. T. & Stern, D. M. Interleukin 1 induces endothelial cell procoagulant while suppressing cell-surface anticoagulant activity. *Proc. Natl. Acad. Sci. U. S. A.* **83,** 3460–3464 (1986).
91. Moore, K. L., Esmon, C. T. & Esmon, N. L. Tumor necrosis factor leads to the internalization and degradation of thrombomodulin from the surface of bovine aortic endothelial cells in culture. *Blood* **73,** 159–165 (1989).
92. MacGregor, I. R., Perrie, A. M., Donnelly, S. C. & Haslett, C. Modulation of human endothelial thrombomodulin by neutrophils and their release products. *Am. J. Respir. Crit. Care Med.* **155,** 47–52 (1997).
93. Glaser, C. B. *et al.* Oxidation of a specific methionine in thrombomodulin by activated neutrophil products blocks cofactor activity. A potential rapid mechanism for modulation of coagulation. *J. Clin. Invest.* **90,** 2565–2573 (1992).
94. Stearns-Kurosawa, D. J., Kurosawa, S., Mollica, J. S., Ferrell, G. L. & Esmon, C. T. The endothelial cell protein C receptor augments protein C activation by the thrombin-thrombomodulin complex. *Proc. Natl. Acad. Sci. U. S. A.* **93,** 10212–10216 (1996).
95. Taylor, F. B., Jr, Peer, G. T., Lockhart, M. S., Ferrell, G. & Esmon, C. T. Endothelial cell protein C receptor plays an important role in protein C activation in vivo. *Blood* **97,** 1685–1688 (2001).
96. Bae, J.-S., Yang, L. & Rezaie, A. R. Receptors of the protein C activation and activated protein C signaling pathways are colocalized in lipid rafts of endothelial cells. *Proc. Natl. Acad. Sci.* **104,** 2867–2872 (2007).
97. Feistritzer, C. *et al.* Protective signaling by activated protein C is mechanistically linked to protein C activation on endothelial cells. *J. Biol. Chem.* **281,** 20077–20084 (2006).

98. Rezaie, A. R. The occupancy of endothelial protein C receptor by its ligand modulates the par-1 dependent signaling specificity of coagulation proteases. *IUBMB Life* **63,** 390–396 (2011).
99. Finigan, J. H. *et al.* Activated Protein C Mediates Novel Lung Endothelial Barrier Enhancement ROLE OF SPHINGOSINE 1-PHOSPHATE RECEPTOR TRANSACTIVATION. *J. Biol. Chem.* **280,** 17286–17293 (2005).
100. Feistritzer, C. & Riewald, M. Endothelial barrier protection by activated protein C through PAR1-dependent sphingosine 1–phosphate receptor-1 crossactivation. *Blood* **105,** 3178–3184 (2005).
101. Burnier, L. & Mosnier, L. O. Novel mechanisms for activated protein C cytoprotective activities involving non-canonical activation of protease-activated receptor 3. *Blood* blood–2013–03–488957 (2013). doi:10.1182/blood-2013-03-488957
102. Kurosawa, S., Stearns-Kurosawa, D. J., Hidari, N. & Esmon, C. T. Identification of functional endothelial protein C receptor in human plasma. *J. Clin. Invest.* **100,** 411–418 (1997).
103. Kurosawa, S. *et al.* Plasma levels of endothelial cell protein C receptor are elevated in patients with sepsis and systemic lupus erythematosus: lack of correlation with thrombomodulin suggests involvement of different pathological processes. *Blood* **91,** 725–727 (1998).
104. Boomsma, M. M. *et al.* Plasma levels of soluble endothelial cell protein C receptor in patients with Wegener's granulomatosis. *Clin. Exp. Immunol.* **128,** 187–194 (2002).
105. Xu, J., Qu, D., Esmon, N. L. & Esmon, C. T. Metalloproteolytic release of endothelial cell protein C receptor. *J. Biol. Chem.* **275,** 6038–6044 (2000).
106. Laszik, Z., Mitro, A., Taylor, F. B., Jr, Ferrell, G. & Esmon, C. T. Human protein C receptor is present primarily on endothelium of large blood vessels: implications for the control of the protein C pathway. *Circulation* **96,** 3633–3640 (1997).
107. Iwaki, T., Cruz, D. T., Martin, J. A. & Castellino, F. J. A cardioprotective role for the endothelial protein C receptor in lipopolysaccharide-induced endotoxemia in the mouse. *Blood* **105,** 2364–2371 (2005).
108. Von Drygalski, A., Furlan-Freguia, C., Ruf, W., Griffin, J. H. & Mosnier, L. O. Organ-specific protection against lipopolysaccharide-induced vascular leak is dependent on the endothelial protein C receptor. *Arterioscler. Thromb. Vasc. Biol.* **33,** 769–776 (2013).
109. Waugh, J. M. *et al.* Local Overexpression of Thrombomodulin for In Vivo Prevention of Arterial Thrombosis in a Rabbit Model. *Circ. Res.* **84,** 84–92 (1999).
110. Kim, A. Y. *et al.* Early Loss of Thrombomodulin Expression Impairs Vein Graft Thromboresistance Implications for Vein Graft Failure. *Circ. Res.* **90,** 205–212 (2002).

111. Tabuchi, N. *et al.* Non-viral in vivo thrombomodulin gene transfer prevents early loss of thromboresistance of grafted veins. *Eur. J. Cardio-Thorac. Surg. Off. J. Eur. Assoc. Cardio-Thorac. Surg.* **26,** 995–1001 (2004).
112. Newby, A. & Baker, A. Targets for gene therapy of vein grafts. [Review] [37 refs]. *Curr. Opin. Cardiol.* **14,** 489–94 (1999).
113. Taylor, F. B. *et al.* Protein C prevents the coagulopathic and lethal effects of Escherichia coli infusion in the baboon. *J. Clin. Invest.* **79,** 918–925 (1987).
114. Bone, R. C. *et al.* DEfinitions for sepsis and organ failure and guidelines for the use of innovative therapies in sepsis. the accp/sccm consensus conference committee. american college of chest physicians/society of critical care medicine. *CHEST J.* **101,** 1644–1655 (1992).
115. Bernard, G. R. *et al.* Efficacy and safety of recombinant human activated protein C for severe sepsis. *N. Engl. J. Med.* **344,** 699–709 (2001).
116. Macias, W. L. *et al.* Pharmacokinetic-pharmacodynamic analysis of drotrecogin alfa (activated) in patients with severe sepsis. *Clin. Pharmacol. Ther.* **72,** 391–402 (2002).
117. Ranieri, V. M. *et al.* Drotrecogin Alfa (Activated) in Adults with Septic Shock. *N. Engl. J. Med.* **366,** 2055–2064 (2012).
118. Mosnier, L. O., Gale, A. J., Yegneswaran, S. & Griffin, J. H. Activated protein C variants with normal cytoprotective but reduced anticoagulant activity. *Blood* **104,** 1740–1744 (2004).
119. Mosnier, L. O., Yang, X. V. & Griffin, J. H. Activated Protein C Mutant with Minimal Anticoagulant Activity, Normal Cytoprotective Activity, and Preservation of Thrombin Activable Fibrinolysis Inhibitor-dependent Cytoprotective Functions. *J. Biol. Chem.* **282,** 33022–33033 (2007).
120. Kerschen, E. J. *et al.* Endotoxemia and sepsis mortality reduction by non-anticoagulant–activated protein C. *J. Exp. Med.* **204,** 2439–2448 (2007).
121. Solis, M. M. *et al.* Intravenous recombinant soluble human thrombomodulin prevents venous thrombosis in a rat model. *J. Vasc. Surg.* **14,** 599–604 (1991).
122. Conway, E. M. *et al.* The Lectin-like Domain of Thrombomodulin Confers Protection from Neutrophil-mediated Tissue Damage by Suppressing Adhesion Molecule Expression via Nuclear Factor κB and Mitogen-activated Protein Kinase Pathways. *J. Exp. Med.* **196,** 565–577 (2002).
123. Van Iersel, T., Stroissnig, H., Giesen, P., Wemer, J. & Wilhelm-Ogunbiyi, K. Phase I study of Solulin, a novel recombinant soluble human thrombomodulin analogue. *Thromb. Haemost.* **105,** 302–312 (2011).
124. Su, E. J. *et al.* The thrombomodulin analog Solulin promotes reperfusion and reduces infarct volume in a thrombotic stroke model. *J. Thromb. Haemost. JTH* **9,** 1174–1182 (2011).
125. Kearon, C. *et al.* Dose-response study of recombinant human soluble thrombomodulin (ART-123) in the prevention of venous thromboembolism after total hip replacement. *J. Thromb. Haemost. JTH* **3,** 962–968 (2005).
126. Saito, H. *et al.* Efficacy and safety of recombinant human soluble thrombomodulin (ART-123) in disseminated intravascular coagulation:

results of a phase III, randomized, double-blind clinical trial. *J. Thromb. Haemost. JTH* **5,** 31–41 (2007).
127. Ding, B.-S. *et al.* Anchoring fusion thrombomodulin to the endothelial lumen protects against injury-induced lung thrombosis and inflammation. *Am. J. Respir. Crit. Care Med.* **180,** 247–256 (2009).
128. Sperling, C., Salchert, K., Streller, U. & Werner, C. Covalently immobilized thrombomodulin inhibits coagulation and complement activation of artificial surfaces in vitro. *Biomaterials* **25,** 5101–5113 (2004).
129. Kishida, A. *et al.* Immobilization of human thrombomodulin onto poly(ether urethane urea) for developing antithrombogenic blood-contacting materials. *Biomaterials* **15,** 848–852 (1994).
130. Han, H. S. *et al.* Studies of a novel human thrombomodulin immobilized substrate: surface characterization and anticoagulation activity evaluation. *J. Biomater. Sci. Polym. Ed.* **12,** 1075–1089 (2001).
131. Zhang, H. *et al.* Bio-inspired liposomal thrombomodulin conjugate through bio-orthogonal chemistry. *Bioconjug. Chem.* **24,** 550–559 (2013).
132. Tseng, P.-Y., Jordan, S. W., Sun, X.-L. & Chaikof, E. L. Catalytic efficiency of a thrombomodulin-functionalized membrane-mimetic film in a flow model. *Biomaterials* **27,** 2768–2775 (2006).
133. Kador, K. E., Mamedov, T. G., Schneider, M. & Subramanian, A. Sequential co-immobilization of thrombomodulin and endothelial protein C receptor on polyurethane: activation of protein C. *Acta Biomater.* **7,** 2508–2517 (2011).
134. Lu, R. L., Esmon, N. L., Esmon, C. T. & Johnson, A. E. The active site of the thrombin-thrombomodulin complex. A fluorescence energy transfer measurement of its distance above the membrane surface. *J. Biol. Chem.* **264,** 12956–12962 (1989).
135. Tsiang, M., Lentz, S. R. & Sadler, J. E. Functional domains of membrane-bound human thrombomodulin. EGF-like domains four to six and the serine/threonine-rich domain are required for cofactor activity. *J. Biol. Chem.* **267,** 6164–6170 (1992).
136. Albelda, S. M., Muller, W. A., Buck, C. A. & Newman, P. J. Molecular and cellular properties of PECAM-1 (endoCAM/CD31): a novel vascular cell-cell adhesion molecule. *J. Cell Biol.* **114,** 1059–1068 (1991).
137. Newman, P. J. The biology of PECAM-1. *J. Clin. Invest.* **99,** 3–8 (1997).
138. Teasdale, M. S., Bird, C. H. & Bird, P. Internalization of the anticoagulant thrombomodulin is constitutive and does not require a signal in the cytoplasmic domain. *Immunol. Cell Biol.* **72,** 480–488 (1994).
139. Moll, S. *et al.* Phase I study of a novel recombinant human soluble thrombomodulin, ART-123. *J. Thromb. Haemost. JTH* **2,** 1745–1751 (2004).
140. Van Iersel, T., Stroissnig, H., Giesen, P., Wemer, J. & Wilhelm-Ogunbiyi, K. Phase I study of Solulin, a novel recombinant soluble human thrombomodulin analogue. *Thromb. Haemost.* **105,** 302–312 (2011).
141. Zaitsev, S. *et al.* Sustained thromboprophylaxis mediated by an RBC-targeted pro-urokinase zymogen activated at the site of clot formation. *Blood* **115,** 5241–5248 (2010).

142. Chacko, A.-M., Nayak, M., Greineder, C. F., DeLisser, H. M. & Muzykantov, V. R. Collaborative Enhancement of Antibody Binding to Distinct PECAM-1 Epitopes Modulates Endothelial Targeting. *PLoS ONE* **7,** e34958 (2012).
143. Sun, J. *et al.* Contributions of the extracellular and cytoplasmic domains of platelet-endothelial cell adhesion molecule-1 (PECAM-1/CD31) in regulating cell-cell localization. *J. Cell Sci.* **113,** 1459–1469 (2000).
144. Weiler-Guettler, H. *et al.* A targeted point mutation in thrombomodulin generates viable mice with a prethrombotic state. *J. Clin. Invest.* **101,** 1983–1991 (1998).
145. Newman, P. J. The Role of PECAM-1 in Vascular Cell Biologya. *Ann. N. Y. Acad. Sci.* **714,** 165–174 (1994).
146. Maruyama, I. & Majerus, P. W. The turnover of thrombin-thrombomodulin complex in cultured human umbilical vein endothelial cells and A549 lung cancer cells. Endocytosis and degradation of thrombin. *J. Biol. Chem.* **260,** 15432–15438 (1985).
147. Fukudome, K. & Esmon, C. T. Molecular Cloning and Expression of Murine and Bovine Endothelial Cell Protein C/Activated Protein C Receptor (EPCR) The Structural and Functional Conservation in Human, Bovine, and Murine EPCR. *J. Biol. Chem.* **270,** 5571–5577 (1995).
148. Fehrenbach, M. L., Cao, G., Williams, J. T., Finklestein, J. M. & DeLisser, H. M. Isolation of murine lung endothelial cells. *Am. J. Physiol. - Lung Cell. Mol. Physiol.* **296,** L1096–L1103 (2009).
149. Van Buul, J. D. *et al.* Inside-Out Regulation of ICAM-1 Dynamics in TNF-α-Activated Endothelium. *PLoS ONE* **5,** e11336 (2010).
150. Staunton, D. E., Dustin, M. L., Erickson, H. P. & Springer, T. A. The arrangement of the immunoglobulin-like domains of ICAM-1 and the binding sites for LFA-1 and rhinovirus. *Cell* **61,** 243–254 (1990).
151. Dübel, S. *et al.* Isolation of IgG antibody Fv-DNA from various mouse and rat hybridoma cell lines using the polymerase chain reaction with a simple set of primers. *J. Immunol. Methods* **175,** 89–95 (1994).
152. Crowe, J. S., Smith, M. A. & Cooper, H. J. Nucleotide sequence of Y3-Ag 1.2.3. rat myeloma immunoglobulin kappa chain cDNA. *Nucleic Acids Res.* **17,** 7992 (1989).
153. Murciano, J.-C. *et al.* ICAM-directed vascular immunotargeting of antithrombotic agents to the endothelial luminal surface Presented in part as posters at the American Thoracic Society (ATS) Meeting, May 5-10, 2000, Toronto, ON, Canada. *Blood* **101,** 3977–3984 (2003).
154. Greineder, C. F. *et al.* Vascular Immunotargeting to Endothelial Determinant ICAM-1 Enables Optimal Partnering of Recombinant scFv-Thrombomodulin Fusion with Endogenous Cofactor. *PLoS ONE* **8,** e80110 (2013).
155. Christofidou-Solomidou, M. *et al.* Vascular Immunotargeting of Glucose Oxidase to the Endothelial Antigens Induces Distinct Forms of Oxidant Acute Lung Injury. *Am. J. Pathol.* **160,** 1155–1169 (2002).
156. Muro, S., Koval, M. & Muzykantov, V. Endothelial endocytic pathways: gates for vascular drug delivery. *Curr. Vasc. Pharmacol.* **2,** 281–299 (2004).

157. Muro, S. *et al.* A novel endocytic pathway induced by clustering endothelial ICAM-1 or PECAM-1. *J. Cell Sci.* **116,** 1599–1609 (2003).
158. Muller, W. A., Weigl, S. A., Deng, X. & Phillips, D. M. PECAM-1 is required for transendothelial migration of leukocytes. *J. Exp. Med.* **178,** 449–460 (1993).
159. Vaporciyan, A. A. *et al.* Involvement of platelet-endothelial cell adhesion molecule-1 in neutrophil recruitment in vivo. *Science* **262,** 1580–1582 (1993).
160. Yan, H. C. *et al.* Alternative splicing of a specific cytoplasmic exon alters the binding characteristics of murine platelet/endothelial cell adhesion molecule-1 (PECAM-1). *J. Biol. Chem.* **270,** 23672–23680 (1995).
161. Binette, T. M., Taylor, F. B., Peer, G. & Bajzar, L. Thrombin-thrombomodulin connects coagulation and fibrinolysis: more than an in vitro phenomenon. *Blood* **110,** 3168–3175 (2007).
162. Matute-Bello, G., Frevert, C. W. & Martin, T. R. Animal models of acute lung injury. *Am. J. Physiol. - Lung Cell. Mol. Physiol.* **295,** L379–L399 (2008).
163. Nakada, M. T. *et al.* Antibodies Against the First Ig-Like Domain of Human Platelet Endothelial Cell Adhesion Molecule-1 (PECAM-1) That Inhibit PECAM-1-Dependent Homophilic Adhesion Block In Vivo Neutrophil Recruitment. *J. Immunol.* **164,** 452–462 (2000).
164. Salmela, K. *et al.* A randomized multicenter trial of the anti-ICAM-1 monoclonal antibody (enlimomab) for the prevention of acute rejection and delayed onset of graft function in cadaveric renal transplantation: a report of the European Anti-ICAM-1 Renal Transplant Study Group. *Transplantation* **67,** 729–736 (1999).
165. Abeyama, K. *et al.* The N-terminal domain of thrombomodulin sequesters high-mobility group-B1 protein, a novel antiinflammatory mechanism. *J. Clin. Invest.* **115,** 1267–1274 (2005).
166. Nagato, M., Okamoto, K., Abe, Y., Higure, A. & Yamaguchi, K. Recombinant human soluble thrombomodulin decreases the plasma high-mobility group box-1 protein levels, whereas improving the acute liver injury and survival rates in experimental endotoxemia. *Crit. Care Med.* **37,** 2181–2186 (2009).
167. Roopenian, D. C. & Akilesh, S. FcRn: the neonatal Fc receptor comes of age. *Nat. Rev. Immunol.* **7,** 715–725 (2007).
168. Bhowmick, T., Berk, E., Cui, X., Muzykantov, V. R. & Muro, S. Effect of flow on endothelial endocytosis of nanocarriers targeted to ICAM-1. *J. Control. Release Off. J. Control. Release Soc.* **157,** 485–492 (2012).